

## Seafloor biota, rock lobster and demersal fish assemblages of the Tasman Fracture Commonwealth Marine Reserve Region: Determining the influence of the shelf sanctuary zone on population demographics

Jacquomo Monk<sup>1</sup>, Neville Barrett<sup>1</sup>, Justin Hulls<sup>1</sup>, Lainey James<sup>1</sup>, Geoff Hosack<sup>2</sup> Elizabeth Oh<sup>1</sup>, Tara Martin<sup>2</sup>, Stuart Edwards<sup>2</sup>, Amy Nau<sup>2</sup>, Bernadette Heaney<sup>2</sup> and Scott Foster<sup>2</sup>

<sup>1</sup>. Institute for Marine and Antarctic Studies, University of Tasmania

<sup>2</sup>. CSIRO, Hobart.

June 2016



[www.nerpmarine.edu.au](http://www.nerpmarine.edu.au)

Enquiries should be addressed to:  
Neville Barrett  
neville.barrett@utas.edu.au

## Preferred citation

Monk J, Barrett NS, Hulls J, James L, Hosack GR, Oh E, Martin T, Edwards S, Nau A, Heaney B, Foster SD (2016) *Seafloor biota, rock lobster and demersal fish assemblages of the Tasman Fracture Commonwealth Marine Reserve Region: Determining the influence of the shelf sanctuary zone on population demographics*. A report to the National Environmental Research Program, Marine Biodiversity Hub. Published by the University of Tasmania. 97 pp.

ISBN: 9781862958715

## Copyright and Disclaimer

© 2016 NERP Marine Biodiversity Hub. To the extent permitted by law, all rights are reserved and no part of this publication covered by copyright may be reproduced or copied in any form or by any means except with the written permission of NERP Marine Biodiversity Hub.

ISBN 978 1 86295 871 5

## Acknowledgement

This work was undertaken for the Marine Biodiversity Hub, a collaborative partnership supported through funding from the Australian Government's National Environmental Research Program (NERP). NERP Marine Biodiversity Hub partners include the Institute for Marine and Antarctic Studies, University of Tasmania; CSIRO Wealth from Oceans National Flagship, Geoscience Australia, Australian Institute of Marine Science, Museum Victoria, Charles Darwin University and the University of Western Australia.

## Important Disclaimer

The NERP Marine Biodiversity Hub advises that the information contained in this publication comprises general statements based on scientific research. The reader is advised and needs to be aware that such information may be incomplete or unable to be used in any specific situation. No reliance or actions must therefore be made on that information without seeking prior expert professional, scientific and technical advice. To the extent permitted by law, the NERP Marine Biodiversity Hub (including its employees and consultants) excludes all liability to any person for any consequences, including but not limited to all losses, damages, costs, expenses and any other compensation, arising directly or indirectly from using this publication (in part or in whole) and any information or material contained in it.







## Contents

<b>Executive Summary .....</b>	<b>i</b>
<b>1. Introduction .....</b>	<b>1</b>
<b>2. Findings .....</b>	<b>3</b>
2.1 Seabed mapping .....	3
2.1.1 Tasman Fracture CMR sanctuary zone .....	6
2.1.2 Reference sites .....	11
2.2 Population trends of rock lobster .....	15
2.2.1 Descriptive patterns in lobster abundance .....	16
2.2.2 Descriptive patterns in lobster size.....	17
2.2.3 Bycatch in lobster pots.....	25
2.2.4 Detailed modelling of lobster data .....	27
2.2.5 Overview and interpretation of model-based analyses of the spatial and depth distribution of lobster catch.....	32
2.3 Trends in benthic biota.....	33
2.3.1 Tasman Fracture CMR benthic biota assemblage .....	33
2.3.2 Comparison between four Tasmanian CMRs.....	46
2.4 Population trends in demersal fishes.....	50
2.4.1 Distribution of seafloor habitat and substrata type .....	59
2.4.2 Length-frequency analysis and abundance maps .....	60
2.4.3 Detailed modelling of demersal fish data .....	68
2.5 Discussion.....	77
2.5.1 Seabed mapping.....	77
2.5.2 Rock lobster .....	78
2.5.3 Benthic invertebrate assemblages .....	78
2.5.4 Fish assemblages .....	79
2.5.5 Conclusion .....	80
2.6 Summary of key findings.....	81
<b>3. Appendix 1: Bayesian model parameters.....</b>	<b>84</b>



---

## List of Figures

Figure 1. Previous multibeam sonar coverage (at 50 m resolution) of the Tasman Fracture CMR seabed features on the shelf and slope. ....	4
Figure 2. Overview of the area mapped in fine detail in 2014 via <i>R.V Bluefin</i> as a part of the current project (a) and more recently in 2015 (b) a southern addition to this by CSIRO staff on <i>R.V. Investigator</i> sea-trials. The maps indicate the extent of reef systems within the shelf component of the Tasman Fracture CMR sanctuary zone and adjacent control regions, with reefs indicated by regions of raised topography.....	5
Figure 3. Overview of the Tasman Fracture sanctuary zone shelf area mapped in fine resolution during the survey.....	6
Figure 4. The isolated patch reef that provides the most defining feature of the eastern sector of the sanctuary zone.....	8
Figure 5. Extensive dune systems in the NW region of the sanctuary zone of the Tasman Fracture CMR, indicating a region of sediment mobilisation due to swell or current action. Note the parallel linear striations running west-east in the lower mapped area that could represent historical trawl tracks.....	9
Figure 6. Multibeam backscatter map of the Tasman Fracture CMR sanctuary zone. Darker shading generally represents areas of greater “hardness”. The insert shows the unusual mottled nature of the NE section of this zone. ....	10
Figure 7. Extensive cross-bedded features typify the NE section of the Tasman Fracture sanctuary zone and have a characteristic “hard” backscatter signal (see Figure 6) that appear to be primarily comprised of sediment/gravel/cobble inundated low profile reef (as evident by the BRUV drops in the region (see inserts) rather than being purely sedimentary features. ....	11
Figure 8. Reference reef habitat north-west of the Tasman Fracture CMR at depths similar to that found for reef habitat within the Tasman Fracture CMR.....	12
Figure 9. Reference reef habitat offshore of South Cape at depths similar to that found for reef habitat within the Tasman Fracture CMR. ....	13
Figure 10. Reference reef habitat offshore of South East Cape at depths similar to that found for reef habitat within the Tasman Fracture CMR.....	14
Figure 11. Location of the 200 lobster pots in the Tasman Fracture CMR and adjacent fished reference areas. ....	15
Figure 12. Total lobster counts from potting surveys within the Tasman Fracture CMR.....	16
Figure 13. Hotspot analysis of CPUE distribution. Note the clustering of lower abundances (blue) of lobsters inside the CMR and the two clusters of high abundances in the reference sites (red). ...	17
Figure 14. Abundance of legal sized vs sub-legal sized lobsters within fished and CMR reefs. ....	18
Figure 15. Hotspot analysis of size distribution of male lobster caught. Note the clustering of smaller size (blue) of lobsters inside the CMR and the three clusters of larger lobsters (red). ....	19
Figure 16. Hotspot analysis of size distribution of female lobster caught. Note the reduced clustering of larger sizes inside the CMR (red). Also note that few legal (>105 mm) were caught, with none exceeding 110mm carapace length. ....	19
Figure 17. Absolute size frequency of lobsters captured within the CMR sanctuary reefs (top plot) and lobsters captured within fished reference locations (bottom plot). Note the differences in the total count scale reflecting differences in the overall catch between fished and CMR locations.....	21



Figure 18. Comparison of size frequency distributions of lobster populations between the Tasman Fracture and adjacent fished reference locations based on adjustment of CMR abundances for equal numbers of sub-legal lobsters (x4.88 for males, x3.21 for females) to allow for direct evaluation of size distributions. ....	22
Figure 19. Sex related difference in mean carapace length per pot lift with depth estimated from all 200 pot lifts undertaken in the Tasman Fracture CMR survey. ....	23
Figure 20. Size-related pattern of the abundance per pot lift of lobsters with depth in the Tasman Fracture survey area. Size categories are based on sub-legal and legal sized lobsters (105 mm CL females and 110 mm CL males).....	23
Figure 21. Total abundance per pot lift with depth for female and male lobsters from all 200 pot lifts undertaken during the Tasman Fracture survey. ....	24
Figure 22. The cross-shelf distribution of lobster catch per pot-lift based on pre-determined positions.	24
Figure 23. Example of one of the three giant crab ( <i>Pseudocarcinus gigas</i> ) caught during pot sampling for lobster. ....	26
Figure 24. Depth (left) and protection (right) effects on the catch of lobster (abundance). Solid line in left plot is the mean of the expected abundance and shading gives some point-wise credible intervals. Values greater than one in right plot imply greater catch of lobsters inside the CMR. Histogram and smoothed density are taken from the posterior samples. Dashed red vertical line is the mean estimate. ....	29
Figure 25. Depth (left) and protection (right) effects on average male size. Solid line in left plot is the mean of the expected size of male lobster and shading gives some point-wise credible intervals. Values greater than zero in right plot imply greater size in male lobsters inside the CMR. Histogram and smoothed density are taken from the posterior samples. Dashed red vertical line is the mean estimate. ....	30
Figure 26. Depth (left) and protection (right) effects on average female size. Solid line in left plot is the mean of the expected average size of female lobster and shading gives some point-wise credible intervals. Values less than zero in right plot imply smaller size female lobsters inside the CMR. Histogram and smoothed density are taken from the posterior samples. Dashed red vertical line is the mean estimate. ....	30
Figure 27. Depth (left) and protection (right) effects on average abundance of legal sized male lobster. Solid line in left plot is the mean of the expected abundance of legal sized males and shading gives some point-wise credible intervals. Values greater than one in right plot imply greater abundance of legal male lobsters inside the CMR. Histogram and smoothed density are taken from the posterior samples. Dashed red vertical line is the mean estimate. ....	31
Figure 28. Depth (left) and protection (right) effects on the proportion of male vs female lobster in the catch. Solid line in left plot is the mean of the expected proportion of male lobster and shading gives some point-wise credible intervals. Values less than zero in right plot imply smaller proportion of female lobsters inside the CMR. Histogram and smoothed density are taken from the posterior samples. Dashed red vertical line is the mean estimate. ....	31
Figure 29. Depth (left) and protection (right) effects on the proportion of legal sized vs undersized male lobsters caught. Solid line in left plot is the mean of the expected average and shading gives some point-wise credible intervals. Values greater than zero in right plot imply greater proportion of legal male lobsters inside the CMR. Histogram and smoothed density are taken from the posterior samples. Dashed red vertical line is the mean estimate. ....	32
Figure 30. Proposed and completed AUV missions in- and around the Tasman Fracture Commonwealth Marine Reserve. ....	35
Figure 31. Example of the Bryozoa/Cnidaria/Hydroid matrix class (non-descript brown turf) that dominated the assemblage. ....	41



Figure 32. Boulder reefs supporting encrusting yellow and white sponges (colour coded arrows). White encrusting sponges are morphospecies “Encrusting white 6”. Note also the large cup-like (“cup 1 white”) in top image. ....	42
Figure 33. Examples of the variety in cup-like sponges from small (centre of image) to large top left image (“cup 1 white” morphospecies). ....	43
Figure 34. An example image highlighting the extreme abundance in the brittle star community, which appears to dominate the seafloor. Note the large scalp in bottom image. Scalps were a common occurrence in the lobster pots. ....	44
Figure 35. An example of the complex invertebrate assemblages including sponges, <i>Capnella</i> -like soft corals (Coral 2 sift <i>Capnella</i> like) and ascidians. Note the lobster ( <i>Jasus edwardsii</i> ) in the centre of the top image. ....	45
Figure 36. Non-metric multidimensional scaling ordination for centroids morphospecies assemblage between Tasman Fracture, Huon, Freycinet and Flinders CMRs. Hashed lines indicate 30 % similarity between morphospecies assemblages. ....	47
Figure 37. Distribution of the 92 BRUV deployments in the Tasman Fracture CMR and adjacent fished reference areas. ....	54
Figure 38. An example of one of the large schools of butterfly perch observed within the Tasman Fracture CMR and adjacent fished reference reefs. Note the striped trumpeter. ....	54
Figure 39. An example of one of the abundance of ocean perch and grubfish observed within the Tasman Fracture CMR and adjacent fished reference reefs. ....	55
Figure 40. An example of one of the large schools of juvenile jackass morwong observed within the Tasman Fracture CMR and adjacent fished reference reefs. This is an interesting finding as juvenile jackass morwong are thought to be usually associated with estuaries and other sheltered shallow-water regions. ....	55
Figure 41. An example of extremely aggressive arrow squid that are commonly observed attempting to predate on other fish around BRUVS within the Tasman Fracture CMR and adjacent fished reference reefs. ....	56
Figure 42. An example of one of the large striped trumpeter observed within the Tasman Fracture CMR and adjacent fished reference reefs. ....	56
Figure 43. An example of an octopus feeding on the bait on one of the BRUVS deployments within the Tasman Fracture CMR and adjacent fished reference reefs. Note the red cod and reef ocean perch in the background. ....	57
Figure 44. Example of the abundance of lobster attracted to the BRUVS. Note the butterfly perch and cosmopolitan leatherjackets ( <i>Meuschenia scaber</i> ) in the background. ....	57
Figure 45. Large seven gill shark ( <i>Notocrynychus cepedianus</i> ), Morid cods (Moridae) and jack mackerel ( <i>Trachurus declivis</i> ) attracted to the BRUVS. ....	58
Figure 46. Another example of a large elasmobranch (Melbourne Skate; <i>Spiniraja whitleyi</i> ) attracted to the BRUVS. ....	58
Figure 47. Distribution of broad substrata types surveyed using the BRUVs. ....	59
Figure 48. Distribution of broad seabed habitats surveyed using the BRUVs. ....	60
Figure 49. Relative abundance of jackass morwong ( <i>Nemadactylus macropterus</i> ) as measured using BRUVS. ....	62
Figure 50. Length-frequencies for jackass morwong ( <i>Nemadactylus macropterus</i> ) as determined using BRUVs. ....	62
Figure 51. Relative abundance of ocean perch ( <i>Helicolenus percoides</i> ) as measured using BRUVS. 63	



Figure 52. Length-frequencies for ocean perch ( <i>Helicolenus percoides</i> ) as determined using BRUVs. ....	64
Figure 53. Relative abundance of morid cods as measured using BRUVs.....	65
Figure 54. Length-frequencies for morid cods as determined using BRUVs. ....	65
Figure 55. Relative abundance of striped trumpeter ( <i>Latris lineata</i> ) as measured using BRUVs. ....	66
Figure 56. Relative abundance of draughtboard shark ( <i>Cephaloscyllium laticeps</i> ) as measured using BRUVs. ....	67
Figure 57. Depth (left) and protection (right) effects on abundance of jackass morwong ( <i>Nemadactylus macropterus</i> ). Solid line in left plot is the mean of the expected abundance and shading gives some point-wise credible intervals. Values greater than one in right plot imply greater abundance inside the CMR. Histogram and smoothed density are taken from the posterior samples. Dashed red vertical line is the mean estimate.....	70
Figure 58. Depth (left) and protection (right) effects on abundance of ocean perch ( <i>Helicolenus percoides</i> ). Solid line in left plot is the mean of the expected abundance and shading gives some point-wise credible intervals. Values greater than one in right plot imply greater abundance inside the CMR. Histogram and smoothed density are taken from the posterior samples. Dashed red vertical line is the mean estimate. ....	70
Figure 59. Depth (left) and protection (right) effects on abundance of morid cods. Solid line in left plot is the mean of the expected abundance and shading gives some point-wise credible intervals. Values greater than one in right plot imply greater abundance inside the CMR. Histogram and smoothed density are taken from the posterior samples. Dashed red vertical line is the mean estimate.....	71
Figure 60. Depth (left) and protection (right) effects on abundance of striped trumpeter ( <i>Latris lineata</i> ). Solid line in left plot is the mean of the expected abundance and shading gives some point-wise credible intervals. Values greater than one in right plot imply greater abundance inside the CMR. Histogram and smoothed density are taken from the posterior samples. Dashed red vertical line is the mean estimate.....	71
Figure 61. Depth (left) and protection (right) effects on abundance of draughtboard shark ( <i>Cephaloscyllium laticeps</i> ). Solid line in left plot is the mean of the expected abundance and shading gives some point-wise credible intervals. Values greater than one in right plot imply greater abundance inside the CMR. Histogram and smoothed density are taken from the posterior samples. Dashed red vertical line is the mean estimate.....	72
Figure 62. Depth (left) and protection (right) effects on mean size of jackass morwong ( <i>Nemadactylus macropterus</i> ). Solid line in left plot is the mean of the expected size and shading gives some point-wise credible intervals. Values less than zero in right plot imply smaller fish inside the CMR. Histogram and smoothed density are taken from the posterior samples. Dashed red vertical line is the mean estimate.....	72
Figure 63. Depth (left) and protection (right) effects on mean size of ocean perch ( <i>Helicolenus percoides</i> ). Solid line in left plot is the mean of the expected size and shading gives some point-wise credible intervals. Values less than zero in right plot imply smaller fish inside the CMR. Histogram and smoothed density are taken from the posterior samples. Dashed red vertical line is the mean estimate.....	73
Figure 64. Depth (left) and protection (right) effects on mean size of morid cods. Solid line in left plot is the mean of the expected size and shading gives some point-wise credible intervals. Values less than zero in right plot imply smaller fish inside the CMR. Histogram and smoothed density are taken from the posterior samples. Dashed red vertical line is the mean estimate. ....	73
Figure 65. Depth (left) and protection (right) effects on mean size of striped trumpeter ( <i>Latris lineata</i> ). Solid line in left plot is the mean of the expected size and shading gives some point-wise credible intervals. Values greater than zero in right plot imply larger fish inside the CMR. Histogram and	





---

smoothed density are taken from the posterior samples. Dashed red vertical line is the mean estimate..... 74

Figure 66. Depth (left) and protection (right) effects on mean size of draughtboard shark (*Cephaloscyllium laticeps*). Solid line in left plot is the mean of the expected size and shading gives some point-wise credible intervals. Values less than zero in right plot imply smaller fish inside the CMR. Histogram and smoothed density are taken from the posterior samples. Dashed red vertical line is the mean estimate..... 74

Figure 67. Depth (left) and protection (right) effects on the abundance of large-sized jackass morwong (*Nemadactylus macropterus*). Solid line in left plot is the mean of the expected abundance of large-sized fish and shading gives some point-wise credible intervals. Values greater than one in right plot imply greater abundance of large-sized fish inside the CMR. Histogram and smoothed density are taken from the posterior samples. Dashed red vertical line is the mean estimate..... 75

Figure 68. Depth (left) and protection (right) effects on the abundance of large-sized striped trumpeter (*Latris lineata*). Solid line in left plot is the mean of the expected abundance of large-sized fish and shading gives some point-wise credible intervals. Values greater than one in right plot imply greater abundance of large-sized fish inside the CMR. Histogram and smoothed density are taken from the posterior samples. Dashed red vertical line is the mean estimate. .... 75

---

## List of Tables

Table 1. Bycatch of associated with lobster potting using research pots with no escape gaps in the Tasman Fracture CMR and adjacent fished reference locations.	25
Table 2. Summary of model outputs contrasting protection and depth effects on the lobster population in and around the Tasman Fracture CMR. Note probabilities are Bayesian probabilities (from 0 to 1) of each effect. Values >0.95 or <0.05 are considered statistically strong. Values >0.8 or <0.2 indicate increasing strength of the trend. * denotes statistically important result.	28
Table 3. Total observations and percentage contribution of morphospecies and bare substrate type observed in the Tasman Fracture CMR using the AUV.	37
Table 4. PERMANOVA pairwise comparisons indicating significantly different assemblages between CMRs.	47
Table 5. Average morphospecies assemblage similarity within/between CMRs produced by the PERMANOVA pairwise routine. A value of 0 suggest no similarity, while a value of 100 suggest identical morphospecies assemblage.	48
Table 6. Similarity percentages (SIMPER) results highlighting the dominant morphospecies within each CMR.	49
Table 7. Fish species recorded using BRUVs in the Tasman Fracture CMR and adjacent fished areas based on 92 deployments. Relative abundance was measured using MaxN.	52
Table 8. Mean fish length (mm) for selected fish species. The minimum and maximum lengths are provided in parenthesis. Note not all fish were measured thus the addition of number measured column.	60
Table 9. Summary of model outputs contrasting protection and depth effects on fishes in and around the Tasman Fracture CMR. Note probabilities are Bayesian probabilities (from 0 to 1) of each effect. Values >0.95 or <0.05 are considered statistically strong. Values >0.8 or <0.2 indicate increasing strength of the trend. For abundance the CMR effect is a multiplicative on a response scale. For average size the CMR effect is additive on a response scale. * denotes statistically important result.	68



## EXECUTIVE SUMMARY

The Tasman Fracture Commonwealth Marine Reserve (CMR) is the southernmost CMR within the Australian CMR network in continental waters. The Tasman Fracture CMR, as part of its zoning arrangements, includes a no-take zone on the continental shelf. This is the only area of continental shelf habitat included within the south-eastern CMR network that completely prohibits fishing activities through the establishment of a Sanctuary Zone. Despite being protected for over 7-years, little was known about the range of habitats and associated biological diversity occurring on the shelf waters within this CMR, or the extent that protection had influenced the biota of the CMR. In this study, we take a multi-step approach to first identifying the types and distribution of benthic habitats within, and adjacent to the CMR, and then focussing on reef habitat, to use a range of biological sampling tools to describe the associated reef biota. These surveys included contrasts of the biota in, and adjacent to the no-take zone, to determine the extent that the biota may have responded to the 7 years of protection within the CMR. Reef habitat was targeted due to its overall greater species diversity than adjacent soft sediments, and this habitat was known to be actively targeted by fishing activities, including those for southern rock lobster.

In the first phase, an extensive multibeam sonar mapping program provided the first fine-scale 3D survey of the seafloor structures that characterise the Tasman Fracture CMR sanctuary zone and a range of nearby unprotected reference locations on the shelf. Mapping suggests that for rocky reef habitat, most reef systems within the vicinity of the CMR are extensions of coastal features and grade to sediment at depths of around 100 m, with little further extension across the shelf. Within the sanctuary area of the CMR, the reef systems extended to depths of 140 m, but despite extending to greater depths than nearby areas, still only comprise a small part of the overall habitat distribution in the area mapped. These reefs were typically restricted to the NW margin of the sanctuary zone or as part of the western extension of a coastal reef system that extends out from the Mewstone (a small rocky island). A notable exception to this is an isolated reef in the mid NE zone of the CMR to the east of the Mewstone, extending from depths of 80 m to 140 m.

In the second phase of sampling, biological surveys were undertaken using lobster pots for lobsters and lobster fishery bycatch, Baited Underwater Video for sampling fish assemblages, and an Autonomous Underwater Vehicle (AUV) to photographically sample the sessile biota (corals, sponges etc). As well as providing a sound baseline inventory of the typical reef associated species, the sampling program was based on a strong model-based approach. This allowed for quantitative estimates to be derived for the abundance and distribution of southern rock lobsters and reef-associated fish, and for these to be contrasted between the CMR and adjacent fished areas.

Model-based analyses suggest there are significantly more lobsters within the CMR than adjacent fished areas, however, the drivers of this require further investigation. The results suggest that this is in part due to higher proportion of females, that despite rarely reaching legal size in this region, may be subject to capture related mortality in the fishery. For fishes,



several species showed protection-related increases in abundance, including striped trumpeter, jackass morwong, ocean perch and Morid cods. For striped trumpeter and jackass morwong this included increases in the abundance of large, legal-sized individuals. Such changes are not unexpected given the CMR sanctuary zone has been protected from fishing for over 7 years in an area subject to heavy fishing pressure for lobsters in particular.

Due to logistical constraints the AUV survey was restricted to two reef systems within the NW sector of the CMR. Despite the less than planned for coverage, the survey covered several km of reef from 100 m to 140 m depth, providing more than sufficient imagery to characterise the benthic biota of these reef systems. Notable features of this survey were an abundance of brittle stars and a dominant cover of soft corals, that differed markedly from the typical sponge dominated cover seen at these depths within cool-temperate waters. These features appear to be unique to the Tasman CMR when compared to the benthic invertebrate assemblages recorded from previous AUV surveys in the Huon, Freycinet and Flinders CMRs, and illustrates that each CMR represents a distinctly different component of benthic biodiversity.

The results from this study provide considerable new insights into the ecosystem functioning of the deep reef systems of southern Tasmania, and the extent that no-take protection can alter lobster and fish abundances. The overall abundance of lobsters suggests they may play a significant ecological role, while the abundance of brittle stars and soft corals suggest a detritus-driven trophic pathway that differs from that found in the more typical sponge-dominated systems in SE Australia. However, as this was a “snapshot” study, results relating to protection effects need confirming through a time-series to fully differentiate protection-related differences from those relating to spatial differences. Likewise, due to overall differences in the depths able to be sampled between the CMR and reference areas (relating to a lack of mapped reef below 120 m outside the Tasman Fracture CMR to allow for a fully balanced sampling design) this study required model-based designs to allow us to both derive a spatially-balanced survey of the reef systems, as well as contrast changes with adjacent fished areas. We recommend that a similar study be undertaken at a biologically meaningful interval (approximately 5 years), and that in the intervening period, suitable reference reefs at depths of between 120-160 m be identified and mapped as a priority to allow depth stratified sampling to be undertaken in the future to more robustly differentiate depth related and protection related effects.



# 1. INTRODUCTION

The Tasman Fracture Commonwealth Marine Reserve (CMR) is the southernmost CMR within the Australian CMR network in continental waters, and was established as part of the south-eastern CMR network, the first phase of national CMR representation being progressed by the Australian government. The SE CMR network was established for over a period of seven years, with declaration resulting in a range of levels of protection being established within the CMRs as part of the management process. The Tasman Fracture CMR was one of the relatively small areas in the SE CMR network that fully closed an actively fished area on the continental shelf through the establishment of a sanctuary area within the CMR boundary. As research in coastal Tasmanian reserves indicates that target species such as southern rock lobster and striped trumpeter may recover significantly in 7-years following protection, it is timely to assess the extent of similar changes associated with CMR closure, to provide initial feedback on the effectiveness of such management strategies and an understanding of the biological processes occurring. At the same time, the surveys in the current project will also provide the opportunity to develop an initial baseline understanding of the shelf reef habitats within the reserve, and the typical species assemblages associated with them, as well as applying survey and statistical methods developed during National Environmental Research Program (NERP) Marine Biodiversity Hub research projects examining methods for inventory and monitoring of CMRs in offshore waters.

Results evaluating the effectiveness of closures will potentially support the next stage of CMR management plans for areas outside the SE CMR network, as well as informing development of monitoring and inventory projects within the CMR network in general. Overall, the work further contributes to our currently limited understanding of the biodiversity assets of the shelf component of the CMR network in this region, provides a baseline for future monitoring of key habitats and species in the shelf region of the Tasman Fracture CMR, and provides an initial assessment of the extent that sanctuary protection has altered the abundance of targeted species or the ecosystems that support them.

We proposed a survey period including the equivalent of 20 days of at sea fieldwork, which balances the expense of at-sea related research, with the need to take a multi-stage approach to data acquisition and processing, as well as subsequent analysis and reporting. The proposed duration and costs of overall ship-time, field costs and staff time associated with planning, deployments, analysis and reporting were based on costs associated with a similar survey within the Flinders CMR as part of NERP Hub research within the region, and include a considerable in-kind contribution from Hub partners involved, including CSIRO, University of Tasmania (IMAS), IMOS (via the AUV facility) and Geosciences Australia. This report summarises the results of the four phases of this study, including a 5-day multibeam sonar mapping program (equivalent to 8 days due to 24 h mapping while on-station), a 5-day rock lobster potting program, a 6-day AUV survey program, and a 5-day baited underwater stereo video (BRUV) survey of the benthic fish fauna of the CMR.



Objectives for this study were:

1. Map seafloor topography within the northern shelf region of the Tasman Fracture CMR and adjacent fished areas.
2. Contrast the lobster population structure between the CMR and adjacent fished areas based on potting survey.
3. Compare seafloor benthos assemblage structure between the CMR and adjacent fished areas based on imagery obtained from an autonomous underwater vehicle (AUV).
4. Contrast demersal fish population structure between the CMR and adjacent fished areas based on baited remote underwater stereo video stations (BRUVS).

The multibeam data will be retained by the Marine National Facility (CSIRO). The AUV and BRUV data will be retained by IMAS. The AUV imagery is available on Squidle web portal (<https://squidle.acfr.usyd.edu.au/>), with scored data being uploaded to the IODN web portal. All data are available upon request. All metadata associated with the project is available on the AODN web portal.



## 2. FINDINGS

### 2.1 Seabed mapping

The first phase of this study was focussed on surveying the seafloor complexity to identify the extent that rocky reef is found on the shelf in the sanctuary zone of the Tasman Fracture CMR. This was done to provide an inventory of the extent of the reef systems, but also have detailed maps of reef location such that we could plan our more targeted biological sampling. In addition, the work focussed on mapping some similar reef systems in areas adjacent to those found in the CMR, such that biological assemblages in the CMR could be contrasted with typical fished habitat within this region. We targeted the mapping and survey effort on reef systems as these were perceived *a priori* to have been likely to have been subject to greater fishing effort than other habitats prior to protection, and therefore show the most marked changes following closure.

Survey planning was guided by knowledge obtained over the past decade as a result of multibeam sonar (MBS) survey lines undertaken by the research vessel *Southern Surveyor* while either on targeted surveys or on transits through the area. These survey lines were obtained using deep-water MBS that, while lacking the fine-scale resolution at shelf depths necessary to produce detailed maps for biological survey planning, still provide sufficient information to identify major reef systems and features. This prior mapping (Figure 1) indicated that reef systems were primarily clustered around the north western margin of the reserve, with some indication from backscatter signals that additional hard bottom may be found in the north eastern sector as well, but with little evidence of substantive reef found further south across the shelf until the shelf-break is reached.

Our mapping therefore targeted the northern sector on the sanctuary zone to both map all known reef systems in this region, as well as produce a full coverage map to identify the full range of habitat features present for future research and management purposes. Mapping was undertaken from the Australian Maritime College (UTas) vessel *Bluefin* on an at-cost charter to the NERP Hub. This vessel, at 35 m in length, is suitable for 24 h operations at sea under moderate weather conditions, so cruise planning incorporated 24 h/day mapping. The MBS mapping was obtained by the Kongsberg 2040C sonar system of CSIRO's, and operated by the Marine National Facility mapping staff who completed all post-processing to remove artefacts. Post-processing of acquired data was undertaken in Caris.

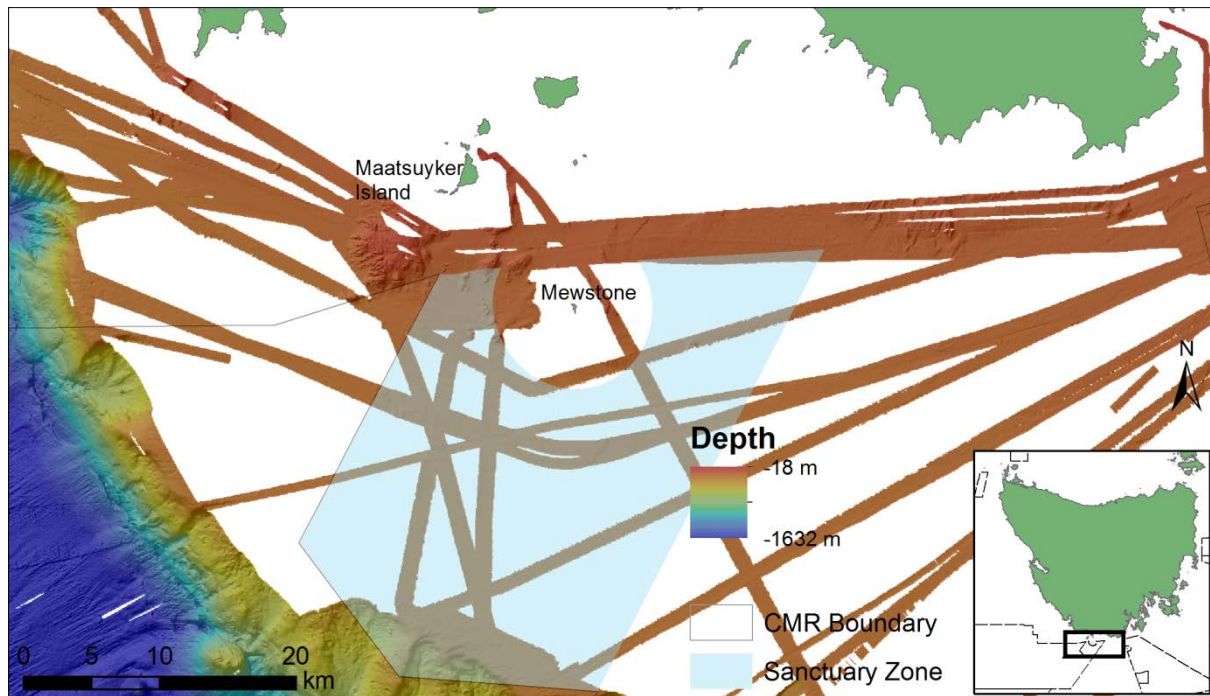


Figure 1. Previous multibeam sonar coverage (at 50 m resolution) of the Tasman Fracture CMR seabed features on the shelf and slope.

The MBS mapping undertaken over 2 x 24h days within the CMR, starting from the NW corner. Several initial east-west passes contained some residual heave in the mapping outputs due to a 3 m swell, however, underway adjustments to the equipment settings allowed these artefacts to be mostly removed from subsequent passes, resulting in high quality map products to be obtained despite the persistent swell and sea-state. At the completion of 2 x 24 h days mapping within the CMR, mapping provided full coverage of the area extending from the northern boundary southward to approximately 2 km below the incision around the Mewstone rock (Figure 2a). At this stage it was evident that finding reef outcrops further south was increasingly more unlikely, and soft sediment features had become homogenous due to increasing depth, so mapping effort switched to focus on obtaining suitable reference reef habitats in adjacent fished areas at matching depth and substrate complexity. These efforts were guided by regional availability of hard substrata identified by the previous surveys aboard the *Southern Surveyor*, and included reef south and west of the Mewstone, north and NW of the NW sanctuary zone boundary, 5 km offshore from South Cape and 5 km offshore from South East Cape (Figure 2a). Note, since the *Bluefin* MBS mapping survey the *R.V. Investigator*, while transiting the region has MBS mapped a larger portion of the CMR out to the shelf break (Figure 2b). Visual inspection of this new mapping data from the *R.V. Investigator* transits has revealed that region south of the Mewstone is largely devoid of any significant high-relief reef systems.





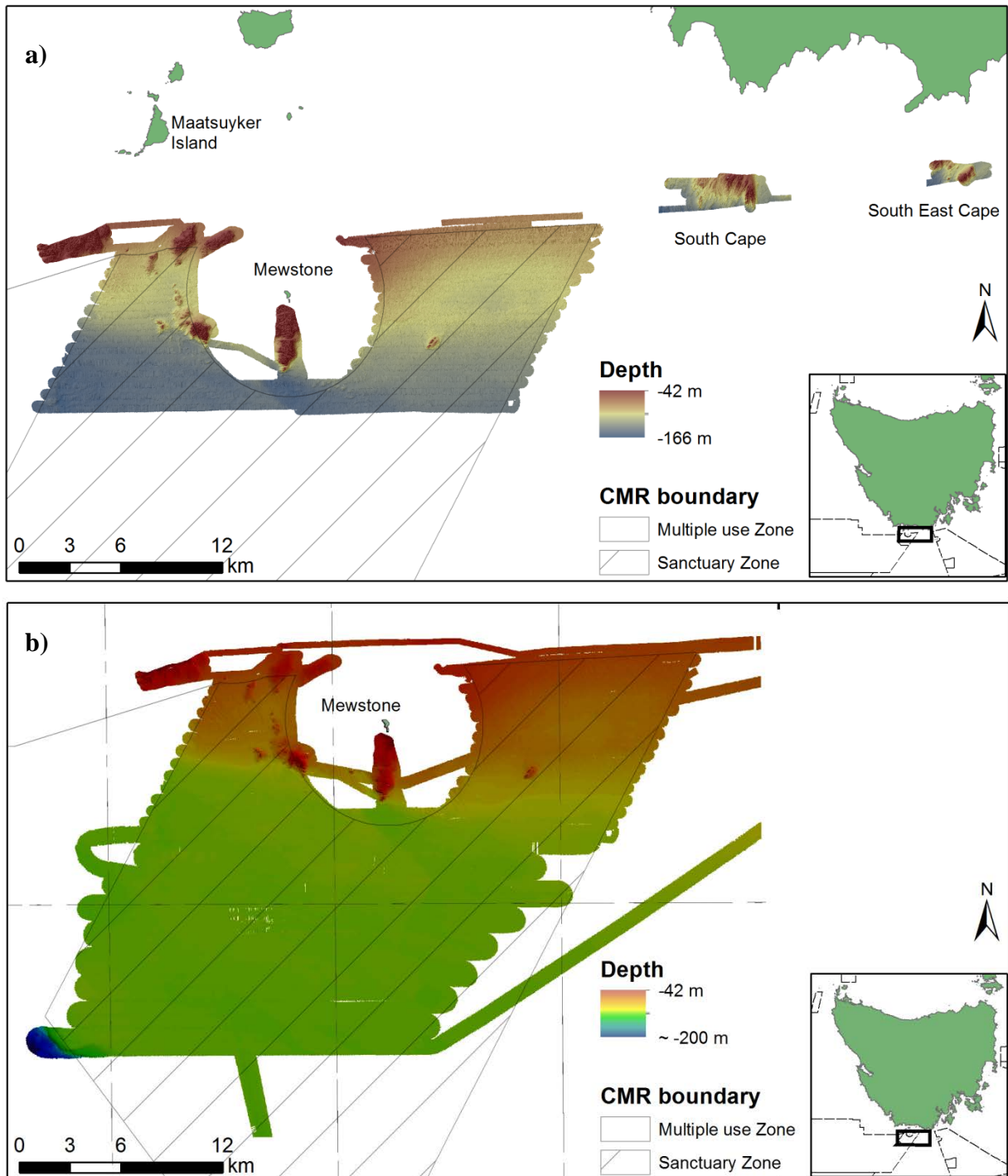


Figure 2. Overview of the area mapped in fine detail in 2014 via *R.V. Bluefin* as a part of the current project (a) and more recently in 2015 (b) a southern addition to this by CSIRO staff on *R.V. Investigator* sea-trials. The maps indicate the extent of reef systems within the shelf component of the Tasman Fracture CMR sanctuary zone and adjacent control regions, with reefs indicated by regions of raised topography.

In all of the areas mapped, most of the reef systems appear to grade to sediment at depths of around 100 m with little further significant extension of significant reef systems across the shelf (Figure 2b). This possibly corresponds to historical sea-level stands where wave action during glacial periods has eroded the deeper reef systems that have subsequently become

inundated with sand/sediment. At depths of up to 130 m the sand/sediment appears to be sculpted by either wave exposure or strong currents or both (Figure 5), however, beyond this depth, extending across the shelf such structuring actions appear to cease and the seabed sediments are relatively featureless.

### 2.1.1 Tasman Fracture CMR sanctuary zone

Within the sanctuary area of the CMR, the exposed reef systems only comprise a small part of the overall habitat distribution in the area mapped (Figure 3). These are generally restricted to the NW margin of the sanctuary zone or as part of the western extension of the coastal reef system that extends out from the Mewstone, a large rocky island surrounded by State waters (Figure 3).

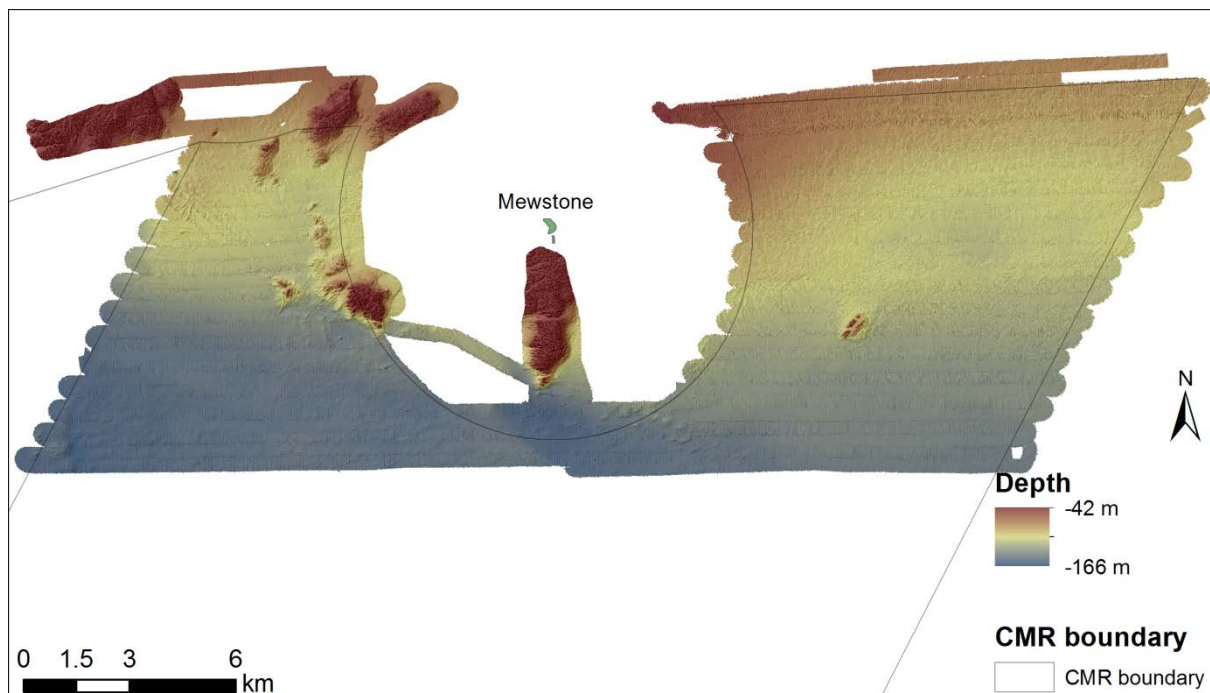


Figure 3. Overview of the Tasman Fracture sanctuary zone shelf area mapped in fine resolution during the survey.

The one exception to that is an isolated reef shown here in the mid NE zone of the CMR to the east of the Mewstone (Figure 4). This reef is approximately 1 km in length and is reasonably high profile, rising from the seabed in approximately 140 m to a top of around 90 m (Figure 4). In addition to being an isolated feature it is also the deepest reef habitat mapped within the area surveyed. Given its isolation, this will be a central target of subsequent phases of fieldwork given it may be also the most protected component by way of that isolation. Discussions with commercial lobster fishermen who worked this area prior to establishment of the CMR indicate it was well known to them and occasionally fished as productive bottom. Unfortunately, no matching reefs at similar maximum depths (140 m) were mapped as part of surveys for external reference reef systems. This was primarily because no such features were indicated for this region, either from navigation charts or previous MBS transits, to inform targeted mapping, and if present, finding such features by



survey of adjacent fished areas would be beyond the time available for this component of the study.

Other notable features within the sanctuary zone include distinct sand-wave formations in the mid-western zone (Figure 5). These seabed dune features indicate that a possible mix of large oceanic swells and strong currents sweeping around southern Tasmania are still able to shape seabed features at depths from 120-140 m. A particular feature of this area is the presence of linear striations extending from the western boundary in an east to SE direction (Figure 5) that could possibly be relict benthic trawl marks through these sediments that have yet to be obscured by sediment movement. Some discussion with trawl fishermen who operate in this region is necessary to determine if the pattern follows typical trawl depths and directions in such habitats. An AUV mission across these tracks was planned to both define the nature of the dune systems as well as examining whether the faunal composition of the “tracks” differ in any way from the surrounding substrata. These missions are discussed later in the report.



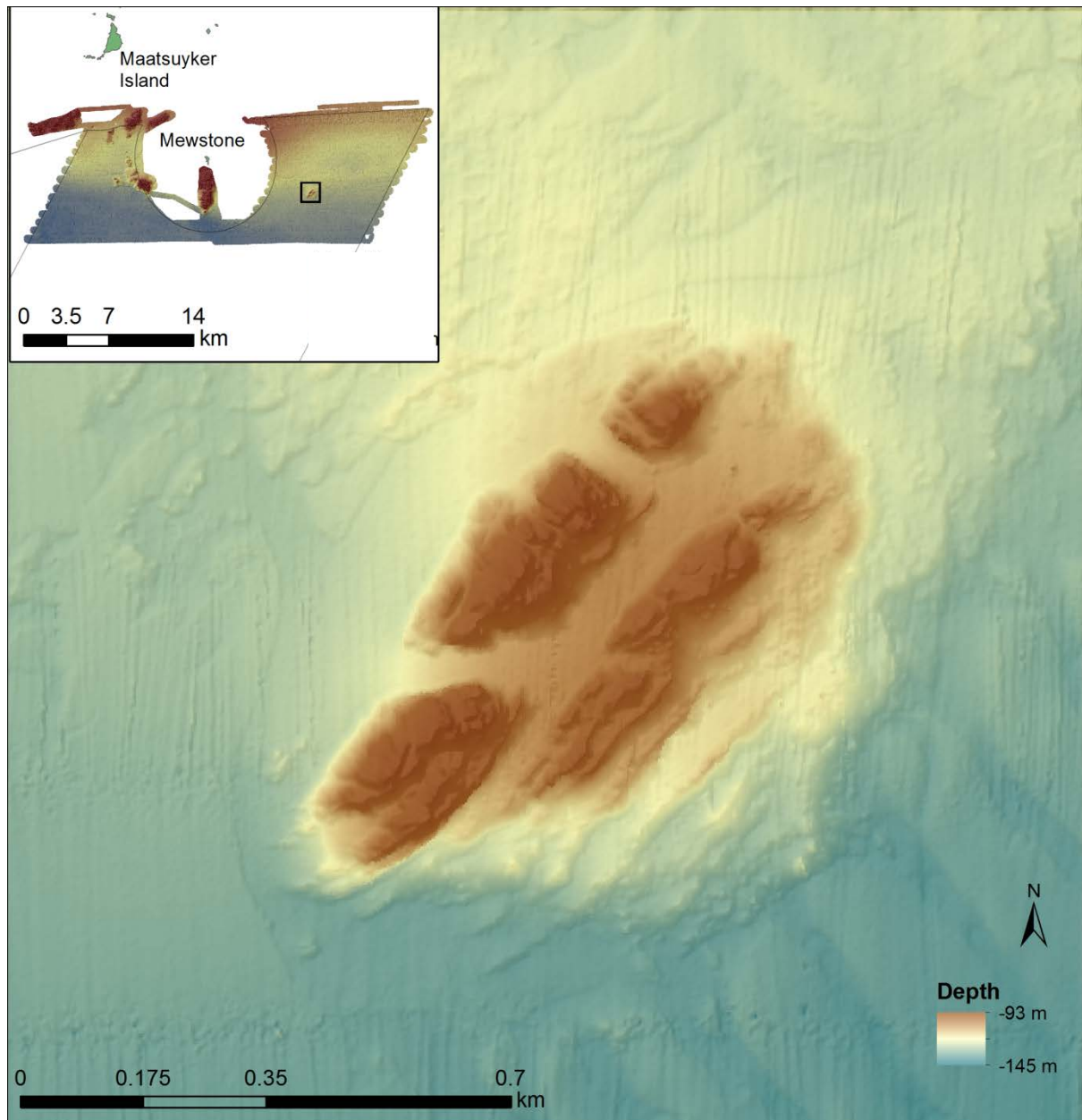


Figure 4. The isolated patch reef that provides the most defining feature of the eastern sector of the sanctuary zone.



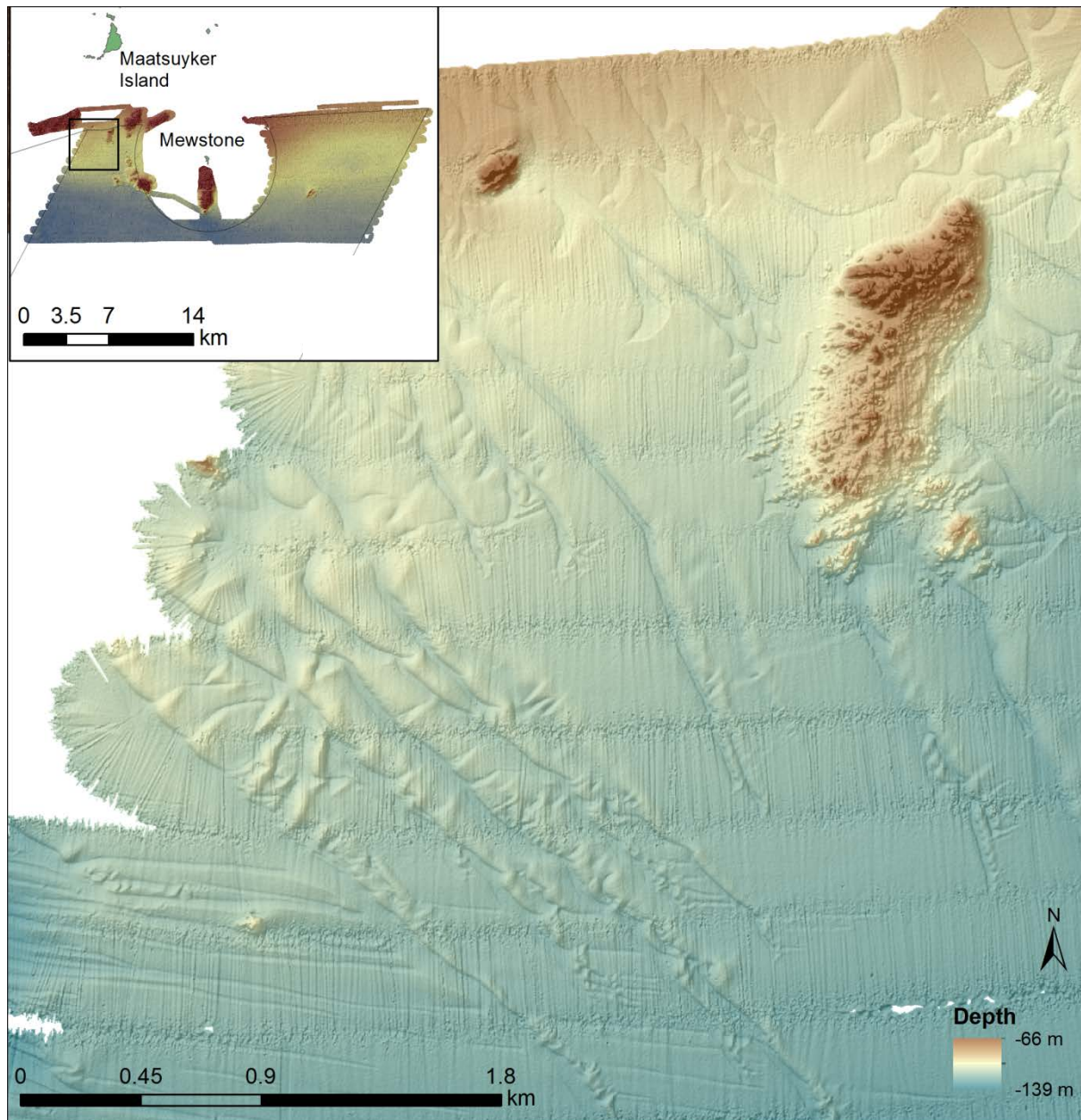


Figure 5. Extensive dune systems in the NW region of the sanctuary zone of the Tasman Fracture CMR, indicating a region of sediment mobilisation due to swell or current action. Note the parallel linear striations running west-east in the lower mapped area that could represent historical trawl tracks.

The final notable feature of the mapped region within the CMR was an extensive area of hummocky seabed in the NE region (Figure 6). This seabed feature corresponded to a region of “hard-bottom” identified from backscatter processing of historical MBS transits through the area. Examination of the backscatter of the new fine-scale MBS data (Figure 6) revealed a uniquely mottled backscatter pattern that was suggestive of an area of extensive cross-cutting gravel hummocks or cobble beds that are structured by large swell events and/or strong currents at these depths. As part of a trial of the effectiveness of BRUVs at such depths during the recent lobster potting survey, five BRUVs were deployed on the seabed within this area for initial ground-truthing (Figure 7). These revealed that these



seabed features were a relatively complex combination of sandy dune features, gravel/cobble beds, and isolated low profile reef patches (Figure 7).

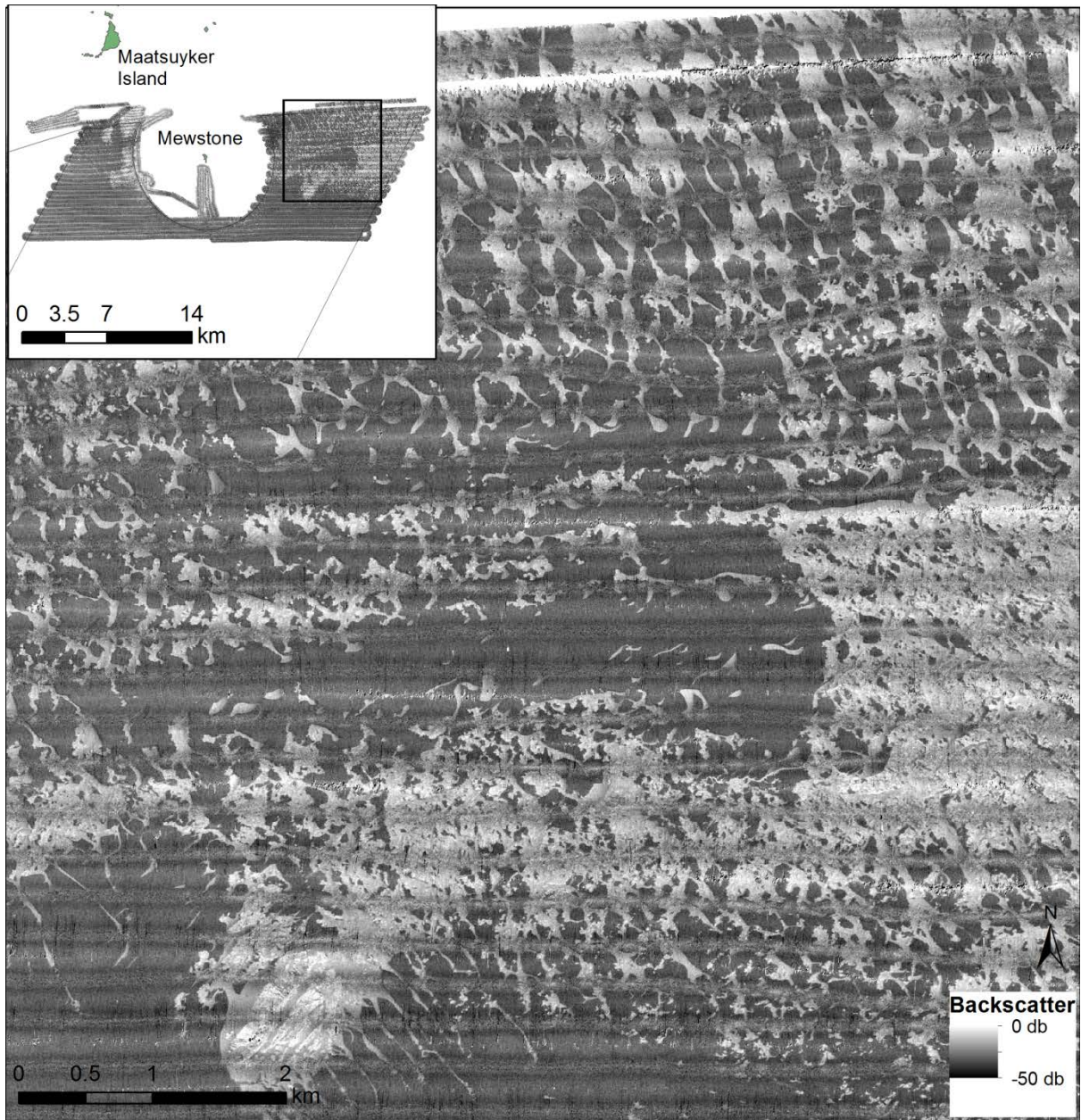


Figure 6. Multibeam backscatter map of the Tasman Fracture CMR sanctuary zone. Darker shading generally represents areas of greater “hardness”. The insert shows the unusual mottled nature of the NE section of this zone.



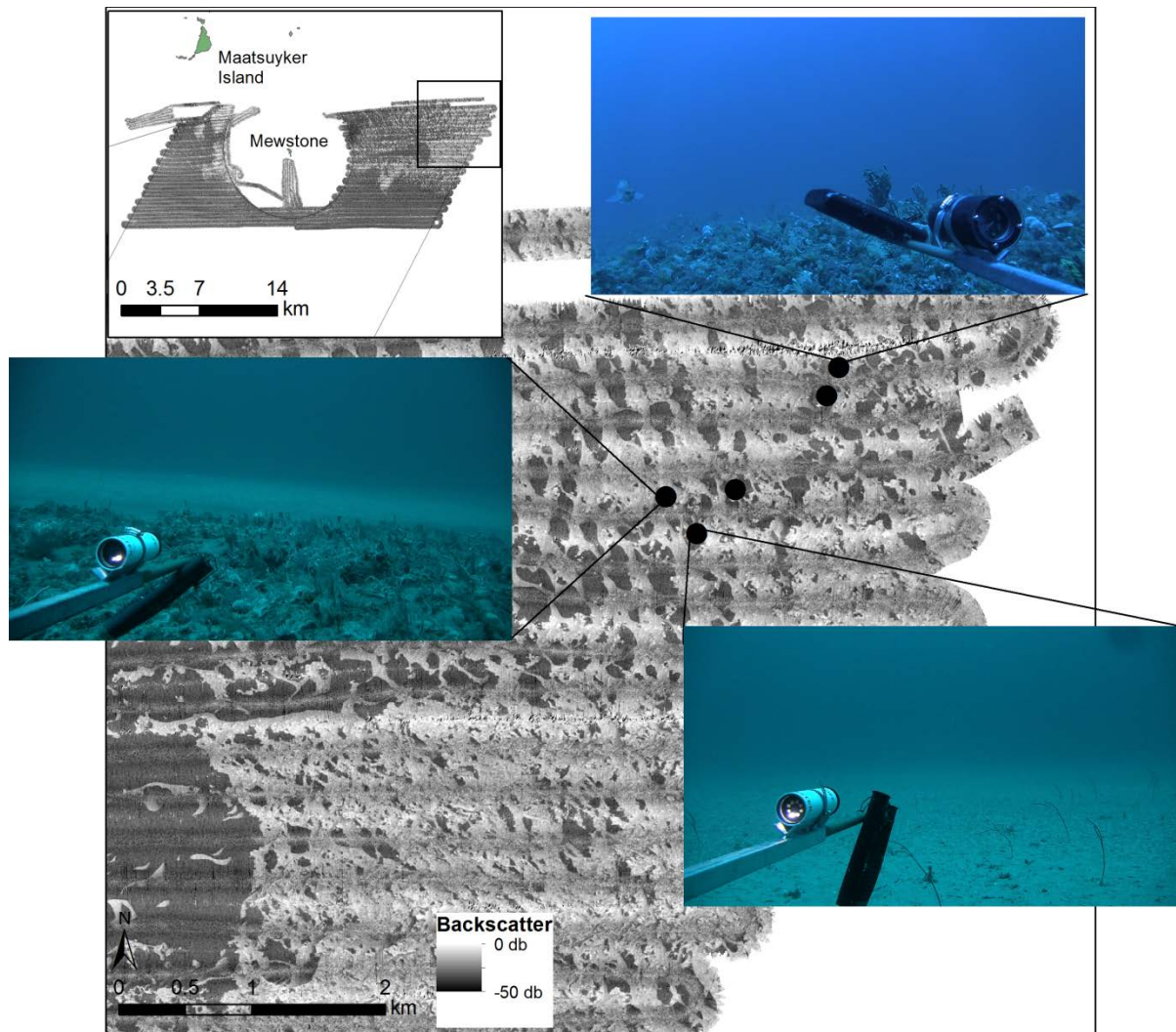


Figure 7. Extensive cross-bedded features typify the NE section of the Tasman Fracture sanctuary zone and have a characteristic “hard” backscatter signal (see Figure 6) that appear to be primarily comprised of sediment/gravel/cobble inundated low profile reef (as evident by the BRUV drops in the region (see inserts) rather than being purely sedimentary features.

### 2.1.2 Reference sites

As discussed previously, a range of external fished reference locations were mapped throughout the region to match as closely as possible with the depth and reef complexity found within the CMR sanctuary zone (Figure 2). Several of these were cross-boundary continuations of reef systems that were mapped within the CMR, including the significant system west of the Mewstone and reef systems extending across the NW boundary (Figure 8). These systems not only provide close-proximity reference sites of similar reef structure and depth, but will also provide the opportunity to examine boundary effects relating to fishing activity and target species mobility. To ensure that reference locations were representative of the regional fishery, and were likely to be “known” to a range of fishing vessels, the mapped control reefs included systems identified nearby off South Cape and South-east Cape (Figure 9, Figure 10). Both these reef systems included the known offshore extensions of major offshore reef systems associated with South and South-east Capes



respectively, and their approximate outer boundaries were known from deeper tracks mapped by *Southern Surveyor* during transits of the area. Both reef systems generally have similar complexity to reefs found within the CMR sanctuary zone. However, a notable exception includes the far eastern portion of the South Cape reef system, which contains a more complex boulder bottom readily seen in Figure 9. We anticipate that this differing complexity may support differing lobster densities; hence work within such locations not only acts as to better inform the relative magnitude of changes within the CMR, but also informs fishery management about the structural control of seabed type on lobster productivity and other natural resource attributes.

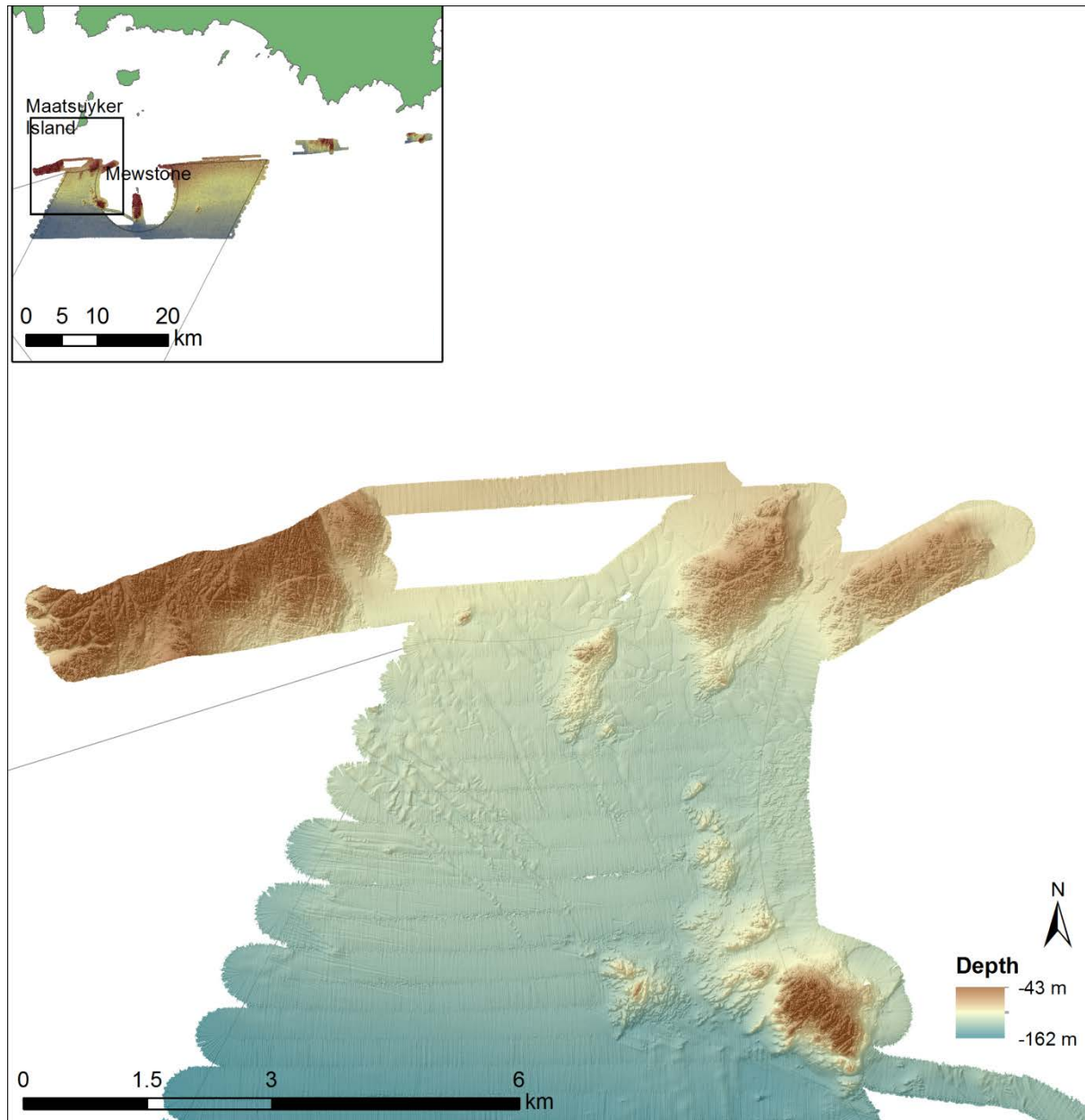


Figure 8. Reference reef habitat north-west of the Tasman Fracture CMR at depths similar to that found for reef habitat within the Tasman Fracture CMR.





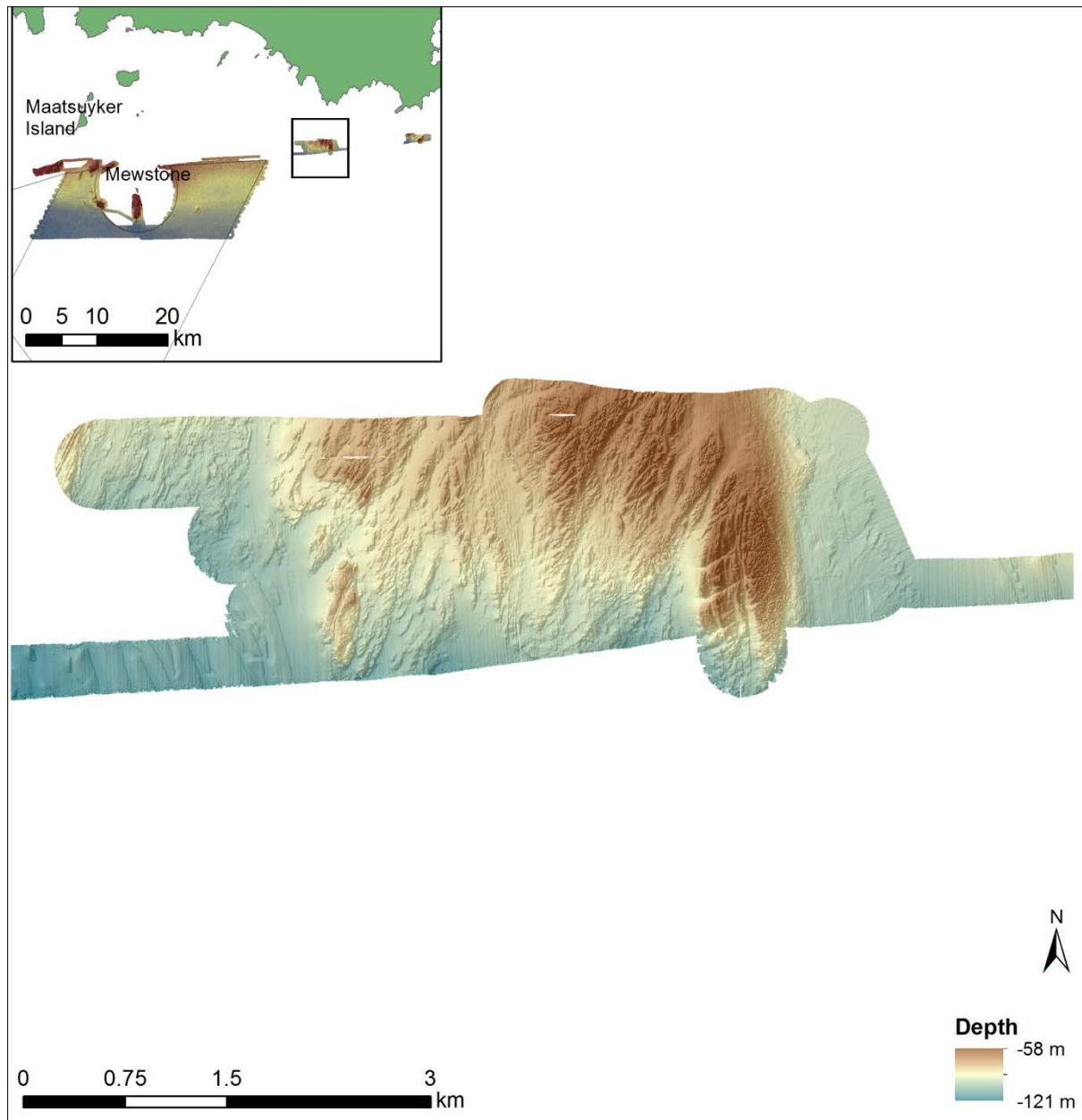


Figure 9. Reference reef habitat offshore of South Cape at depths similar to that found for reef habitat within the Tasman Fracture CMR.

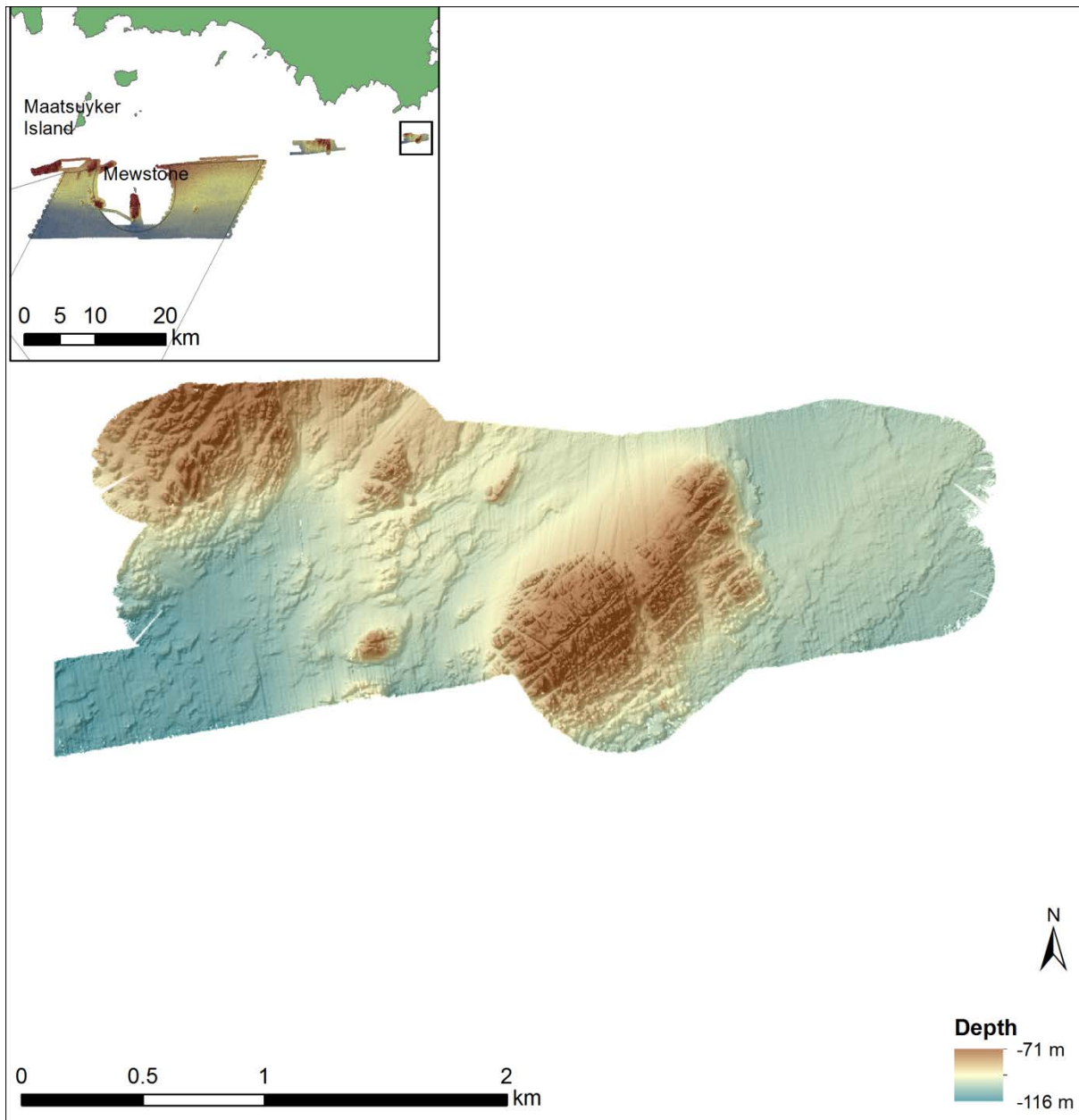


Figure 10. Reference reef habitat offshore of South East Cape at depths similar to that found for reef habitat within the Tasman Fracture CMR.

Overall, the mapping component of this study was highly successful. It indicated that the combination of a shelf-capable seagoing vessel such as the AMC (UTas) vessel *Bluefin*, capable of round-the clock operation in favourable weather and up to 3 m swells, and readily available MBS equipment and expert staff from CSIRO, was a particularly cost-effective combination for the essential task of mapping and inventory of CMR habitats across the shelf in remote areas.



## 2.2 Population trends of rock lobster

The aim of this component of the research was quantify the abundance, depth distribution and size distribution of lobsters within the no-take zone of the CMR and contrast these with patterns observed in adjacent fished reference habitats. Initial planning involved identification and selection of potential reef in the region based on the prior mapping. Reef outlines were manually digitised based on visual inspection of the MBS data. Any considerable within reef (internal) sand patches (>50 m scale) that may result in low or no captures if potted were also removed from this reef extent data. To ensure reference reefs were sampled at appropriate matching depths, depths shallower than that of the shallowest reef found within the CMR were also excluded from the survey design. The survey design involved a planned deployment of 200 scientific lobster pots (as used for all Tasmanian fishery assessment research) with no escape gaps, with 100 deployed within the CMR and 100 deployed at the reference sites (Figure 11). A statistically-based, spatially balanced design was used to *a priori* select the location of each pot deployment location and depth, such that model-based approaches could be used to derive a quantitative estimate of population sizes and distributions in the sampled areas.

The lobster potting fieldwork was undertaken between the 29 November and 3 December 2014 with an average of 50 pots set per night. Fieldwork was delayed for over a month from the initial planned date due to adverse weather in the highly exposed Tasman Fracture CMR region. All planned pot deployments were set on the location intended, resulting in over 30 km of line being set and retrieved over four nights of deployment.

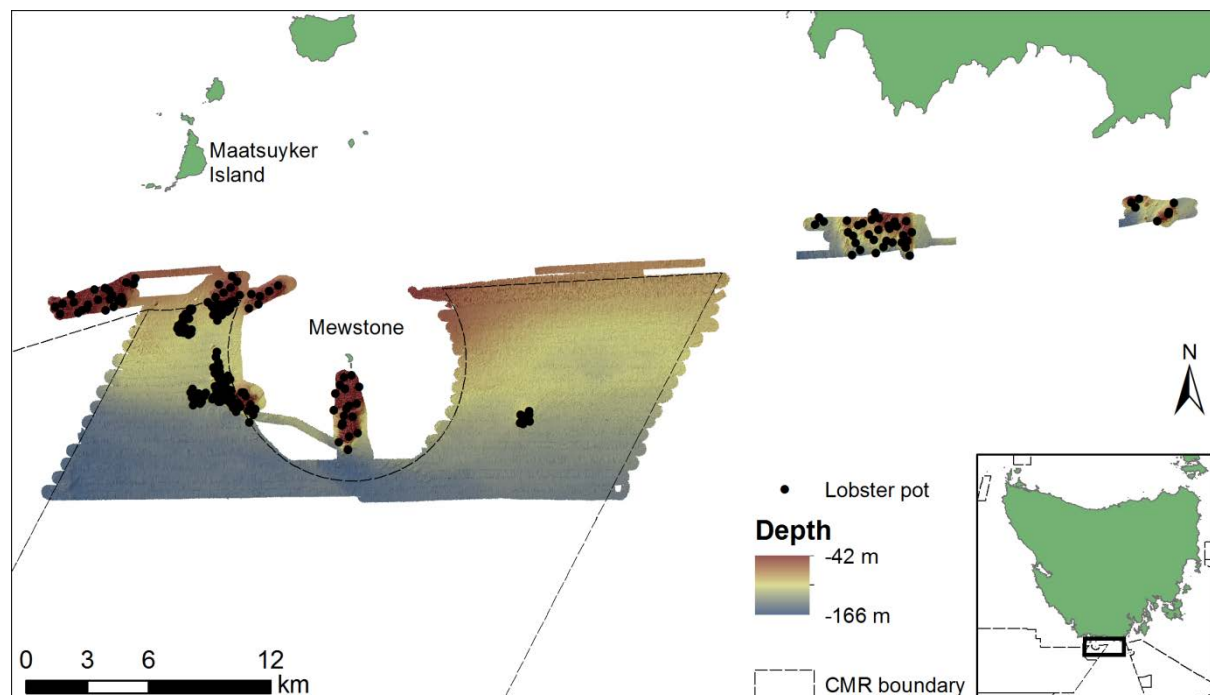


Figure 11. Location of the 200 lobster pots in the Tasman Fracture CMR and adjacent fished reference areas.



### 2.2.1 Descriptive patterns in lobster abundance

There was a marked discrepancy between capture rates within the CMR and the adjacent fished reefs (Figure 12). On average 3.5 lobsters were caught per pot in the CMR compared to 9.2 lobsters per pot within the fished locations, with a total of 1277 lobsters captured overall.

Spatial patterns in the catch data was assessed using the local Getis-Ord Gi statistic calculated using in the Spatial Statistics tool in ArcMap 10.0. This determined the areas with high and low values of CPUE, which were designated as hotspot (z-score > 1.65) and coldspot (z-score < -1.65) areas, respectively. This approach determines statistically significant local autocorrelation and dependence among neighbouring pots. The 675-m fixed distance band was chosen for hotspot analysis following the analysis of Moran's autocorrelation where this distance band resulted in high z-score values as an indication of clustering patterns in CPUE data.

Based on the hotspot analysis significant spatial clustering was observed in the distribution of lobster abundance data (Figure 13). Significant hotspots (represent high CPUE in red in Figure 13) were only recorded in reference sites (i.e. on the reefs NW west of the CMR and at South Cape). A significant coldspot (representing low CPUE in blue in Figure 13) was observed inside the CMR, indicating an area of low lobster abundance.

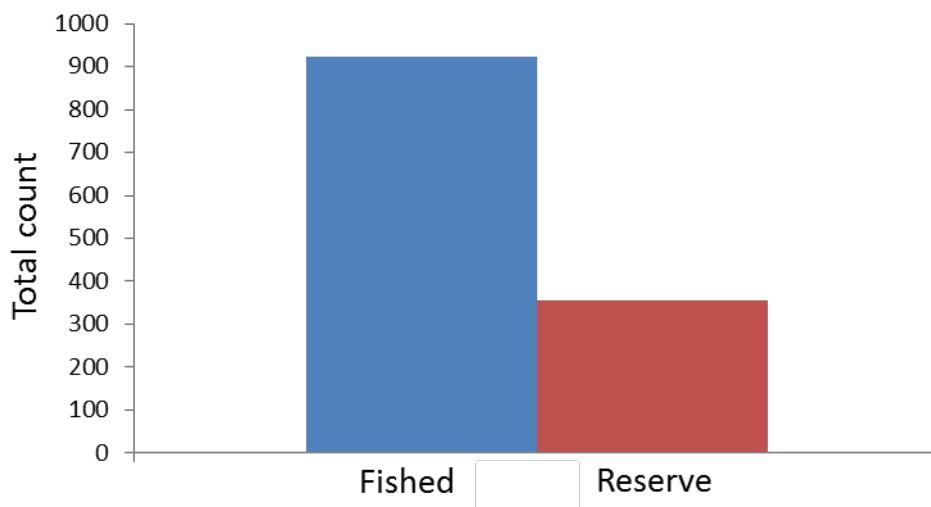


Figure 12. Total lobster counts from potting surveys within the Tasman Fracture CMR.



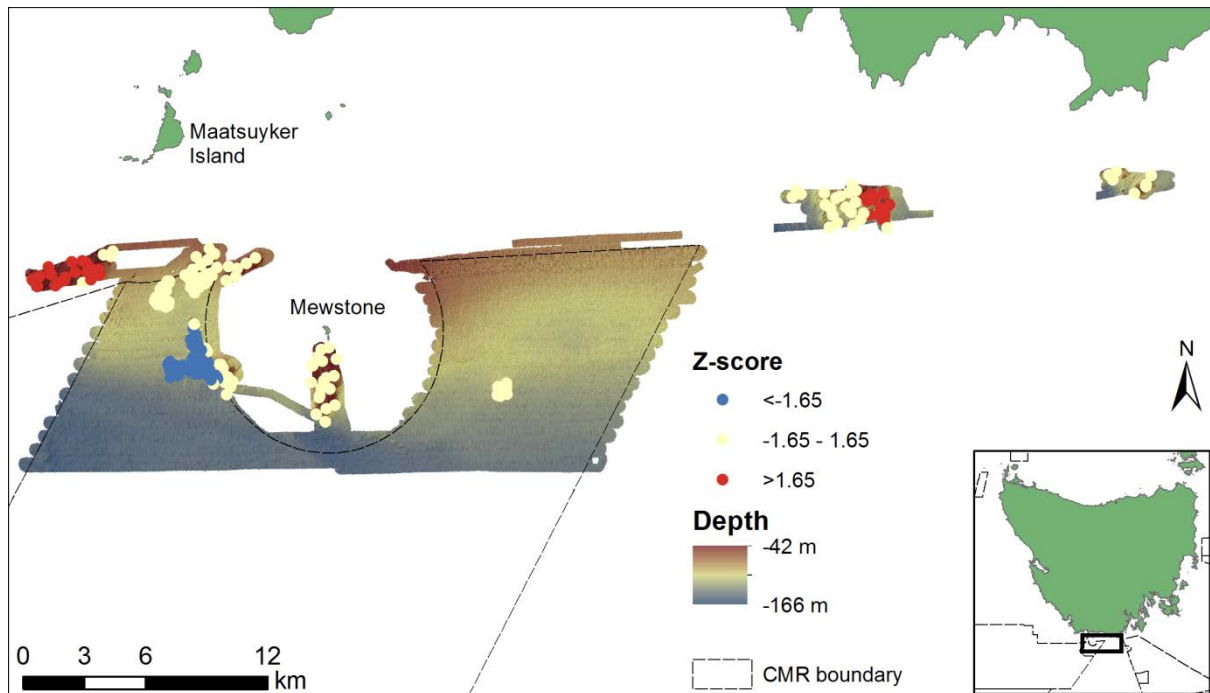


Figure 13. Hotspot analysis of CPUE distribution. Note the clustering of lower abundances (blue) of lobsters inside the CMR and the two clusters of high abundances in the reference sites (red).

### 2.2.2 Descriptive patterns in lobster size

There was also a marked difference in the ratio of legal size v's undersize male lobsters between the fished areas and the CMR (Figure 14), with legal sized males ( $> 110$  mm carapace length) representing 45 % of the catch in the CMR v's 18 % in the fished reference areas. For females, however, the story was very different. Irrespective of location very few females were legal size (7 % of the captured females within the CMR and only 2 % of the captured females within the fished reference locations; Figure 14). The growth rates of female lobster in this region are known to be extremely low. Therefore, the CMR offers no additional protection other than reduced capture-related mortality if potting effort is high within the fishery.



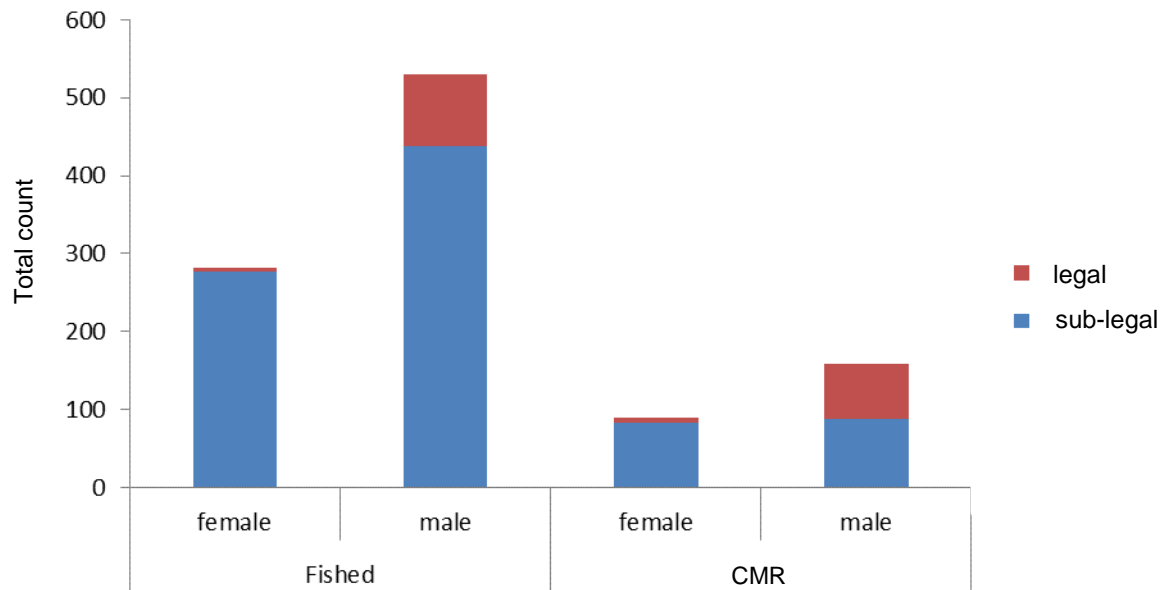


Figure 14. Abundance of legal sized vs sub-legal sized lobsters within fished and CMR reefs.

A hotspot analysis was also run on the size data to detect any significant clustering in large and small lobster. Similar to the abundance data, significant spatial clustering was observed in the distribution of male and female lobster abundance data (Figure 15, Figure 16). For male lobster size, significant hotspots of large lobster abundance (large lobsters in red in Figure 15) were recorded in the CMR on the bridging reef near the upper northwest boundary of the CMR, as well as on the isolated patch reef in the SE of the CMR, and on the reefs NW west of the CMR in the reference site. A significant coldspot (representing small lobsters in blue in Figure 15) was again observed inside the CMR, indicating an area of small lobsters on the reefs west of the Mewstone.

A similar pattern in clustering was observed for female lobster size (Figure 16). Notable differences can be observed on the isolated patch reef in the SE of the CMR, which had reduced clustering in large female lobsters. Interestingly the coldspot on the reefs west of the Mewstone was markedly smaller when compared to the male lobster hotspot analysis (Figure 16).



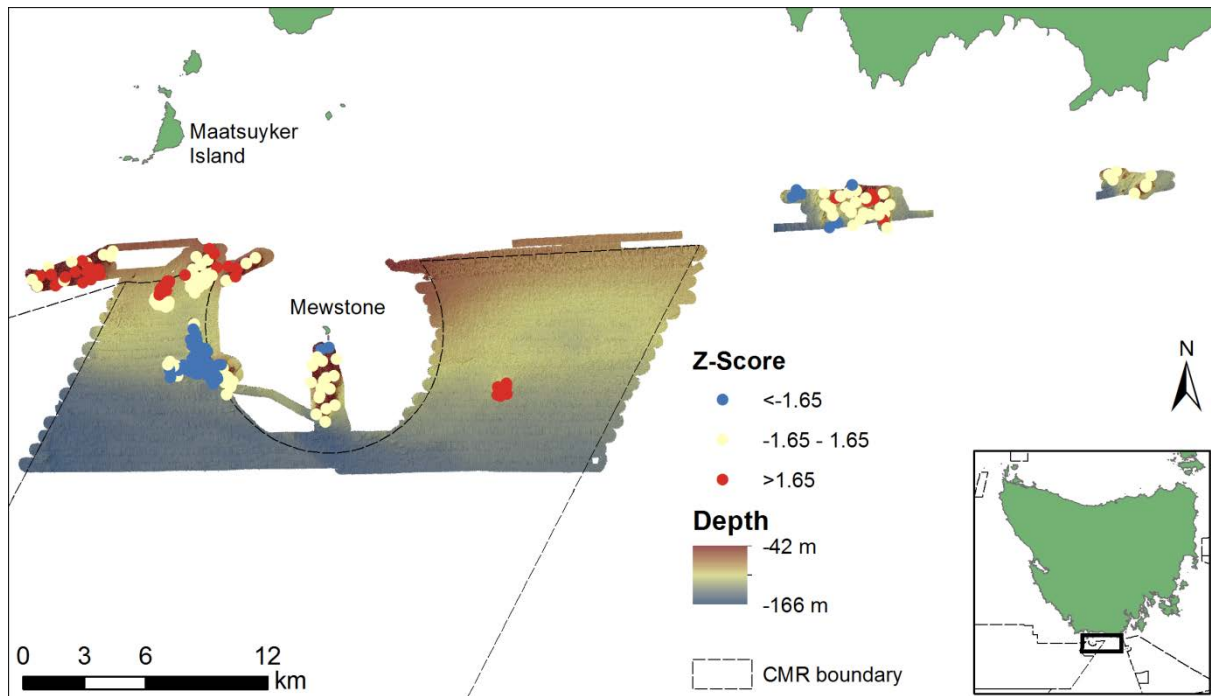


Figure 15. Hotspot analysis of size distribution of male lobster caught. Note the clustering of smaller size (blue) of lobsters inside the CMR and the three clusters of larger lobsters (red).

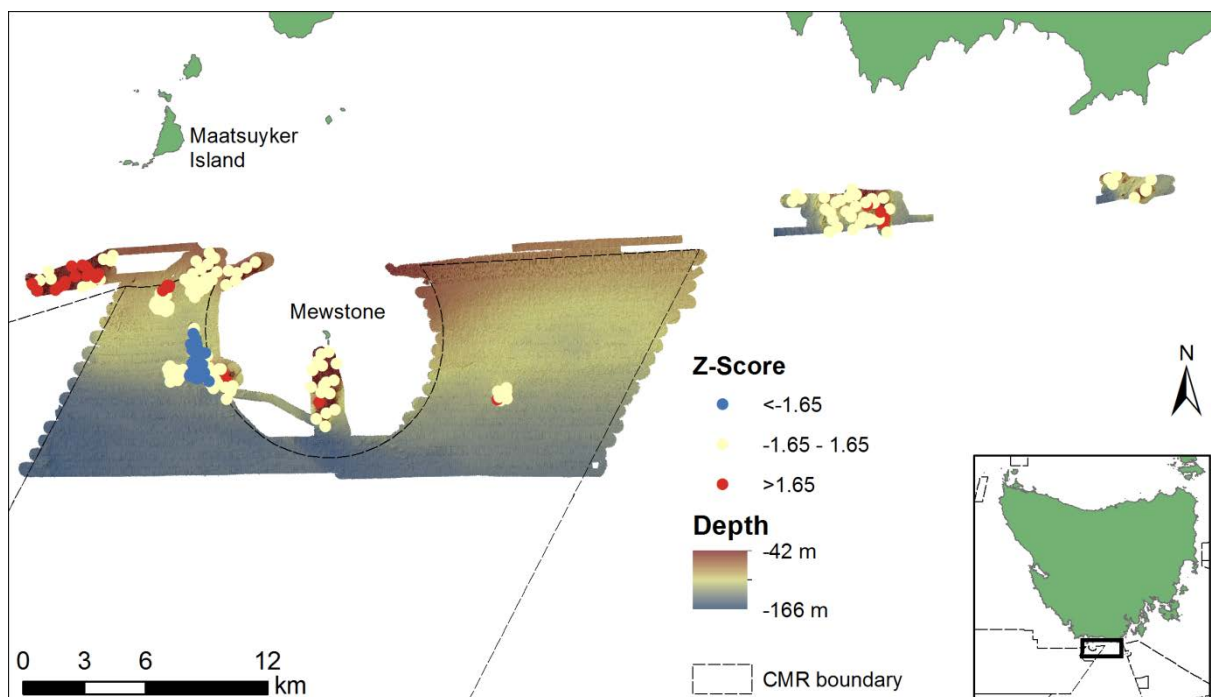


Figure 16. Hotspot analysis of size distribution of female lobster caught. Note the reduced clustering of larger sizes inside the CMR (red). Also note that few legal (>105 mm) were caught, with none exceeding 110mm carapace length.

Despite the limited maximum female size, and that clearly the frequency distribution could not be skewed due to removal of larger lobsters by fishing, there was still a substantial difference in the overall frequency distribution between fished and CMR locations (Figure

17) with the peak in abundance being for smaller size classes (81-85 mm relative to the CMR: 96-100 mm). Such a difference may be related to factors independent of the level of protection, for example a cross-shelf gradient in recruitment success (reflected by the markedly differing abundances between the fished and CMR locations) and/or differential growth rates driven by density dependent resource limitation. However, these differences could also be related to fishing effort through mortality associated with repeated captures of females within the fishery, and associated mortality due to octopus kills, damage due to handling, translocation to unsuitable habitat (e.g. sand) during vessel movements, and seal and other predator induced mortality when being thrown back after capture. Further work is required to explain these observed size-distribution differences.

A similar but more marked differentiation was seen in the male lobsters (Figure 17). As indicated by the ratio of legal to sub legal sized lobsters (Figure 14), there were substantially more large lobsters within the CMR than the fished reference locations when examined as a proportion of the population caught, although the total number of legal sized lobsters captured in and out of the CMR were approximately similar due to the lower capture rates within the CMR. While differential growth rates due to density effects may explain part of this pattern, marked truncation above the legal size limit for males (110 mm) would be expected to be similar for that found in the fished areas under fished conditions, yet this was not the case (Figure 17), suggesting there was a substantial build-up of large lobsters within the CMR due to the 7-yr period of protection from fishing, despite the overall lower population density.





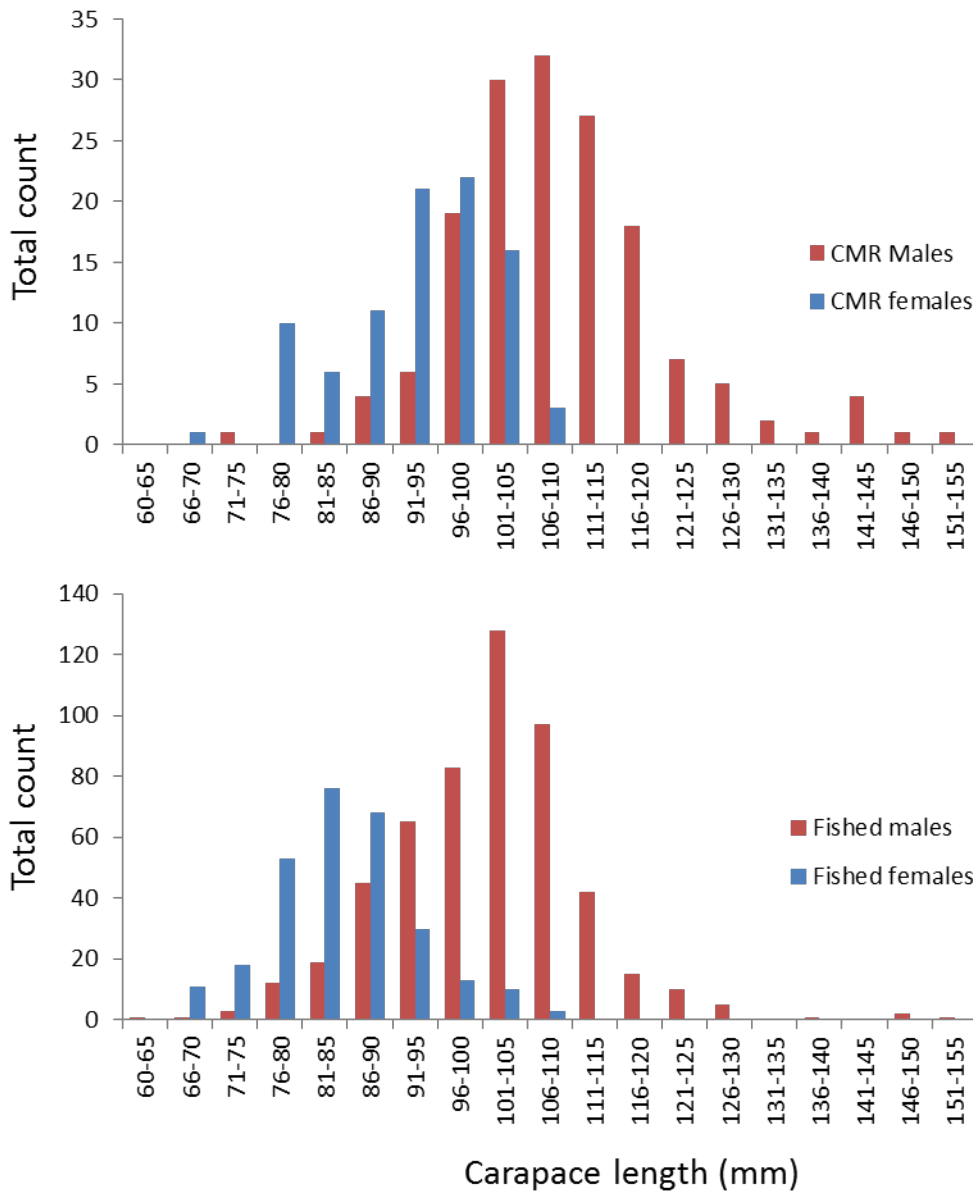


Figure 17. Absolute size frequency of lobsters captured within the CMR sanctuary reefs (top plot) and lobsters captured within fished reference locations (bottom plot). Note the differences in the total count scale reflecting differences in the overall catch between fished and CMR locations.

To better illustrate differences between size distributions within and near the CMR, the abundance of lobsters within the CMR was adjusted for the same number of sub-legal lobsters found within the fished reference locations (Figure 18). This shows the substantially differing distributions in size between the CMR and the fished reference locations for both females and males. Again, while this is clearly related to biophysical processes (and/or fishing related mortality) rather than protection of legal-sized animals for females, the particularly high proportion of males above legal size within the CMR indicates, that at least for males, there is a significant effect of protection within the sanctuary zone.

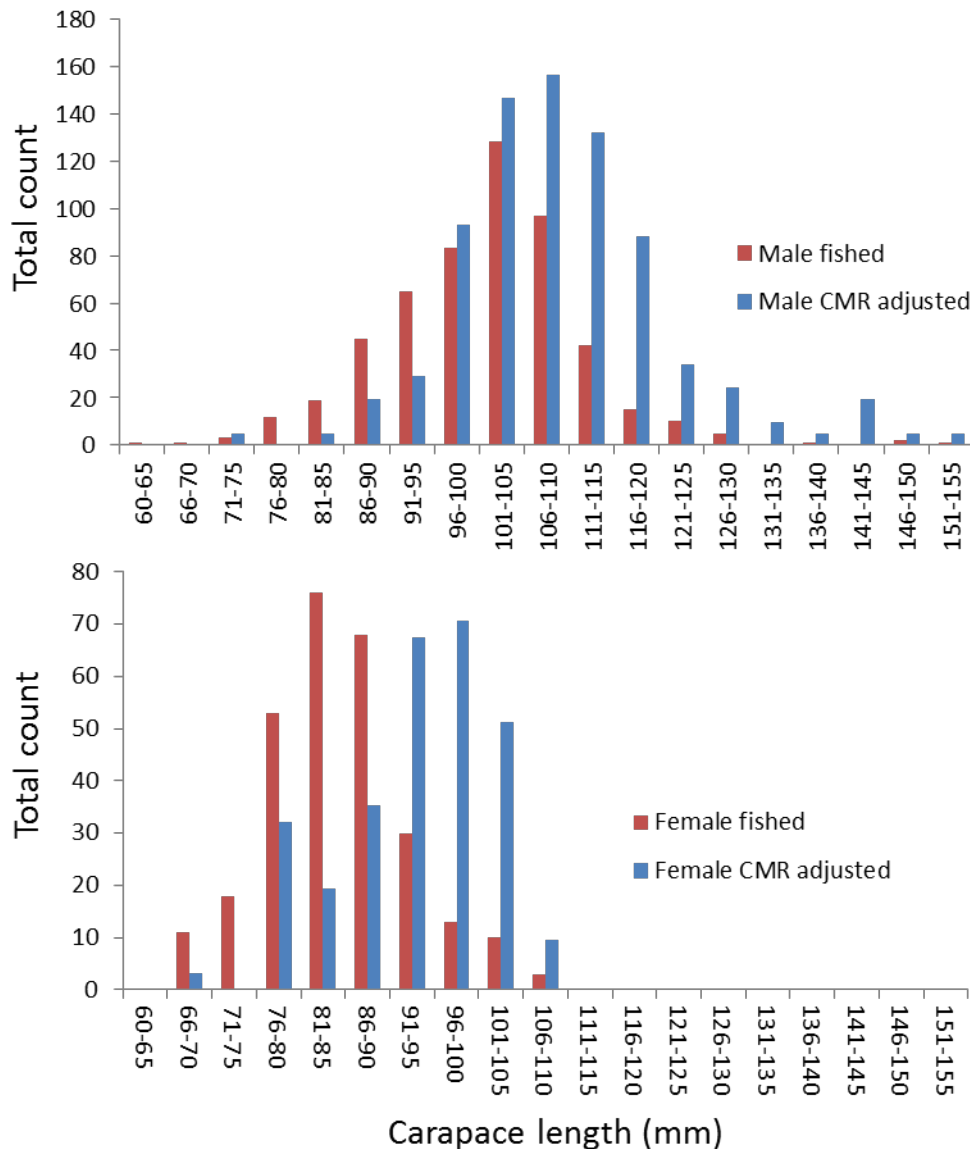


Figure 18. Comparison of size frequency distributions of lobster populations between the Tasman Fracture and adjacent fished reference locations based on adjustment of CMR abundances for equal numbers of sub-legal lobsters (x4.88 for males, x3.21 for females) to allow for direct evaluation of size distributions.

Examination of depth-related trends indicated that there was indeed a strong depth related positive trend in mean size for both sexes (Figure 19) and that this was predominantly determined by a decline with depth in the abundance of sub-legal lobsters rather than even changes with depth across the size spectrum (Figure 20). A major part of this is almost certainly driven by the overall cross-shelf/depth distribution of lobster abundance. For both males and females this pattern was particularly strong (Figure 21; Figure 22), and perhaps reflects differential recruitment to shallower waters by lobsters as they settle from planktonic larval stages. This pattern is certainly confounded by protection effects, as CMR reefs were on average deeper than control reefs, and model-based approaches in a subsequent section of this report are utilised to better untangle the relative contribution of depth to overall lobster

density, and the consequent interaction of this with the influence of CMR no-take protection for males.

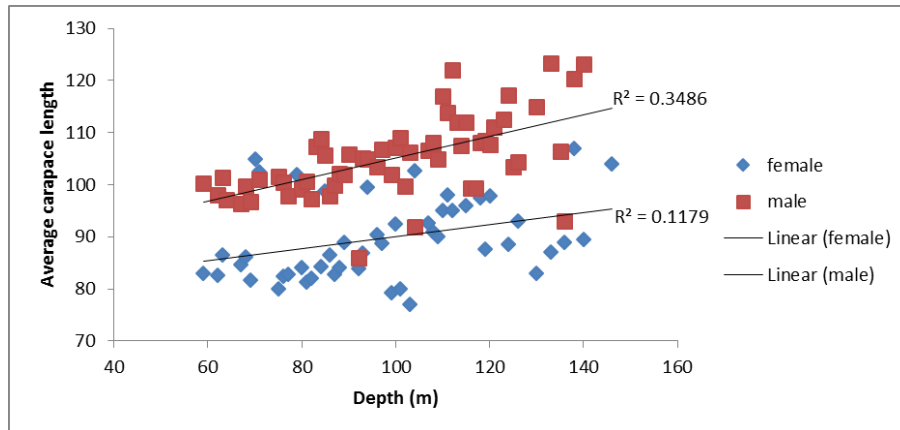


Figure 19. Sex related difference in mean carapace length per pot lift with depth estimated from all 200 pot lifts undertaken in the Tasman Fracture CMR survey.

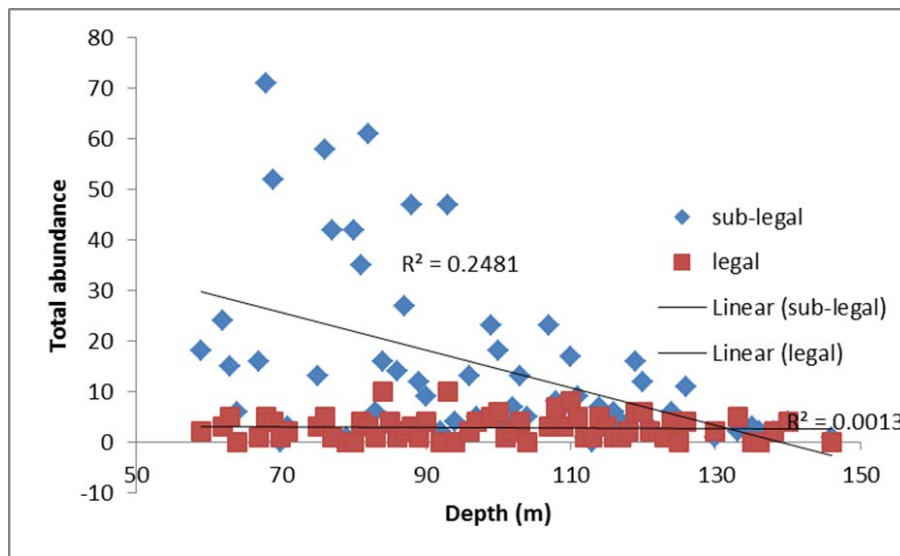


Figure 20. Size-related pattern of the abundance per pot lift of lobsters with depth in the Tasman Fracture survey area. Size categories are based on sub-legal and legal sized lobsters (105 mm CL females and 110 mm CL males).

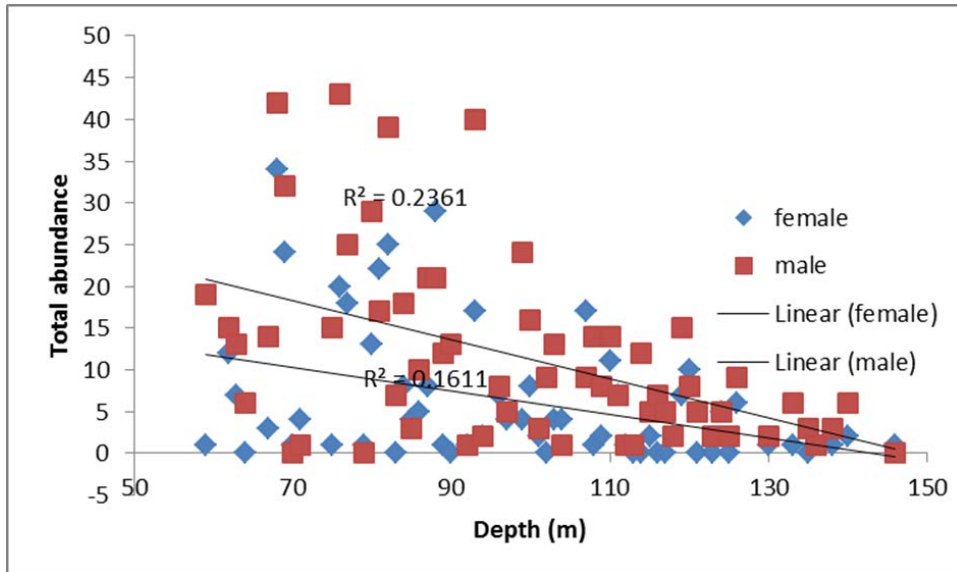


Figure 21. Total abundance per pot lift with depth for female and male lobsters from all 200 pot lifts undertaken during the Tasman Fracture survey.

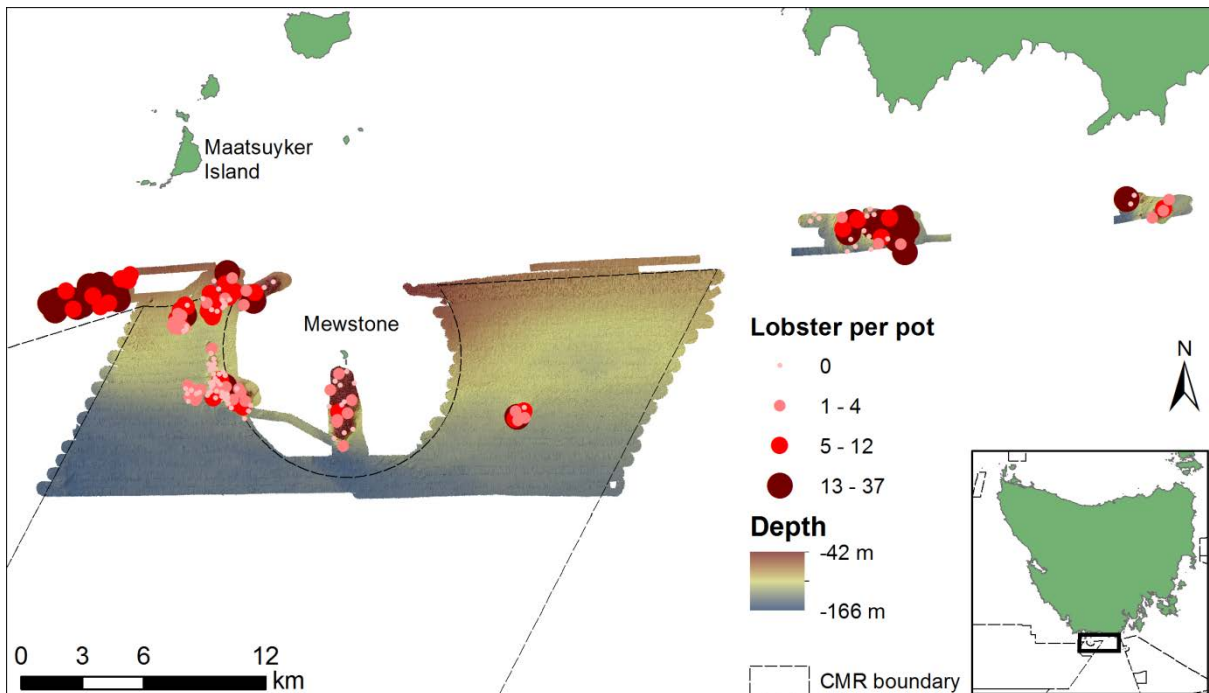


Figure 22. The cross-shelf distribution of lobster catch per pot-lift based on pre-determined positions.

### 2.2.3 Bycatch in lobster pots

Overall bycatch numbers were relatively low in this region and were predominantly composed of draughtboard sharks (*Cephaloscyllium laticeps*), hermit crabs (possibly *Strigopagurus strigimanus*), ocean perch (*Helicolenus percoides*), red cod (*Pseudophycis bachus*) and conger eels (*Conger verreauxi*). Draughtboard sharks contributed to the majority of the catch (Table 1). The majority of species captured were able to be returned to the water unharmed and were observed swimming to the seabed. Exceptions were red cod which suffered barotrauma from swim-bladder inflation, and a moderate proportion of reef ocean perch that were slow to swim to depth. These were routinely predated by shy albatross (*Thalassarche cauta*) that actively followed the vessel while fishing in this region. A large colony of shy albatross exists on the Mewstone. A notable minor bycatch component was the giant crab (*Pseudocarcinus gigas*) with three individuals captured incidentally within the CMR (Figure 23). While this bycatch data does indicate typical numbers that may be expected in the commercial pot fleet for larger species such as sharks, eels and giant crabs, the lack of an escape gap in the research pots means that captures of smaller fish species such as reef ocean perch or rosy wrasse (*Pseudolabrus rubicundus*) may well be elevated in this data due to lesser opportunities to escape.

Table 1. Bycatch of associated with lobster potting using research pots with no escape gaps in the Tasman Fracture CMR and adjacent fished reference locations.

Bycatch	CMR	Fished
<i>Asymbolus rubiginosus</i> (Orange spotted cat shark)	0	1
<i>Cephaloscyllium laticeps</i> (Draughtboard shark)	20	37
<i>Conger verreauxi</i> (Conger eel)	7	6
<i>Helicolenus percoides</i> (Ocean perch)	26	8
<i>Latris lineata</i> (Striped trumpeter)	1	0
<i>Nectocarcinus</i> spp. (Red velvet crab)	0	4
<i>Nemadactylus macropterus</i> (Jackass morwong)	1	0
<i>Octopus maorum</i> (Maori Octopus)	0	2
<i>Octopus</i> spp.	2	0
<i>Pseudocarcinus gigas</i> (Giant crab)	3	0
<i>Pseudolabrus rubicundus</i> (Rosy wrasse)	0	2
<i>Pseudophycis bachus</i> (Red cod)	10	6
<i>Ranella australasia</i> (Whelk)	0	1
<i>Strigopagurus strigimanus</i> (Hermit crab)	27	30
Unidentified decorator crab	2	4





Figure 23. Example of one of the three giant crab (*Pseudocarcinus gigas*) caught during pot sampling for lobster.

## 2.2.4 Detailed modelling of lobster data

In addition to the basic descriptive patterns in the lobster catch data already given, a Bayesian model-based approach was used to further contrast the patterns in lobster catch and size between the CMR and adjacent fish reference reef areas across depth. Appendix 1 contains specific details on the modelling approach.

Six geostatistical models were run to examine the effects of depth and protection on: (1) overall lobster catch, (2) catch of legal sized male lobster, (3) average size of male lobster, (4) average size of female lobster, (5) abundance of legal-sized lobster, and (6) proportion of males in population (Table 2). Models revealed some interesting patterns in lobster abundance, size and gender ratios (Table 2). In a traditional hypothesis testing framework (e.g. with p-values) most, but not all, of these patterns would be a non-significant.

Here, the effect of protection, on each of the outcome variables, is summarised in four ways: 1) the modelled CMR effect (e.g. how many more/less lobsters were caught inside the CMR, as described by the mean of the posterior distribution), 2) the (posterior) distribution of likely values of the CMR effect, 3) the (posterior) probability that the CMR effect is greater than parity, and 4) a plot of the likely (posterior) response to depth. Posterior probability values close to 0 or 1 suggest that there is strong evidence that the MPA has an effect on that variable, whereas values close to 0.5 suggest that positive or negative effects are equally likely.

As an illustrative example, consider the catch of lobsters (abundance) in Table 2 and Figure 24. The effect of the CMR was that pots set inside the CMR expected to have 3.68 times the catch of pots outside the CMR (Table 2). There is substantial evidence that this effect is statistically important (probability of being greater than parity is 0.97), which is reflected by the distribution of the CMR effect in right hand panel in Figure 24. This implies that the probability of a negative CMR effect is just 0.03. Further, there appears to be a depth preference of around 80 metres, as shown in Figure 24 (left hand panel), but there is plenty of uncertainty in this effect.



Table 2. Summary of model outputs contrasting protection and depth effects on the lobster population in and around the Tasman Fracture CMR. Note probabilities are Bayesian probabilities (from 0 to 1) of each effect. Values >0.95 or <0.05 are considered statistically strong. Values >0.8 or <0.2 indicate increasing strength of the trend. \* denotes statistically important result.

Analysis	Probability	CMR effect	Depth effect
Catch of lobster	0.97 *	3.68 (multiplicative on a response scale)	Monotonic trend with peak at ~80 m
Catch of legal sized males	0.59	1.01 (multiplicative on a response scale)	No clear effect
Average size of males	0.62	0.82 (additive on a response scale)	No clear effect
Average size of females	0.43	-0.57 (additive on a response scale)	No clear effect
Proportion of legal sized males	0.71	0.45 (additive on a logit scale)	Proportion of legal-sized male lobsters caught declines at depths below 100 m
Proportion of male lobsters (gender ratio)	0.41	-0.61 (additive on logit scale)	Slight decline in the proportion of male lobster caught around 90 m





### *Effect of protection and depth on lobster catch (abundance)*

Based on the model-based approach, there was a strong probability (i.e. 0.97) that lobster abundance was significantly influenced by CMR. On average, the model suggest that lobster abundance was 3.68 times higher inside the CMR than those outside (Figure 24). The depth effect on catch was interesting with a striking non-monotonic trend (Figure 24), with what appears to be an increase in catch around 80 m depth that decreases for deeper and shallower pots.

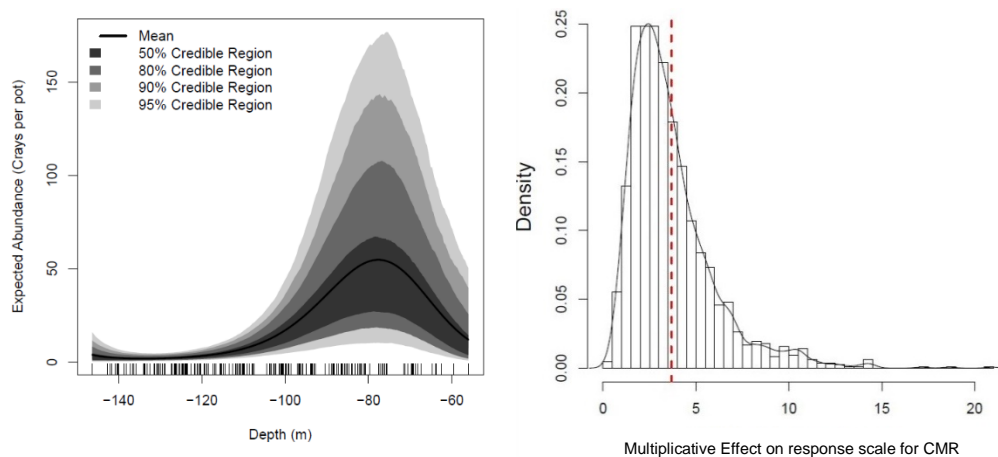


Figure 24. Depth (left) and protection (right) effects on the catch of lobster (abundance). Solid line in left plot is the mean of the expected abundance and shading gives some point-wise credible intervals. Values greater than one in right plot imply greater catch of lobsters inside the CMR. Histogram and smoothed density are taken from the posterior samples. Dashed red vertical line is the mean estimate.

### *Effect of protection and depth on average lobster size*

Models based on mean male lobster size were, on average, 0.82 mm larger inside the CMR than those outside (Figure 25). The reverse was true for females, with the probability of catching smaller females slightly less inside the CMR, where lobster were 0.57 mm smaller (Figure 26). However, for both males and females, the size of this effect is not overly strong with probabilities of 0.62 and 0.43, respectively.

Depth had no discernible effect on male or female lobster size (Figure 25, Figure 26).

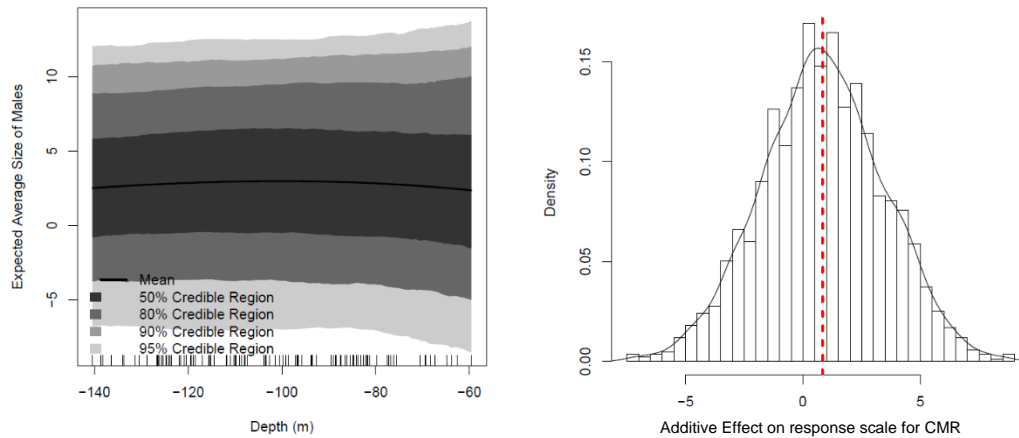


Figure 25. Depth (left) and protection (right) effects on average male size. Solid line in left plot is the mean of the expected size of male lobster and shading gives some point-wise credible intervals. Values greater than zero in right plot imply greater size in male lobsters inside the CMR. Histogram and smoothed density are taken from the posterior samples. Dashed red vertical line is the mean estimate.

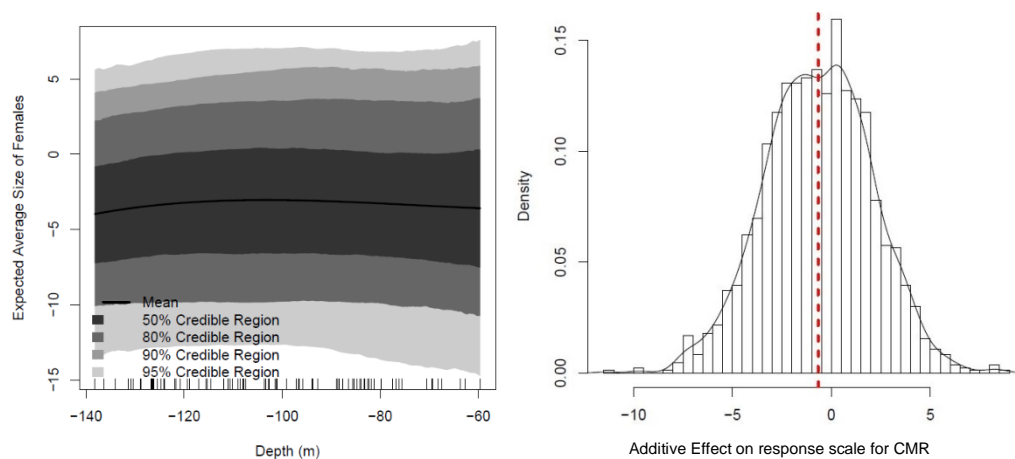


Figure 26. Depth (left) and protection (right) effects on average female size. Solid line in left plot is the mean of the expected average size of female lobster and shading gives some point-wise credible intervals. Values less than zero in right plot imply smaller size female lobsters inside the CMR. Histogram and smoothed density are taken from the posterior samples. Dashed red vertical line is the mean estimate.

### *Effect of protection and depth on legal male lobster abundance*

Models based on average abundance of legal male lobster were found to have, on average, a greater probability of catching more legal sized male lobsters inside the CMR than those outside (Figure 27). However, this proportion was very small, with the model suggesting that there were 1.01 times more legal sized lobster inside the CMR (i.e. just over the same abundance). Again, and not surprisingly given the very small difference, the size of this effect is not strong at 0.59.

Depth had no discernible effect on the average abundance of legal size male lobsters (Figure 27).

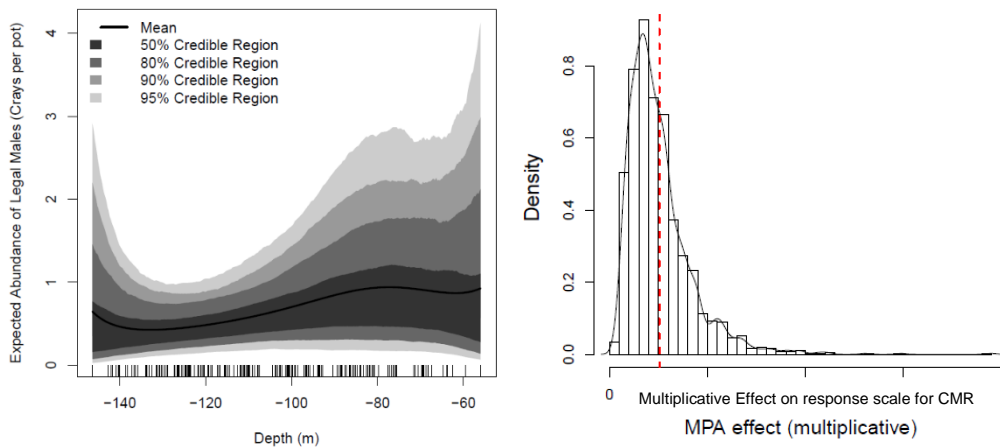


Figure 27. Depth (left) and protection (right) effects on average abundance of legal sized male lobster. Solid line in left plot is the mean of the expected abundance of legal sized males and shading gives some point-wise credible intervals. Values greater than one in right plot imply greater abundance of legal male lobsters inside the CMR. Histogram and smoothed density are taken from the posterior samples. Dashed red vertical line is the mean estimate.

*Effect of protection and depth on the proportion of male lobster (sex ratio)*

Models based on the ratio of male and female lobsters caught indicated that the population was dominated by males, with the 64 % males inside the CMR compared to 78 % outside the CMR. The model also suggested that there were less males in the lobster population inside the CMR (Figure 28). As with the previous analyses the size of this effect is quite small (i.e. 0.45).

Depth showed a slight decline in the proportion of male lobster caught around -90 m (Figure 28).

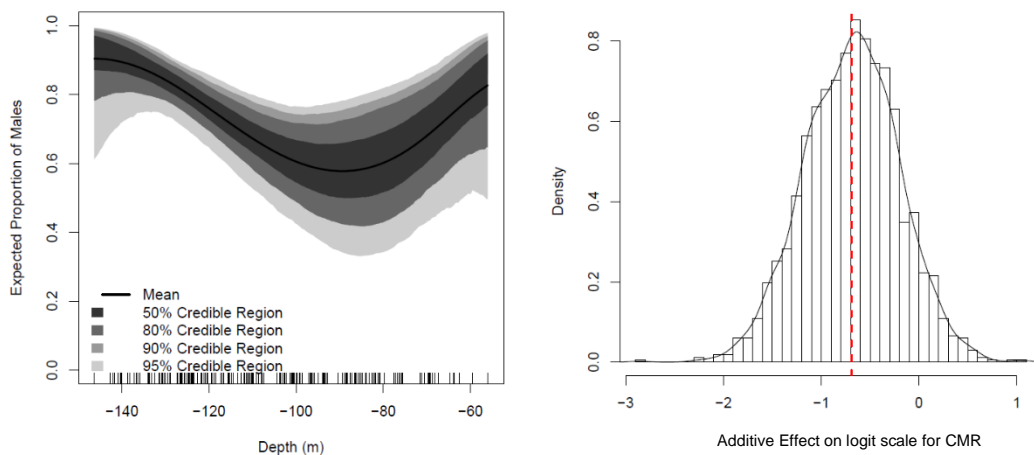


Figure 28. Depth (left) and protection (right) effects on the proportion of male vs female lobster in the catch. Solid line in left plot is the mean of the expected proportion of male lobster and shading gives some point-wise credible intervals. Values less than zero in right plot imply smaller proportion of female lobsters inside the CMR. Histogram and smoothed density are taken from the posterior samples. Dashed red vertical line is the mean estimate.

### *Effect of protection and depth on the proportion of legal male lobster caught*

Models based on the proportion of legal sized male lobster caught suggested that, on average, legal males made up 24 % and 17 % of the male lobster population inside and outside of the CMR, respectively. This suggests that there is a greater proportion of legal males inside the CMR than outside (Figure 29). Again, the size of this effect is quite small (i.e. 0.45).

Depth had a discernible but slight effect on the proportion of legal-sized male lobsters caught, with the proportion declining somewhat at depths below 100 m (Figure 29).

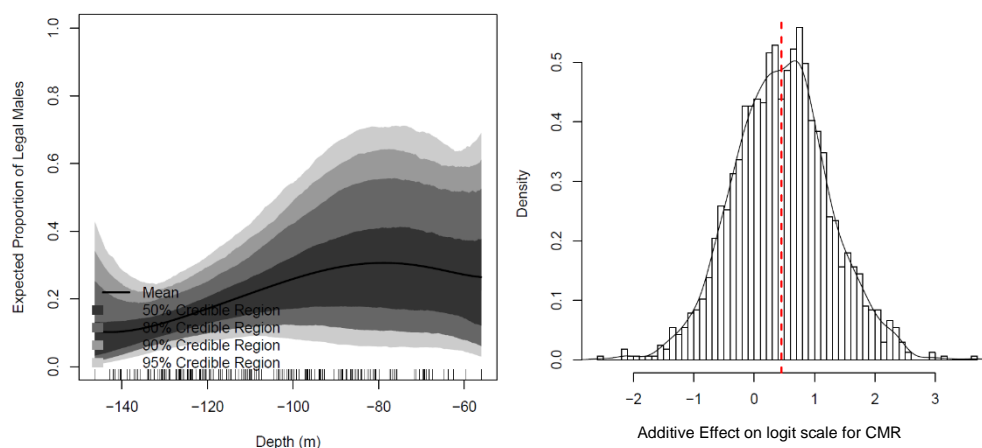


Figure 29. Depth (left) and protection (right) effects on the proportion of legal sized vs undersized male lobsters caught. Solid line in left plot is the mean of the expected average and shading gives some point-wise credible intervals. Values greater than zero in right plot imply greater proportion of legal male lobsters inside the CMR. Histogram and smoothed density are taken from the posterior samples. Dashed red vertical line is the mean estimate.

#### 2.2.5 Overview and interpretation of model-based analyses of the spatial and depth distribution of lobster catch

While simple examination of the lobster catch data would suggest some clear trends with respect to depth and CMR protection, these results were partially confounded with differing depths and sample dates between sampled CMR and fished locations. Despite our best attempts to map and sample representative depths within the CMR and associated reference fished locations, there was a depth disparity between the mapped areas, with the CMR containing more deep reef below 120 m than could be found in adjacent areas based on our prior knowledge and the time allocated to new mapping. The results were therefore partially confounded by the strong depth related patterns in overall lobster abundance as catch per pot-lift declined markedly below 100 m, whereas much of the reef within the CMR was at depths of 100 to 140 m. The model-based analysis allows some of these confounding factors to be untangled, but is substantially driven by analysis of relationships within depth ranges that the CMR and fished sites have in common.

However, despite these limitations, the model-based analysis indicated that there were in fact, significantly more lobsters per pot-lift within the CMR when depth factors are accounted

for, suggesting that the CMR no-take protection has resulted in increased lobster numbers as predicted. This was coupled with the model-based analysis showing greater average male size and marginally greater abundance of legal sized males within the CMR, again as expected, as larger males are protected from fishing within the CMR. This was reinforced by a trend for a greater proportion of legal v's sub-legal lobsters in the CMR relative to fished reference sites. With exception to overall catch (abundance) which yielded a strong trend, the remaining results are statistically weak, and will rely on additional surveys to strengthen (or invalidate) the confidence in these patterns.

Overall, the model based results suggest lobster abundances were substantially greater within the CMR on a depth by depth basis, and that while some of this was driven by a greater proportion of legal sized lobsters, the majority of it may be driven by an increased abundance of sub-legal female lobsters. If this proves to be the case, it would imply that female lobsters are encountering substantial fishing-induced mortality outside the CMR, as a result of repeated captures in pots, despite nominally being protected by the minimum legal size limit.

While the models should account for the imbalance between sampling depths between fished and CMR sites, further sampling should be undertaken to provide certainty in the interpretation of patterns found in this region in response to protection. A priority action for future work is therefore to map out suitable deeper reef locations within adjacent fished habitats on which to allow a more balanced sampling design, and flesh out the real patterns with depth and level of protection.

Regardless of some of the unresolved questions from this sampling, the research has greatly improved our understanding of the extent that cross-shelf reefs within the CMR are utilised by lobsters, including their declining abundances with depth beyond 80 m and with distance offshore, as well as the potential impacts of the lobster fishery in this region on sub-legal females. The current results will act as an appropriate baseline for future studies documenting changes in this CMR following protection, and will inform refinement of the experimental design to best separate CMR related trends from patterns driven by habitat variability.

## 2.3 Trends in benthic biota

### 2.3.1 Tasman Fracture CMR benthic biota assemblage

We planned to survey the benthic biota of the CMR and adjacent fished areas to provide a baseline inventory of sessile benthic biota (such as sponges, soft corals, bryozoans) of the CMR and broader region, to validate the physical seabed structures interpreted from multibeam sonar surveys, and to examine the extent that the biota may be influenced through ecosystem effects of fishing, either now, or in the future. This survey was planned to be undertaken using the IMOS AUV facility *Sirius* over a four-day period, deployed from *R. V. Bluefin*. The underpinning survey design was based on gathering an extensive coverage of CMR and reference reef systems by the broad grid transect design used in IMOS and CERF/NERP Hub deployments (planned tracks shown in Fig. 33). Unfortunately, only two of the 21 proposed AUV missions were successfully completed due to a “perfect storm” of

logistical constraints. These included unanticipated delays in vessel availability, technical malfunctions with the AUV itself, deteriorating weather conditions off southern Tasmania, and the need to on-ship the AUV to Perth rather than wait out the poor weather pattern. This region is an extremely remote and exposed to all weather conditions. Weather conditions change quickly and aligning vessel and AUV availability with a suitable weather window proved to be extremely difficult, as the weather deteriorated outside forecast conditions from the outset, resulting in a number of days on site, but where it was unsafe to deploy the AUV. Despite these set-backs, the two successful transects yielded 18,420 images of seafloor benthos. These images may be viewed by the AUV imagery viewer Squidle (<https://squidle.acfr.usyd.edu.au/>), or via the IMOS AUV image viewer (<https://auv.aodn.org.au/auv/>) while the associated metadata have now been uploaded onto the AODN data portal (<https://auv.aodn.org.au/auv/>). Images from the AODN image viewer can be downloaded via a tiff link, and, as they are usually underexposed, brightened using any image enhancement software. The two transects completed were on the reefs inside the CMR west of the Mewstone (Figure 30) and encompassed reefs typical of the CMR from depths of 80-130 m, thus while the survey was not comprehensive, it did provide a substantial amount of imagery and has significantly improved our understanding of the biota of this region within the CMR.



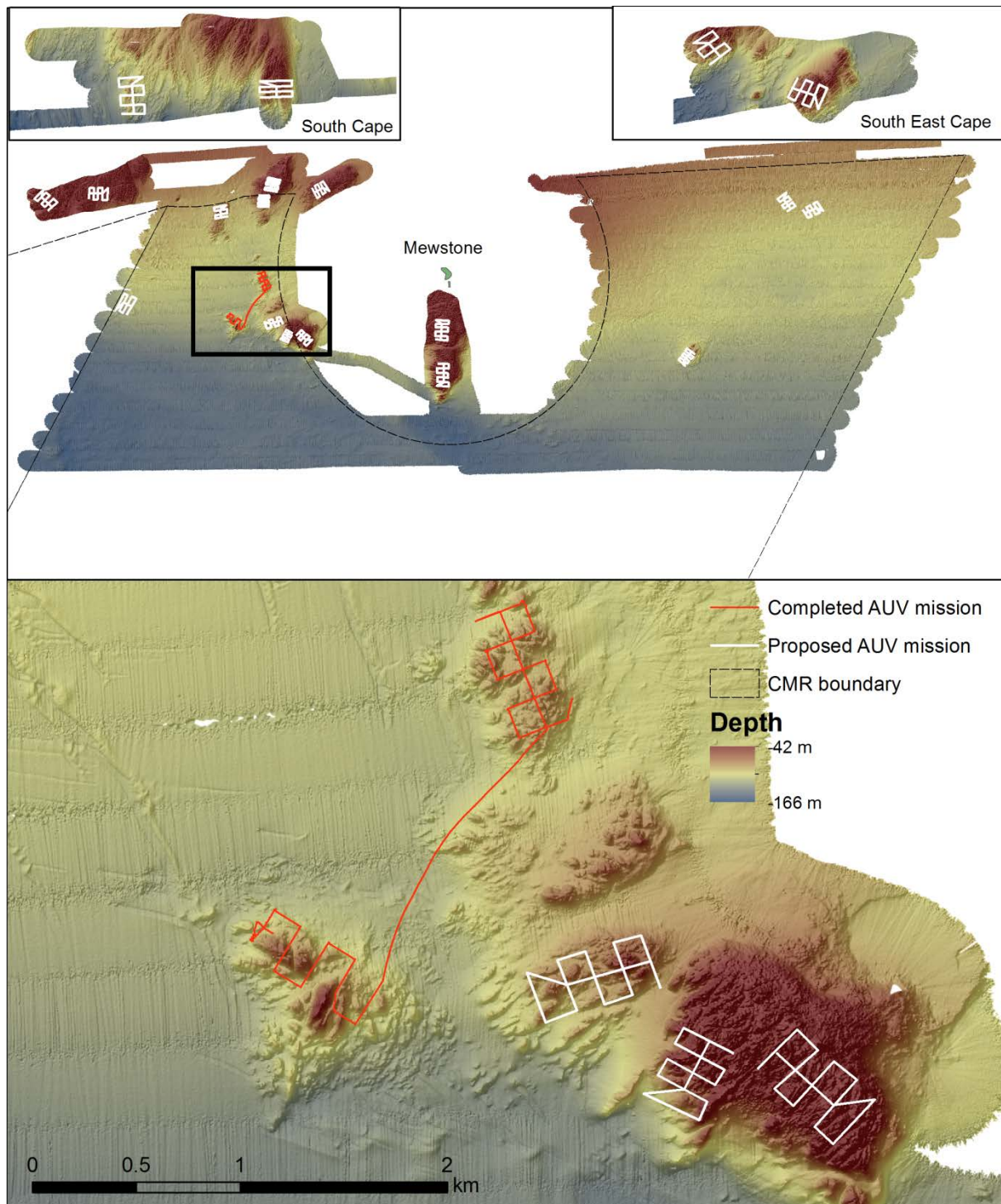


Figure 30. Proposed and completed AUV missions in- and around the Tasman Fracture Commonwealth Marine Reserve.

From these two AUV missions 261 images, representing sampling of approximately every 50<sup>th</sup> image, or one image every 25 m along transect, were scored for percentage cover of benthic invertebrate and substrate cover using a count of cover below each of 25 randomly placed points per image.



A highly diverse assemblage was recorded, with 149 biological morphospecies being identified and three substratum types (Table 3). Similar to other deep water environments around Tasmania (such as the Flinders CMR), a matrix of low-profile, finely-structured invertebrate cover was the most common biogenic substrata feature (morphospecies “Bryozoan/Cnidaria/Hydroid matrix” Figure 34; Table 3) providing 16% of the total cover. For the larger, more visible invertebrates, sponges formed the most significant identifiable component of the fauna (17.6 %) . Of these, the morphospecies “Encrusting white 6” (Figure 32), was the dominant sponge, representing 4.8% of the total cover. Overall, the remaining biota was typical of that found in deep reef assemblages on previous studies in the region, with very few species approaching cover of 2%, and with the vast majority significantly less than that. A large number of sponge morphospecies were encountered (110 morphospecies), including a number of structure forming species such as “cup 1 white” (Figure 32) .

Two quite notable features of the overall invertebrate cover were (1) the abundance of mobile brittle stars (Figure 34, 1.9% cover), and (2) the abundance of octocoral species which at 5.7% overall, was markedly higher than encountered on similar surveys in the SE region of Australia, and may be a unique feature of this region. The soft coral “soft *Capnella* like” (Figure 35) was the most abundant of these at 1.9% cover. Likewise, the broad scale abundance of brittle stars throughout the imagery (1.9% cover) is a feature not yet seen elsewhere in AUV-based surveys although they are a conspicuous component of trawl catch in some soft sediment locations. Their abundance potentially indicates this environment is rich in detrital food sources.

Nearly 29 % of morphospecies were singletons (i.e. only seen once) and nearly half the morphospecies in the assemblage were seen less than twice (Table 3). This suggests that the benthic assemblage in the Tasman Fracture consists of a morphospecies that are highly diverse and spatially rare.





Table 3. Total observations and percentage contribution of morphospecies and bare substrate type observed in the Tasman Fracture CMR using the AUV.

CATAMI (Level 1)	Morphospecies	Total observations	Percentage contribution
Ascidians	Ascidian 12 Colonial Red	1	0.02
	Ascidian 2 <i>Clavelina</i> like	2	0.03
	Unidentified Species No 16	1	0.02
	Unidentified Species No 29	3	0.05
	Unidentified Species No 7	7	0.11
<b>Total ascidian cover</b>			<b>0.23</b>
Biota	Unknown Biology	65	1.00
Bryozoa	Bryozoan 2 soft <i>Amathia</i> like	3	0.05
	Bryozoan 3 <i>Canticella</i> like	70	1.07
	Bryozoan 5 Lace	16	0.25
	Bryozoan 7 Hard	8	0.12
	Unidentified Species No 109	43	0.66
<b>Total bryozoan species cover</b>			<b>2.2</b>
Bryozoa/Cnidaria/Hydroid matrix	Bryozoa/Cnidaria/Hydroid matrix	1042	15.97
Bryozoa/Sponge matrix	Bryozoa/Sponge matrix	240	3.68
Cnidaria	Bramble <i>Acabaria</i> sp	46	0.70
	Bramble <i>Asperaxis karenii</i>	9	0.14
	Coral 2 soft <i>Capnella</i> like	123	1.89
	Coral 6 soft blue	6	0.09
	Coral orange solitary	6	0.09
	Gorgonian pink 1	7	0.11
	Gorgonian red 2	55	0.84
	Hydroid 1	73	1.12
	Hydroid 2	3	0.05
	Hydroid White	7	0.11
	Sea whip 1	21	0.32
	Unidentified Species No 101	6	0.09
	Unidentified Species No 176	4	0.06
	Unidentified Species No 179	1	0.02
Unidentified Species No 85	4	0.06	
Zooanthid 1 cf <i>Epizooanthus</i>	1	0.02	
<b>Total cnidarian cover</b>			<b>5.7</b>
Crustacea	<i>Jasus edwardsii</i> (Lobster)	1	0.02
Echinoderms	Brittle star	124	1.90
	Holothuroidea	2	0.03
Fishes	<i>Caesioperca lepidoptera</i> (Butterfly Perch)	1	0.02
	<i>Helicolenus percoides</i> (Red Gurnard Perch)	3	0.05
Jellies	Salps	8	0.12
Macroalgae	Brown algae (drift)	1	0.02
Molluscs	Scallop	4	0.06
Sponges	Arborescent 10 orange/brown fingers	1	0.02
Sponges cont.	Arborescent 12 brown thorny	2	0.03
	Arborescent 13 orange	2	0.03

CATAMI (Level 1)	Morphospecies	Total observations	Percentage contribution
	Arborescent 14 black	2	0.03
	Arborescent 15 white short	15	0.23
	Arborescent 17 stumpy grey	5	0.08
	Arborescent 5 white	5	0.08
	Arborescent 6 yellow	10	0.15
	Arborescent 8 tan	1	0.02
	Branching 1 Orange	2	0.03
	Branching 3 Purple	1	0.02
	Branching 4 Brown	2	0.03
	Cup 1 white	13	0.20
	Cup 2 white frilly	1	0.02
	Cup 6 pink thick	2	0.03
	Cup 7 light pink flat thick	9	0.14
	Cup 8 yellow	7	0.11
	Encrusting 1 orange	77	1.18
	Encrusting 2 light orange	13	0.20
	Encrusting 3 yellow	76	1.16
	Encrusting 4 blue	35	0.54
	Encrusting 5 brown	119	1.82
	Encrusting 6 white	313	4.80
	Fan 10 thick large oscules	2	0.03
	Fan 12 brown thin	2	0.03
	Fan 14 white thin	1	0.02
	Fan 3 orange flat	5	0.08
	Fan 4 pink	2	0.03
	Fan 6 yellow	3	0.05
	Fan 7 orange thin blade	2	0.03
	Fan 9 orange thick	1	0.02
	Globular 2 white <i>Tethya</i> like	1	0.02
	Massive 11 white holey	3	0.05
	Massive 12 yellow papillate	3	0.05
	Massive 17 white lumpy	1	0.02
	Massive 18 orange holey	4	0.06
	Massive 20 pink	1	0.02
	Massive 22 Yellow holey	4	0.06
	Massive 5 fungi	1	0.02
	Orange Massive Ball 1	2	0.03
	Papillate 2 yellow	2	0.03
	Tubular 7 pink thorny	1	0.02
	Tubular 3 white colony	6	0.09
	Tubular 4 tan	1	0.02
Sponges cont.	Tubular 6 white thorny	3	0.05
	Tubular 9 pink small oscules	3	0.05
	Unidentified Species No 1	12	0.18
	Unidentified Species No 102	6	0.09
	Unidentified Species No 104	1	0.02



CATAMI (Level 1)	Morphospecies	Total observations	Percentage contribution
	Unidentified Species No 105	1	0.02
	Unidentified Species No 111	1	0.02
	Unidentified Species No 113	2	0.03
	Unidentified Species No 114	1	0.02
	Unidentified Species No 115	2	0.03
	Unidentified Species No 121	1	0.02
	Unidentified Species No 123	1	0.02
	Unidentified Species No 124	3	0.05
	Unidentified Species No 134	1	0.02
	Unidentified Species No 136	9	0.14
	Unidentified Species No 137	61	0.93
	Unidentified Species No 143	1	0.02
	Unidentified Species No 144	9	0.14
	Unidentified Species No 146	2	0.03
	Unidentified Species No 148	1	0.02
	Unidentified Species No 151	16	0.25
	Unidentified Species No 152	6	0.09
	Unidentified Species No 154	3	0.05
	Unidentified Species No 157	9	0.14
	Unidentified Species No 159	1	0.02
	Unidentified Species No 160	1	0.02
	Unidentified Species No 163	1	0.02
	Unidentified Species No 166	1	0.02
	Unidentified Species No 168	12	0.18
	Unidentified Species No 170	2	0.03
	Unidentified Species No 177	2	0.03
	Unidentified Species No 178	3	0.05
	Unidentified Species No 18	2	0.03
	Unidentified species No 180	1	0.02
	Unidentified Species No 19	12	0.18
	Unidentified Species No 21	1	0.02
	Unidentified Species No 24	13	0.20
	Unidentified Species No 27	13	0.20
	Unidentified Species No 3	6	0.09
	Unidentified Species No 33	1	0.02
	Unidentified Species No 35	3	0.05
	Unidentified Species No 37	2	0.03
	Unidentified Species No 38	8	0.12
	Unidentified Species No 41	8	0.12
	Unidentified Species No 49	1	0.02
Sponges cont.	Unidentified Species No 51	2	0.03
	Unidentified Species No 52	1	0.02
	Unidentified Species No 53	1	0.02
	Unidentified Species No 55	1	0.02
	Unidentified Species No 57	1	0.02
	Unidentified Species No 58	2	0.03



CATAMI (Level 1)	Morphospecies	Total observations	Percentage contribution
	Unidentified Species No 6	2	0.03
	Unidentified Species No 62	2	0.03
	Unidentified Species No 63	4	0.06
	Unidentified Species No 68	1	0.02
	Unidentified Species No 75	4	0.06
	Unidentified Species No 78	1	0.02
	Unidentified Species No 84	1	0.02
	Unidentified Species No 87	1	0.02
	Unidentified Species No 88	3	0.05
	Unidentified Species No 95	2	0.03
	Unidentified Species No 97	2	0.03
	Unidentified Species No 98	15	0.23
	Unidentified Species No 99	83	1.27
	Yellow French Fires 1	4	0.06
	Yellow Shapeless Smooth 1	2	0.03
<b>Total sponge cover</b>			<b>17.6</b>
Worms	Tube Worm sp1	4	0.06
	Unidentified Species No 34	2	0.03
Substratum	Biological Rubble	1123	17.21
	Rock	492	7.54
	Sand	1781	27.3
Unscorable	Unscorable	3	0.05



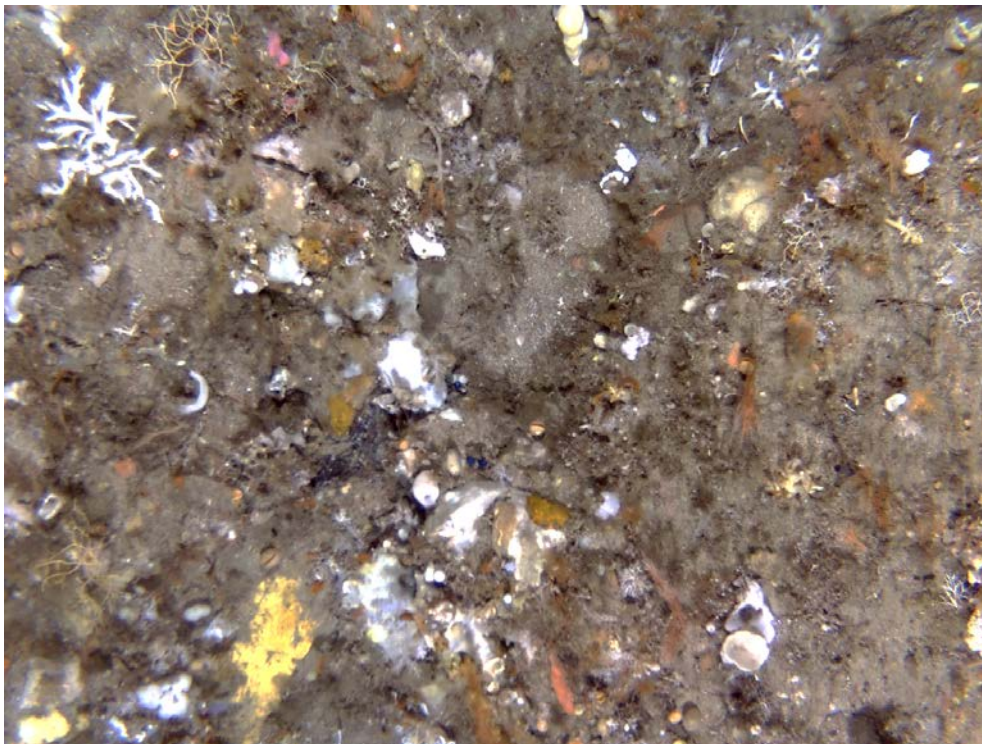


Figure 31. Example of the Bryozoa/Cnidaria/Hydroid matrix class (non-descript brown turf) that dominated the assemblage.

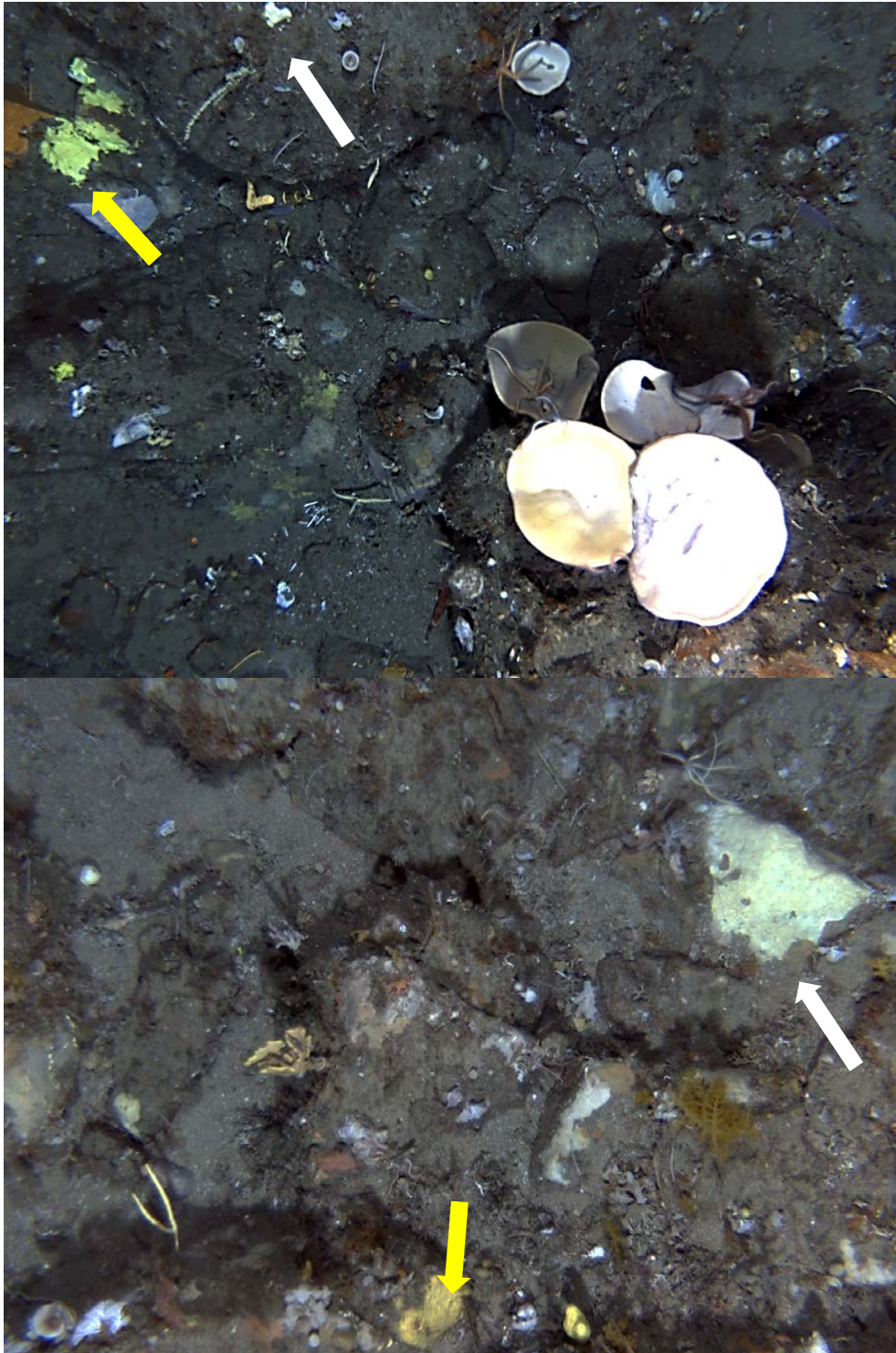


Figure 32. Boulder reefs supporting encrusting yellow and white sponges (colour coded arrows). White encrusting sponges are morphospecies "Encrusting white 6". Note also the large cup-like ("cup 1 white") in top image.



Figure 33. Examples of the variety in cup-like sponges from small (centre of image) to large top left image (“cup 1 white” morphospecies).

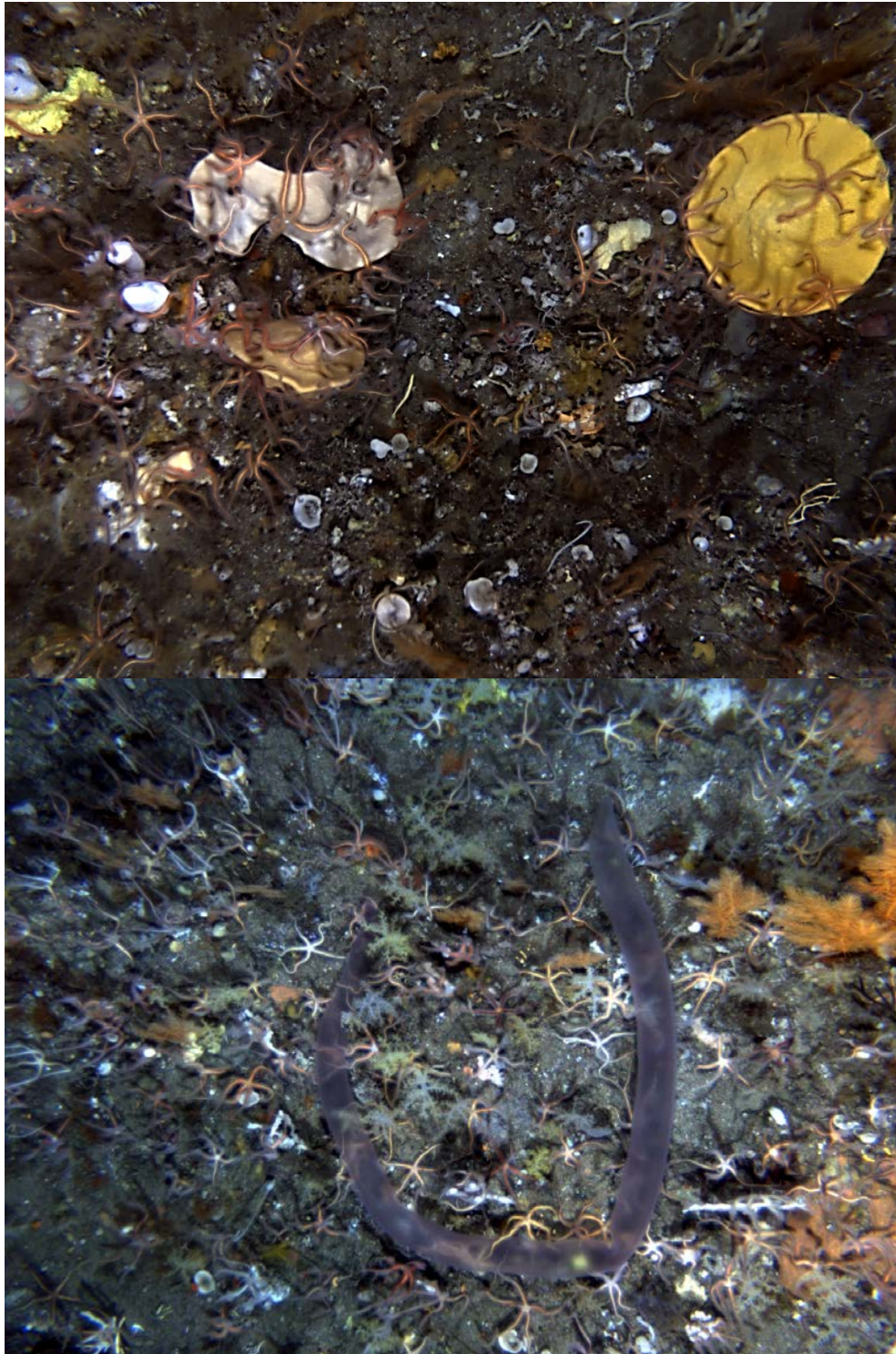


Figure 34. An example image highlighting the extreme abundance in the brittle star community, which appears to dominate the seafloor. Note the large scallop in bottom image. Scalps were a common occurrence in the lobster pots.



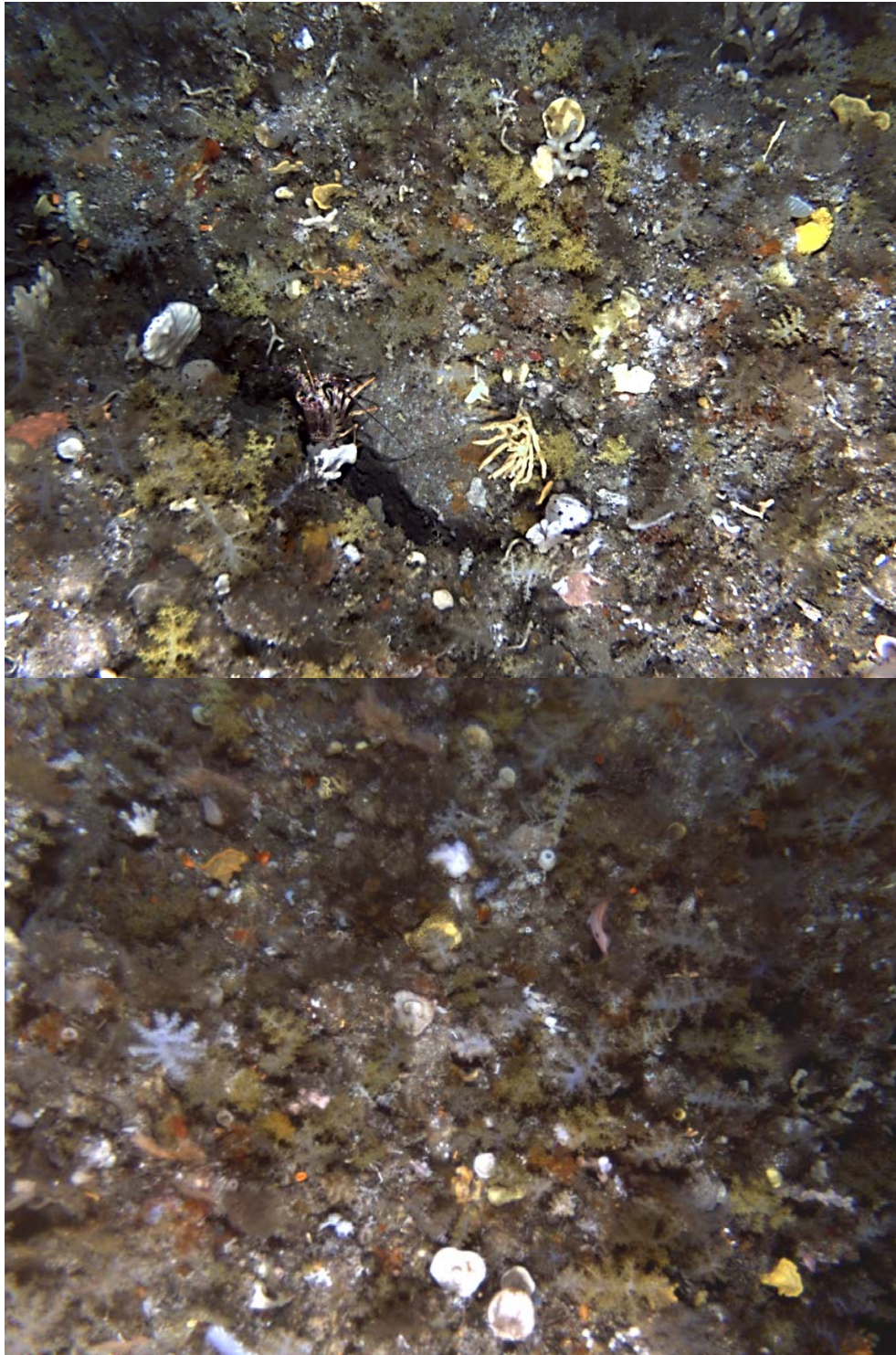


Figure 35. An example of the complex invertebrate assemblages including sponges, *Capnella*-like soft corals (Coral 2 silt *Capnella* like) and ascidians. Note the lobster (*Jasus edwardsii*) in the centre of the top image.

### 2.3.2 Comparison between four Tasmanian CMRs

As corresponding AUV-derived descriptions of benthic invertebrate cover were available from a range of other CMRs in the SE region, we used this data to examine the extent that the CMRs represented similar or markedly different sessile benthic biota on deep reef systems. This comparison was made between the communities recorded from the Tasman Fracture, Huon, Freycinet and Flinders CMRs. A permutational analysis of variance (PERMANOVA) was used to determine significant differences in morphospecies assemblages between CMRs, and, where significant differences were detected a pair-wise comparison was undertaken to further differentiate between areas. The PERMANOVA, and associated pairwise analysis, were run using an unrestricted permutation of raw data with 9999 permutations. Similarity measures were based Bray-Curtis of the assemblage cover. Cluster analysis and non-metric multi-dimensional scaling (nMDS) were used to visualize the patterns in morphotype assemblages. Distances among centroids were calculated for the nMDS to aid in interpretation of the graph. Similarity percentages routine (SIMPER) was also run to determine which combinations of morphospecies were responsible for observed differences. All of these analyses were run in PRIMER v6 + PERMANOVA-addon. The PERMANOVA found that the morphospecies assemblages between all CMRs were significantly different (Pseudo-f = 84.54, P(perm) = 0.001). Pairwise comparisons suggested that the assemblages in all CMRs were significantly different from each other (Table 4). The nMDS suggested that there was also a distinct divide between the two southern CMRs (Tasman Fracture and Huon) with the two northern CMRs (Freycinet and Flinders) (Figure 36).

The PERMANOVA pairwise routine also identifies the relative sizes of average similarities (or dissimilarities) between CMRs, which suggested that the morphospecies assemblages within the Tasman Fracture and Huon CMRs had highly variable assemblages and were quite dissimilar to all other CMRs (Table 5). Conversely, the Freycinet and Flinders CMRs had lower variation (i.e. high similarity within) and also were quite similar to each other (i.e. 42 % similarity; Table 5).

The SIMPER analysis revealed that variations in the cover of Bryozoa/Cnidaria/Hyrdoid matrix, the increased presence of *Capnella*-like soft corals and greater abundance brittle stars and sponge cover were the major morphospecies responsible for structuring biological differences between the CMRs (Table 6). It should be noted that the differences in these assemblages could be driven by inherent discrepancies in depth and seabed structure. For example, Freycinet and Flinders CMRs consist of comparatively more sand-inundated low-profile reef than the Tasman Fracture and Huon CMRs. These differences have not been taken into account in the current analysis and should be kept in mind when interpreting the trends in the assemblage structure presented here.

Table 4. PERMANOVA pairwise comparisons indicating significantly different assemblages between CMRs.

Comparisons	<i>t</i>	<i>P</i> (perm)
Tasman Fracture CMR, Flinders CMR	8.38	<0.001
Tasman Fracture CMR, Huon CMR	7.47	<0.001
Tasman Fracture CMR, Freycinet CMR	8.07	<0.001
Flinders CMR, Huon CMR	10.71	<0.001
Flinders CMR, Freycinet CMR	8.27	<0.001
Huon CMR, Freycinet CMR	9.92	<0.001

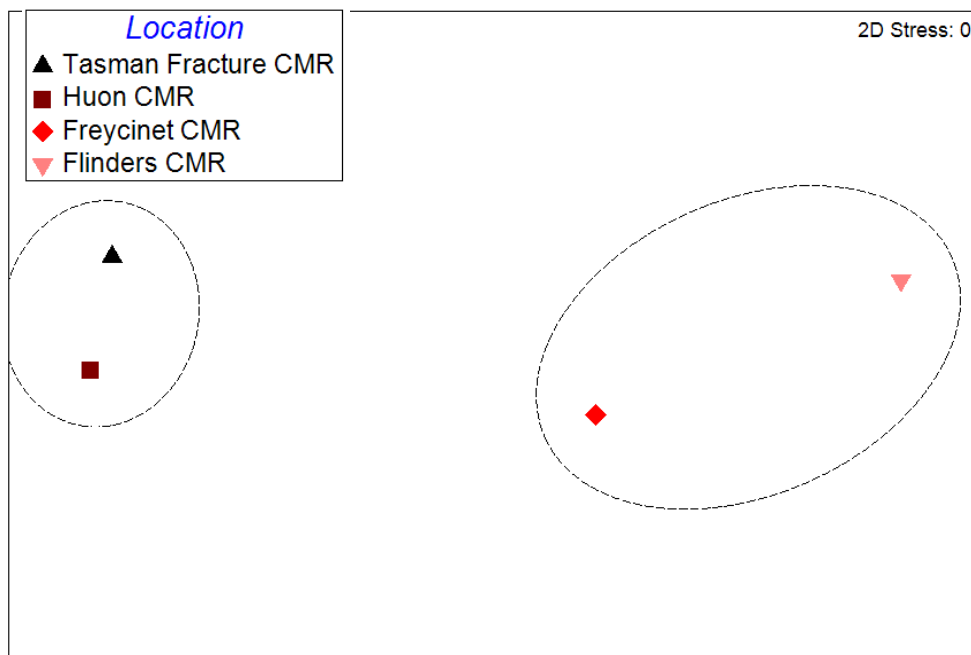


Figure 36. Non-metric multidimensional scaling ordination for centroids morphospecies assemblage between Tasman Fracture, Huon, Freycinet and Flinders CMRs. Hashed lines indicate 30 % similarity between morphospecies assemblages.

Table 5. Average morphospecies assemblage similarity within/between CMRs produced by the PERMANOVA pairwise routine. A value of 0 suggest no similarity, while a value of 100 suggest identical morphospecies assemblage.

	<b>Tasman Fracture CMR</b>	<b>Huon CMR</b>	<b>Freycinet CMR</b>	<b>Flinders CMR</b>
Tasman Fracture CMR	28			
Huon CMR	23	29		
Freycinet CMR	31	33	50	
Flinders CMR	29	27	42	51



Table 6. Similarity percentages (SIMPER) results highlighting the dominant morphospecies within each CMR.

CMR	Morphospecies	Average cover	Average Similarity	Standard deviation similarity	Contribution (%)
Tasman Fracture	Bryozoa/Cnidaria/Hydroid matrix	4.12	9.91	0.71	58.8
	Encrusting 6 white sponge	1.2	2.17	0.46	12.88
	Bryozoa/Sponge matrix	0.92	1.34	0.18	7.97
	Encrusting 5 brown sponge	0.46	0.48	0.23	2.84
	Coral 2 soft <i>Capnella</i> like	0.47	0.34	0.2	2
	Brittle star	0.48	0.32	0.16	1.88
	Encrusting 1 orange sponge	0.3	0.3	0.22	1.78
	Encrusting 3 yellow sponge	0.29	0.29	0.2	1.72
	Huon	Bryozoa/Cnidaria/Hydroid matrix	12.42	18.68	0.79
Screw shell		0.99	0.77	0.13	3.68
Freycinet	Bryozoa/Cnidaria/Hydroid matrix	4.47	29.37	0.98	90.94
Flinders	Bryozoa/Cnidaria/Hydroid matrix	2.18	6.02	0.38	85.38
	Bioturbation	0.13	0.69	0.1	9.75



## 2.4 Population trends in demersal fishes

To establish a baseline understanding of the reef-associated benthic fish assemblages of the CMR and surrounding reef systems, and to evaluate potential changes in these fish assemblages following protection within the no-take zone, fish assemblages in this zone were compared with adjacent fished habitat using baited underwater stereo video stations (stereo BRUVS). Sites were selected in advance based on a spatially balanced statistical design, which planned for a total of 100 deployments, evenly balanced between CMR and fished locations (Figure 37). The central aim of the study was to document possible changes in key targeted species such as striped trumpeter and jackass morwong in response to protection, as well as providing a baseline inventory of the benthic fish assemblages of the CMR shelf reef habitats. Deployments followed standard BRUV protocols that were evaluated and utilised during NERP Hub studies, with protocols including one-hour length deployments, use of ~ 800 g of pilchards for bait, standard SeaGIS BRUV frames, and minimum separation between concurrent BRUV deployments of at least 250 m ([http://frdc.com.au/research/Documents/Final\\_reports/2010-002-DLD.pdf](http://frdc.com.au/research/Documents/Final_reports/2010-002-DLD.pdf)). Following an initial trial of BRUVS during the lobster potting fieldwork, it was decided that artificial lighting was required for the BRUVS deployments as natural lighting was insufficient at depths below 60 m for cameras to operate effectively. Raytech lights, consisting of 7 royal blue CREE LEDs, were obtained and attached to each BRUV during deployment. A total of 92 deployments were achieved from the planned 100 deployments over four days from 29 April to 2 May 2015 (Figure 37). The parameter MaxN was used as the measure of relative abundance for all subsequent analysis. The MaxN is the maximum number of fish in any one species seen in one segment of video where all fish can be identified as different individuals. This measure prevents repeated counting of the same individual, but may significantly underestimate the abundance of any one species. For key species, the stereo imagery was also used to identify the length of individuals in the MaxN frames.

Based on the BRUV footage it is clear that a variety of fish species and habitats are present in the CMR and adjacent fished regions (Figure 38-Figure 46). While it was not a central aim of this study, the variety of substratum types evident from the BRUV footage within the CMR also provides complimentary information to the AUV images to assist in description and validation of habitats identified from the multibeam sonar surveys. This is particularly valuable for habitat interpretation following the inability to deploy the AUV as widely as planned. These habitats support a variety of commercially important fishes (including striped trumpeter and jackass morwong; Figure 38; Figure 40) as well as a large abundance of butterfly perch (*Caesioperca lepidoptera*), ocean reef perch, red cod, grubfish (*Paraperca* spp), lobster and even the occasional elasmobranch and cephalopod (including arrow squid, *Nototodarus* spp, octopus, seven gill shark and skate; Figure 38-Figure 46). The observation of large schools of juvenile jackass morwong, which are usually associated with estuaries and other shallow-water coastal regions, is of note.

A total of 92 BRUV deployments were achieved, with approximately equal drops in the CMR and in the fished areas. A total of 20929 individual fishes were recorded represented by 47 species from 33 families (Table 7). Of these, 34 species were recorded in the CMR compared to 39 in the fished area. More individuals were recorded inside the CMR (Table 7). The most abundant species were baitfish (Clupeiformes: 12816 individuals), butterfly perch (*Caesioperca lepidoptera*; 3748 individuals), jack mackerel (*Trachurus declivis*; 1100

individuals), splendid perch (*Callanthis australis*; 326 individuals), jackass morwong (*Nemadactylus macropterus*; 316 individuals) and ocean perch (*Helicolenus percoides*; 282 individuals) (Table 7).

While some species were present in high numbers, many of these were pelagic species that are likely to be transient residents of the area. These included the *Trachurus* species (jack mackerel), species in the order clupeiformis (small bait fish), and even yellowfin or bluefin tuna (*Thunnus* sp). The latter could not be differentiated from each other in the imagery.

Of the reef resident species, schooling planktivore species were most abundant, including the splendid perch and butterfly perch. Common and generally widespread species included the ocean perch, jackass morwong, rosy wrasse, cosmopolitan leatherjacket and red cod (*Pseudophycis bachus*), all predominantly benthic feeding species ranging from piscivores to micro-carnivores. Striped trumpeter (*Latris lineata*) were less common, with only 32 individuals encountered (based on MaxN) across the 92 BRUV deployments, despite these deployments being in optimal depth ranges and habitat for this species. Interestingly, draughtboard sharks (*Cephaloscyllium laticeps*) were not commonly encountered either, despite being well represented in lobster potting bycatch.



Table 7. Fish species recorded using BRUVs in the Tasman Fracture CMR and adjacent fished areas based on 92 deployments. Relative abundance was measured using MaxN.

Family	Species name	Common name	Fished	CMR	Habitat preference	Trophic group
Berycidae	<i>Centroberyx sp</i>	Redfish	1	0	Reef/Pelagic	Demersal carnivore
Brachionichthyidae	<i>Brachionichthyidae sp</i>	Handfish	1	0	Reef	Demersal carnivore
Callanthiidae	<i>Callanthias australis</i>	Splendid perch	265	61	Reef/Pelagic	Demersal planktivore
Carangidae	<i>Trachurus declivis</i>	Jack mackerel	670	430	Pelagic	Pelagic carnivore
	<i>Trachurus sp</i>	Mackerel	1331	66	Pelagic	Pelagic carnivore
Centrolophidae	<i>Seriolella brama</i>	Blue warehou	2	0	Pelagic	Pelagic planktivore
Cheilodactylidae	<i>Nemadactylus macropterus</i>	Jackass morwong	102	214	Soft sediment	Demersal invertivore
Congridae	<i>Conger verreauxi</i>	Conger eel	0	2	Reef/Soft sediment	Demersal carnivore
Cyttidae	<i>Cyttus australis</i>	Silver dory	7	74	Reef/Soft sediment	Demersal invertivore
Dasyatidae	<i>Dasyatis brevicaudata</i>	Smooth stingray	1	0	Reef/Soft sediment	Demersal invertivore
Fishes (multi-family)	<i>Blenniidae, Gobiidae, Tripterygiidae</i>	Blenny	0	1	Soft sediment	Demersal planktivore
	<i>Order Clupeiformes -</i>	Baitfish	3252	9564	Pelagic	Pelagic planktivore
Gempylidae	<i>Thyrsites atun</i>	Barracouta	8	0	Pelagic	Pelagic carnivore
Hexanchidae	<i>Notorynchus cepedianus</i>	Broadnose sevengill shark	2	0	Pelagic	Pelagic carnivore
Labridae	<i>Notolabrus tetricus</i>	Bluethroat wrasse	1	0	Reef	Demersal invertivore
	<i>Pseudolabrus rubicundus</i>	Rosy wrasse	105	26	Reef	Demersal invertivore
Latridae	<i>Latris lineata</i>	Striped trumpeter	19	13	Reef/Soft sediment	Demersal invertivore
Macroramphosidae	<i>Notopogon lilliei</i>	Crested bellowsfish	0	5	Reef	Demersal invertivore
Monacanthidae	<i>Meuschenia australis</i>	Brownstriped leatherjacket	3	0	Reef	Browsing herbivore
	<i>Meuschenia scaber</i>	Cosmopolitan	149	11	Reef	Demersal invertivore
	<i>Thamnaconus degeni</i>	Bluefin leatherjacket	20	0	Reef	Demersal invertivore
Moridae	<i>Lotella rhacina</i>	Rock cod	1	0	Reef	Demersal carnivore
	<i>Pseudophycis bachus</i>	Red cod	67	66	Reef	Demersal carnivore



Family	Species name	Common name	Fished	CMR	Habitat preference	Trophic group
	<i>Pseudophycis barbata</i>	Southern codling	5	8	Reef	Demersal carnivore
	<i>Pseudophycis sp</i>	Morid cod	0	2	Reef	Demersal carnivore
Narcinidae	<i>Narcine tasmaniensis</i>	Tasmanian numbfish	0	1	Soft sediment	Demersal invertivore
Neosebastidae	<i>Neosebastes scorpaenoides</i>	Common gurnard perch	8	1	Reef/Soft sediment	Demersal invertivore
Ophidiidae	<i>Genypterus tigerinus</i>	Rock ling	0	1	Reef/Soft sediment	Demersal invertivore
Ostraciidae	<i>Aracana aurita</i>	Shaw's cowfish	1	0	Reef/Soft sediment	Demersal invertivore
Paraulopidae	<i>Paraulopus nigripinnis</i>	Blacktip cucumberfish	1	1	Soft sediment	Benthic invertivore
Pinguipedidae	<i>Parapercis allporti</i>	Barred grubfish	26	76	Soft sediment	Benthic invertivore
Platycephalidae	<i>Platycephalus sp</i>	Flathead	1	0	Soft sediment	Benthic carnivore
Rajidae	<i>Dentiraja lemprieri</i>	Thornback skate	0	1	Soft sediment	Benthic carnivore
	<i>Spiniraja whiteyi</i>	Melbourne skate	4	2	Soft sediment	Benthic carnivore
Scombridae	<i>Thunnus sp</i>	Tuna	88	1	Pelagic	Pelagic carnivore
Scorpaenidae	<i>Scorpaena papillosa</i>	Southern red scorpionfish	1	3	Reef	Benthic invertivore
Scyliorhinidae	<i>Asymbolus rubiginosus</i>	Orange spotted catshark	3	7	Reef	Benthic carnivore
	<i>Cephaloscyllium laticeps</i>	Draught board shark	15	11	Reef/Pelagic	Demersal carnivore
Sebastidae	<i>Helicolenus percoides</i>	Ocean perch	77	205	Reef	Benthic carnivore
Serranidae	<i>Caesioperca lepidoptera</i>	butterfly perch	3011	737	Reef/Pelagic	Pelagic planktivore
	<i>Caesioperca rasor</i>	barber perch	8	5	Reef/Pelagic	Pelagic planktivore
	<i>Caesioperca sp</i>	perch	31	4	Reef/Pelagic	Pelagic planktivore
	<i>Lepidoperca pulchella</i>	Eastern orange perch	0	8	Reef/Pelagic	Pelagic planktivore
Trachichthyidae	<i>Paratrachichthys macleayi</i>	Sandpaper fish	17	11	Reef	Benthic carnivore
Urolophidae	<i>Urolophus cruciatus</i>	Banded stingaree	2	3	Soft sediment	Benthic invertivore
	<i>Urolophus paucimaculatus</i>	Sparsely-spotted stingaree	2	0	Soft sediment	Benthic invertivore
	<b>Total</b>		<b>9308</b>	<b>11621</b>		

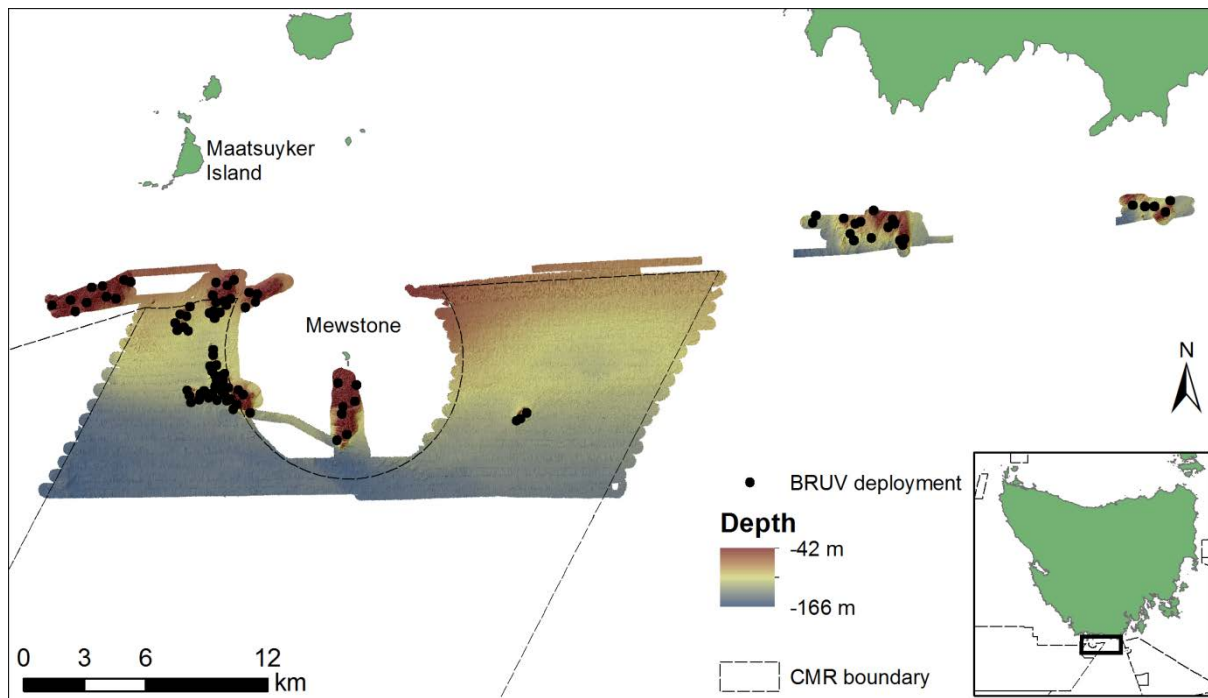


Figure 37. Distribution of the 92 BRUV deployments in the Tasman Fracture CMR and adjacent fished reference areas.



Figure 38. An example of one of the large schools of butterfly perch observed within the Tasman Fracture CMR and adjacent fished reference reefs. Note the striped trumpeter.



Figure 39. An example of one of the abundance of ocean perch and grubfish observed within the Tasman Fracture CMR and adjacent fished reference reefs.



Figure 40. An example of one of the large schools of juvenile jackass morwong observed within the Tasman Fracture CMR and adjacent fished reference reefs. This is an interesting finding as juvenile jackass morwong are thought to be usually associated with estuaries and other sheltered shallow-water regions.



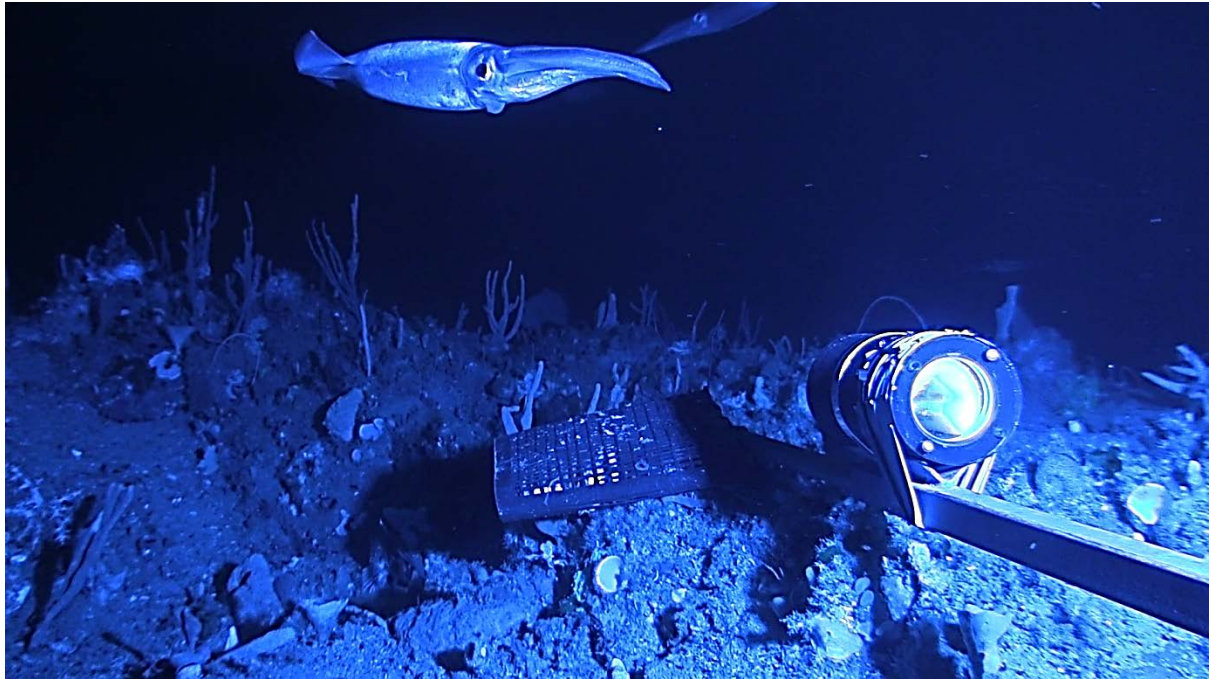


Figure 41. An example of extremely aggressive arrow squid that are commonly observed attempting to predate on other fish around BRUVS within the Tasman Fracture CMR and adjacent fished reference reefs.



Figure 42. An example of one of the large striped trumpeter observed within the Tasman Fracture CMR and adjacent fished reference reefs.



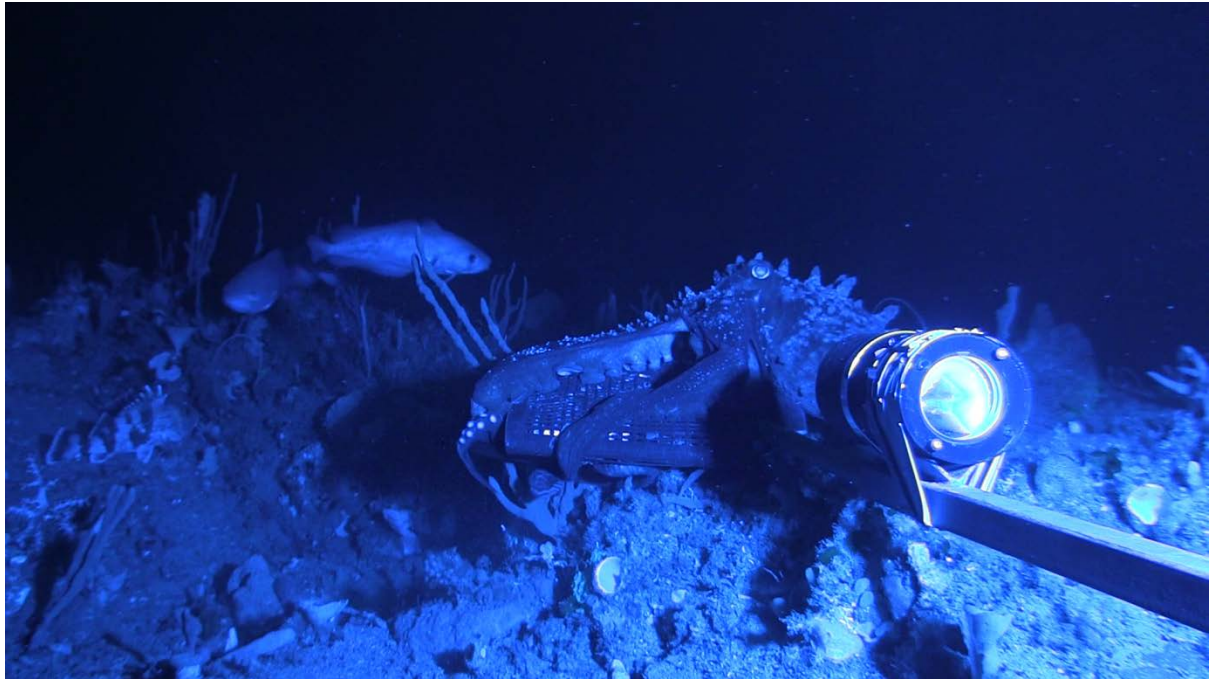


Figure 43. An example of an octopus feeding on the bait on one of the BRUVS deployments within the Tasman Fracture CMR and adjacent fished reference reefs. Note the red cod and reef ocean perch in the background.

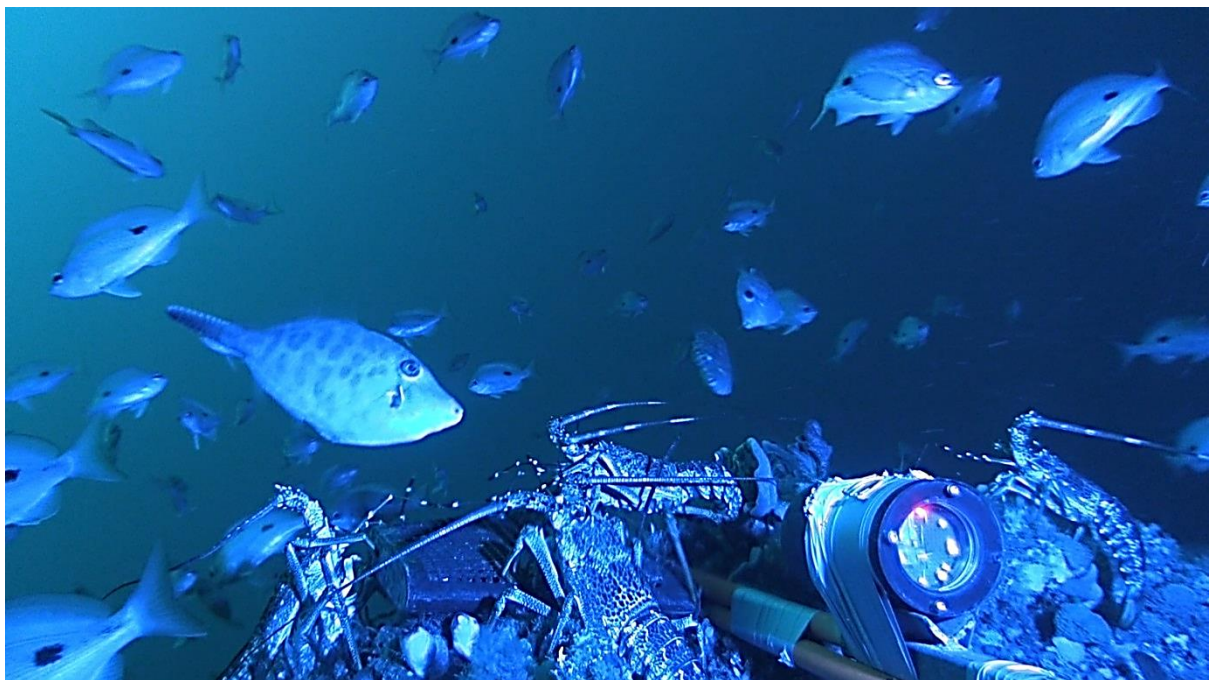


Figure 44. Example of the abundance of lobster attracted to the BRUVS. Note the butterfly perch and cosmopolitan leatherjackets (*Meuschenia scaber*) in the background.



Figure 45. Large seven gill shark (*Notocrynychus cepedianus*), Morid cods (*Moridae*) and jack mackerel (*Trachurus declivis*) attracted to the BRUVS.



Figure 46. Another example of a large elasmobranch (Melbourne Skate; *Spiniraja whitleyi*) attracted to the BRUVS.

### 2.4.1 Distribution of seafloor habitat and substrata type

Although not the primary purpose of a BRUV, bed habitat information can also be extracted. Although the same biological resolution cannot be achieved with the BRUV imagery as from the AUV, this information can be viewed as complimentary, especially considering the limited AUV missions achieved.

Interrogation of this data indicated that 39 % of BRUV deployments landed on solid reef, 33 % on a mixture of reef and sediment, and 28 % landed in sediment substrata (Figure 47). No obvious differences in surveyed substrata type was observed between the CMR and adjacent fished regions (Figure 47).

The broad benthic biological habitat was also scored from the BRUV footage (Figure 48). This data indicated that 33 % of BRUV deployments landed in soft coral dominated habitat, 31 % sponge dominated, 7 % in brittle star dominated. Twenty-eight percent of deployments landed on substrata containing no visible macrobiota. The most striking spatial pattern observed from this data was that the brittle star dominated habitats appear to be found on the reefs surveyed by the AUV. This is not to say they were absent on other deployments, rather did not dominate the assemblage as they did on the reefs west of the Mewstone.

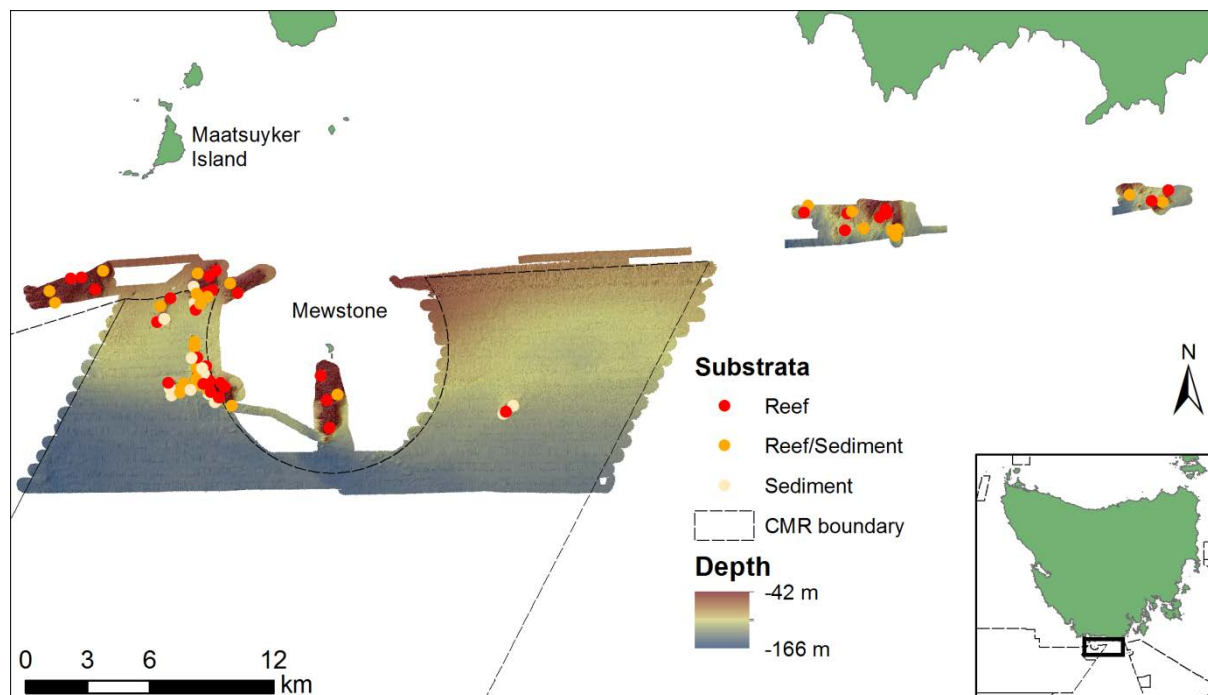


Figure 47. Distribution of broad substrata types surveyed using the BRUVs.

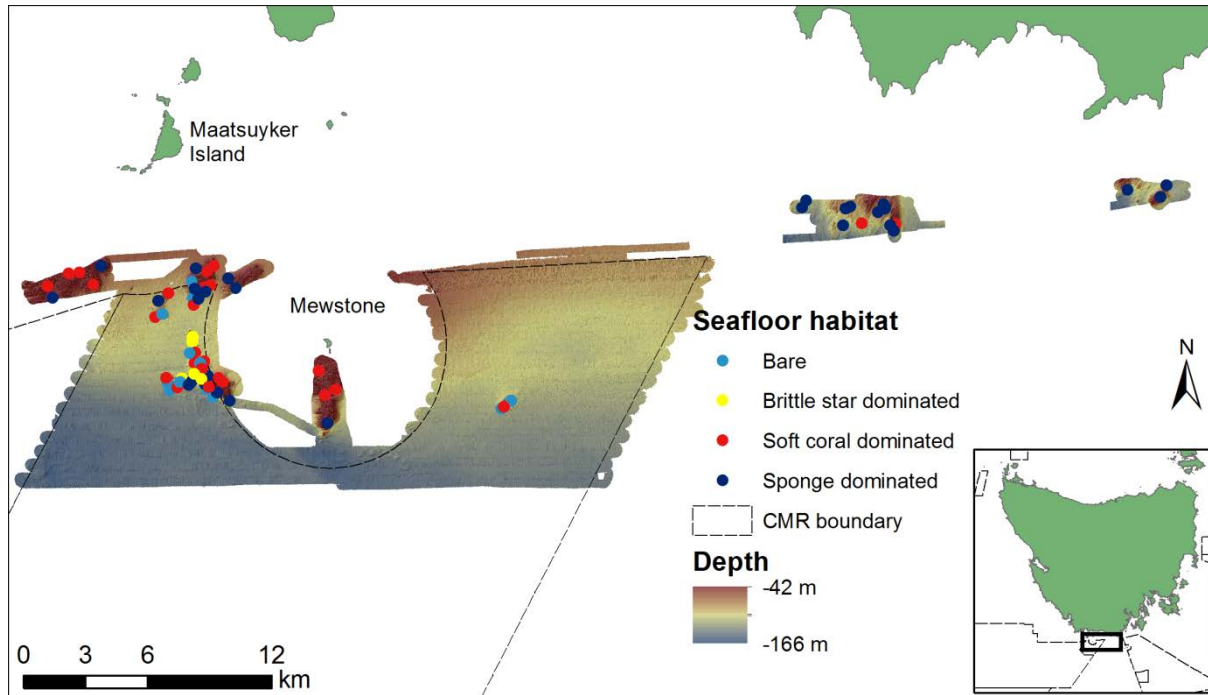


Figure 48. Distribution of broad seabed habitats surveyed using the BRUVs.

## 2.4.2 Length–frequency analysis and abundance maps

Length-frequency plots and abundance maps are shown below for fish species that are potentially affected by fishing pressure and where sufficient numbers were seen and able to be measured from the stereo imagery. These included jackass morwong (*Nemadactylus macropterus*), ocean perch (*Helioclenus percooides*), Morid cods (Moridae), striped trumpeter (*Latris lineata*) and draughtboard shark (*Cephaloscyllium laticeps*), a bycatch species in the lobster fishery.

When examined without accounting for depth related influences on size distribution, with the exception of *L. lineata*, these selected fish species were all smaller in length inside the CMR compared to adjacent fished areas (Table 8).

Table 8. Mean fish length (mm) for selected fish species. The minimum and maximum lengths are provided in parenthesis. Note not all fish were measured thus the addition of number measured column.



	Fished		CMR	
	Mean (Range)	No. measured	Mean (Range)	No. measured
<i>Cephaloscyllium laticeps</i>	576 (369-774)	6	388 (309-466)	5
<i>Helicolenus percoides</i>	219 (78-337)	41	181 (42-307)	85
<i>Latris lineata</i>	609 (488-936)	15	616 (515-743)	6
<i>Nemadactylus macropterus</i>	298 (99-584)	31	137 (40-334)	115
<b>Moridae</b>	320 (78-467)	50	224 (85-592)	52

### *Jackass Morwong (Nemadactylus macropterus)*

There were nearly 2.5 times more jackass morwong inside the CMR compared to adjacent fished areas, with the highest MaxN of 42 inside the CMR (Table 7; Figure 49).

Length-frequency plots that much of this pattern is the result of a significant abundance of juvenile morwong (between 90-150 mm length) that were encountered on deeper reefs within the CMR, a habitat not mirrored within the fished reference sites.

Overall, the length-frequency plot for morwong showed that the CMR was dominated by smaller morwong, with few in larger size categories, while the fished reference areas had substantially more large individuals, albeit at low abundances (Figure 50). Not all individuals could be measured due to camera failure, poor orientation of partial obscuring of one camera. As a result, length frequency graphs do not account for the 88 jackass morwong individuals that could not be measured inside compared the 34 outside. This graph also does not account for depth effects.



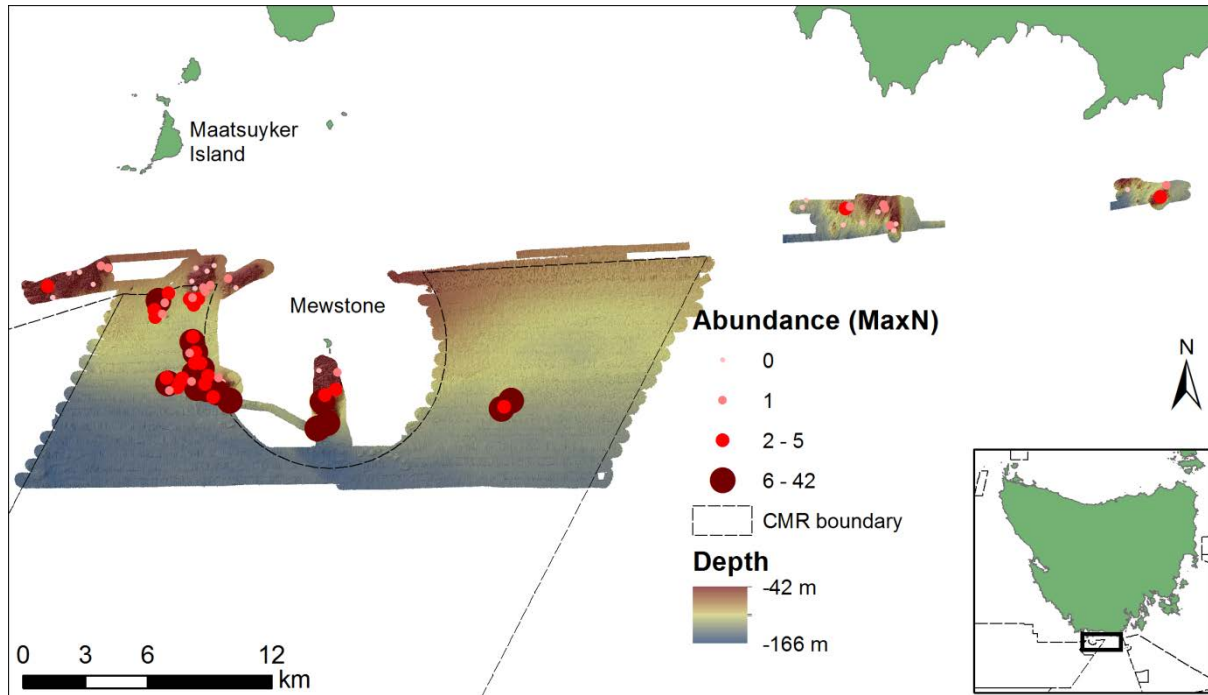


Figure 49. Relative abundance of jackass morwong (*Nemadactylus macropterus*) as measured using BRUVs.

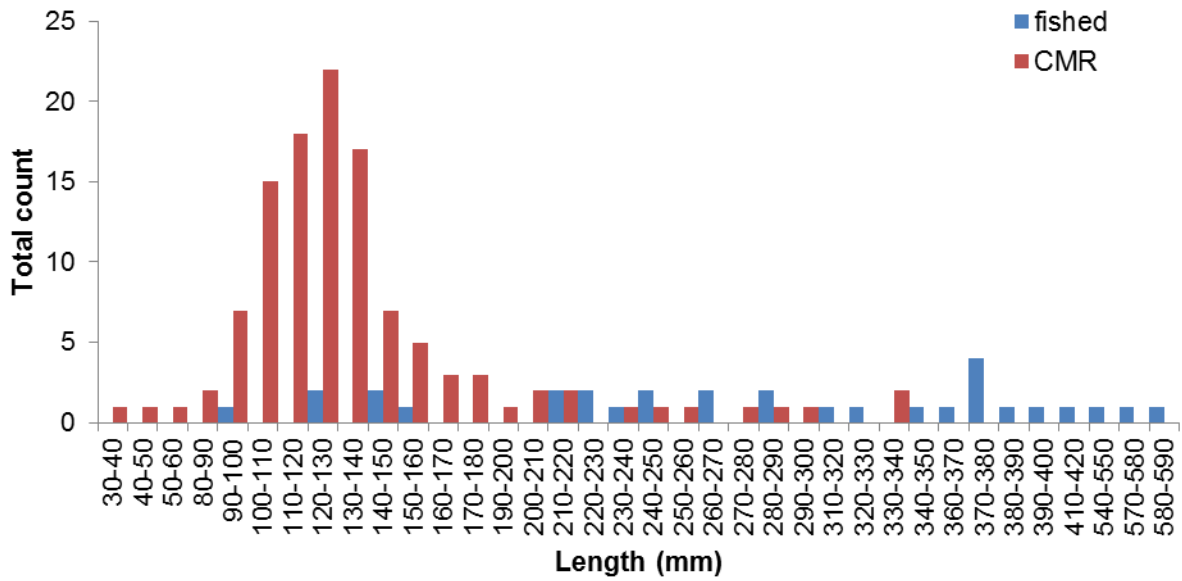


Figure 50. Length-frequencies for jackass morwong (*Nemadactylus macropterus*) as determined using BRUVs.

## Ocean perch (*Helicolenus percoides*)

There were nearly 2.7 times more ocean perch inside the CMR compared to adjacent fished areas, with MaxN of 18 individuals (Figure 51; Table 7) with the reefs inside the CMR west of the Mewstone supporting the highest relative abundances in the region (Figure 51).

When the overall size distribution was examined via length-frequency plots, the distributions had essentially the same shape between the CMR and fished reference locations, indicating no strong protection or depth-related patterns with respect to size (Figure 52).

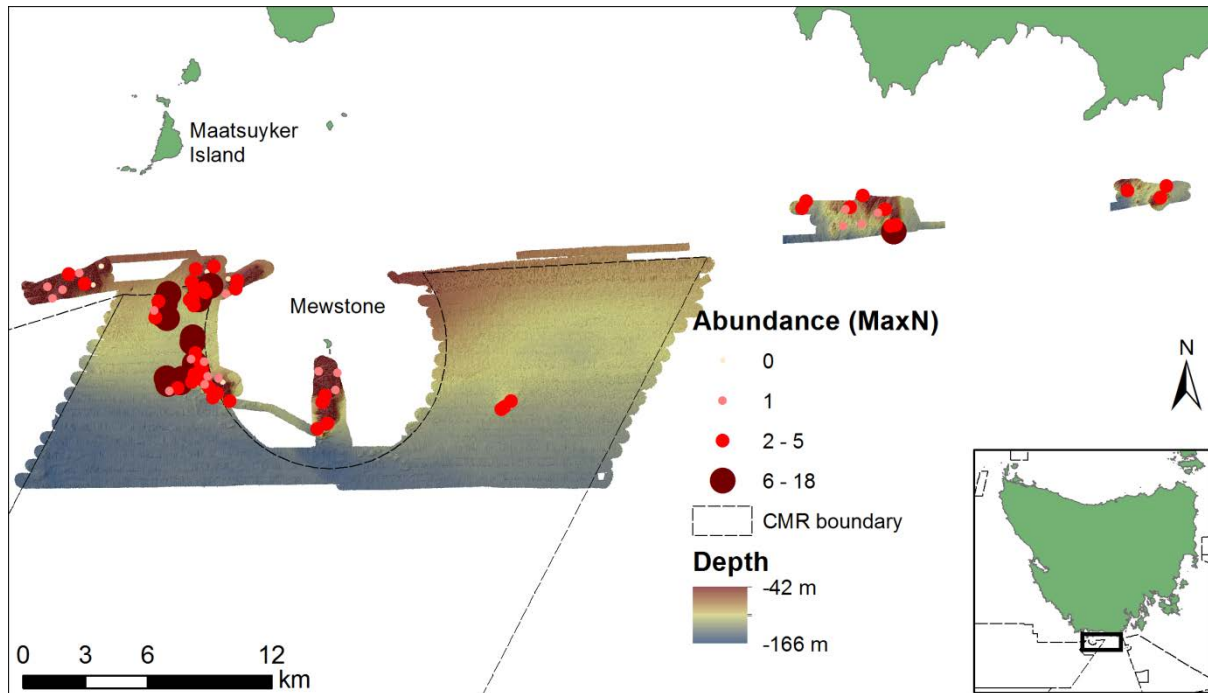


Figure 51. Relative abundance of ocean perch (*Helicolenus percoides*) as measured using BRUVS.



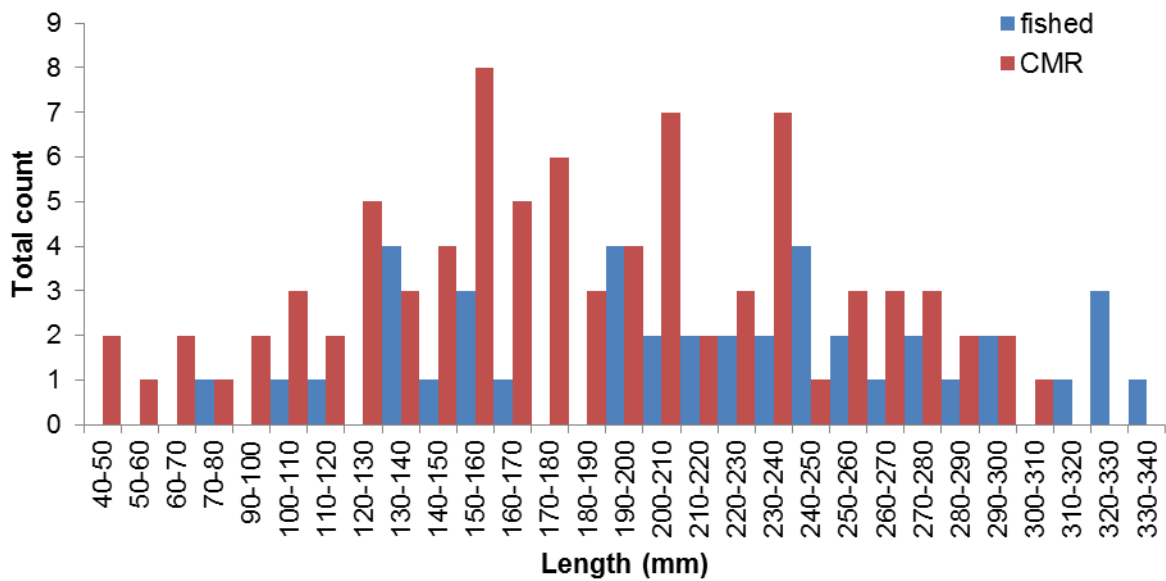


Figure 52. Length-frequencies for ocean perch (*Helioclenus percoides*) as determined using BRUVs.

### Morid cods

The four species of morid cods were combined for subsequent analysis due to relative low abundance and prevalence. No differences in overall abundance were observed for the morid cods with 76 individuals recorded inside the CMR compared to 73 in fished areas (Figure 53).

The length-frequency plots however, suggest that there could be a depth or CMR effect for morid cods, with a cohort of smaller individuals occurring inside in CMR but not in the fished reference areas, while these areas had more of the larger individuals. Of note are the moderate number of individuals 130-170 mm in length found within the CMR, possibly representing juveniles which previously were thought to be found in shallow, sheltered bays and estuaries.

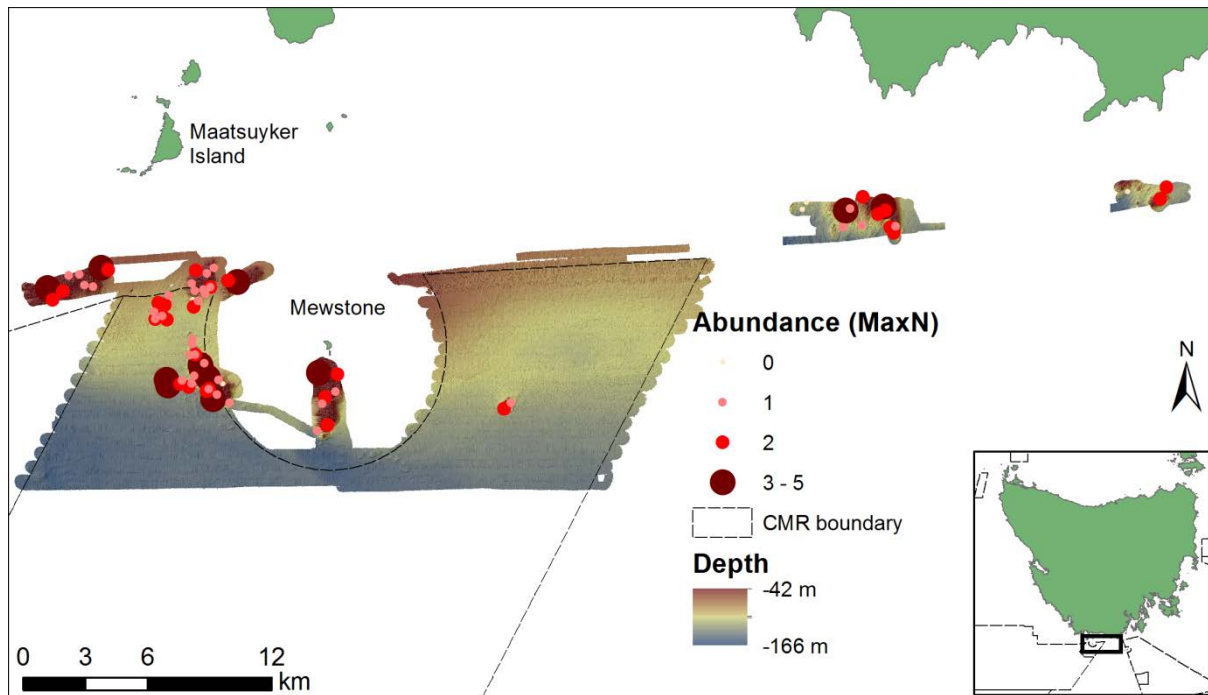


Figure 53. Relative abundance of morid cods as measured using BRUVs.

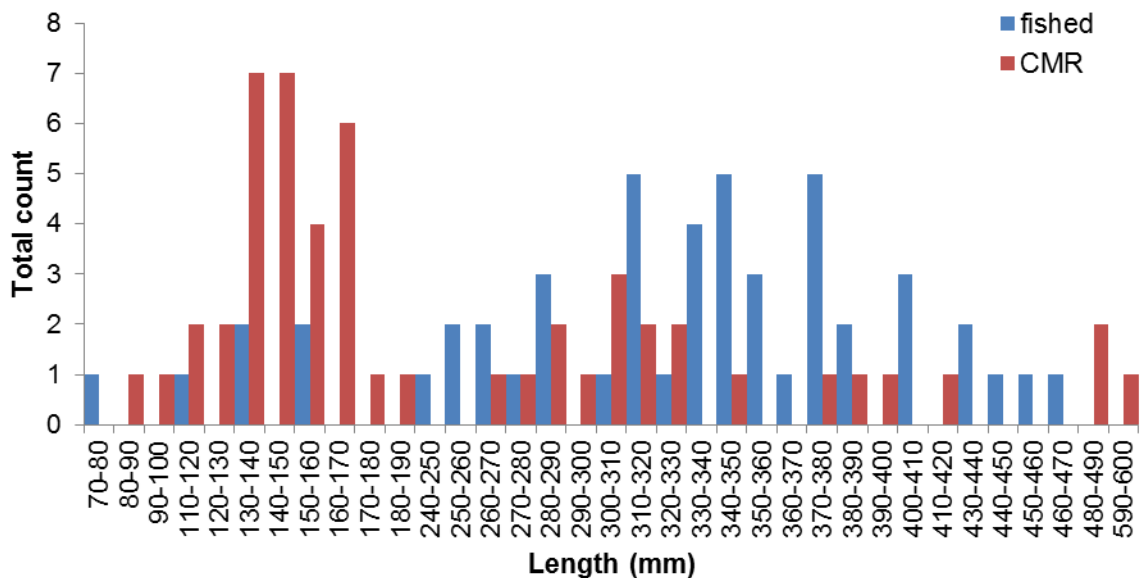


Figure 54. Length-frequencies for morid cods as determined using BRUVs.

### *Striped trumpeter (Latris lineata)*

Striped trumpeter were recorded in relatively low abundance throughout the CMR and adjacent fished areas (19 and 13 respectively), with the distribution of captures shown in Figure 55. At this level of capture, the abundance differences are unlikely to be significant of

biologically meaningful. The largest schools (i.e. 4-6 individuals) were, however, recorded inside the CMR, potentially reflecting habitat effects (depth, reef complexity). Too few individuals could be measured to generate length-frequency plots as not all sighted individuals were able to be sized from the imagery.

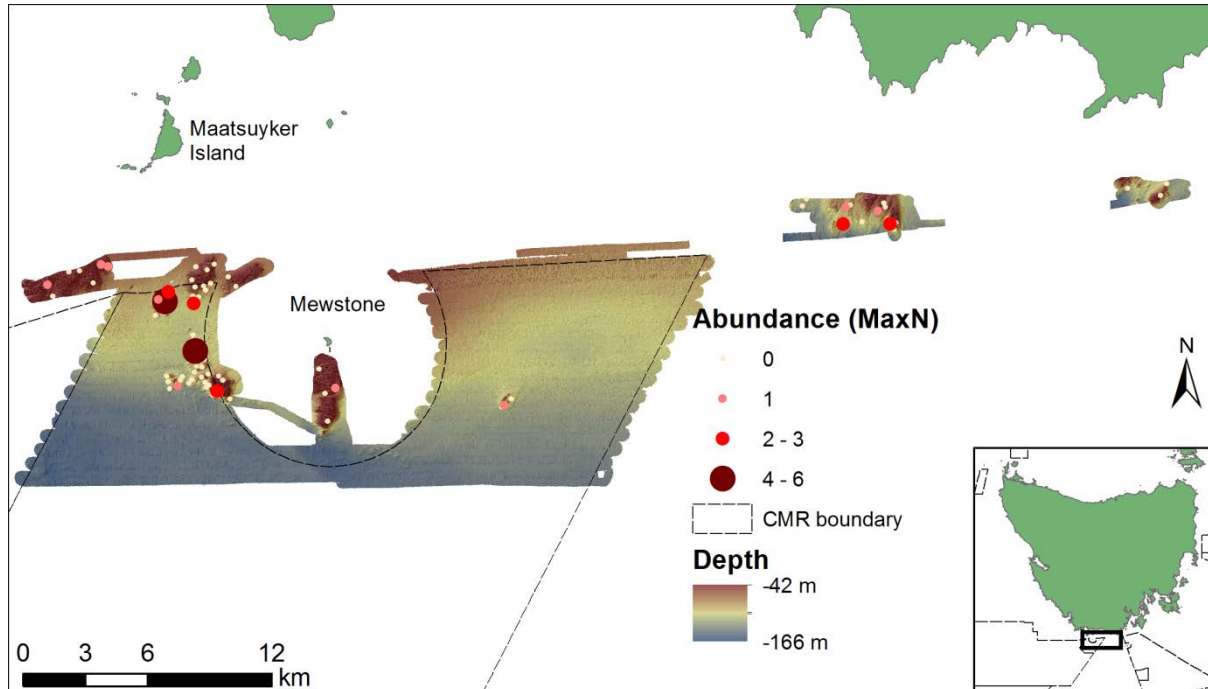


Figure 55. Relative abundance of striped trumpeter (*Latris lineata*) as measured using BRUVS.

### *Draughtboard shark (Cephaloscyllim laticeps)*

Draughtboard shark were recorded in relatively low abundances on the BRUVs with the highest MaxN being two (Figure 56). Roughly equal abundances were recorded inside the CMR compared to the adjacent fished areas, with most individuals being recorded in the shallow reefs of the CMR (Figure 56). There were too few occurrences to generate length-frequency plots.



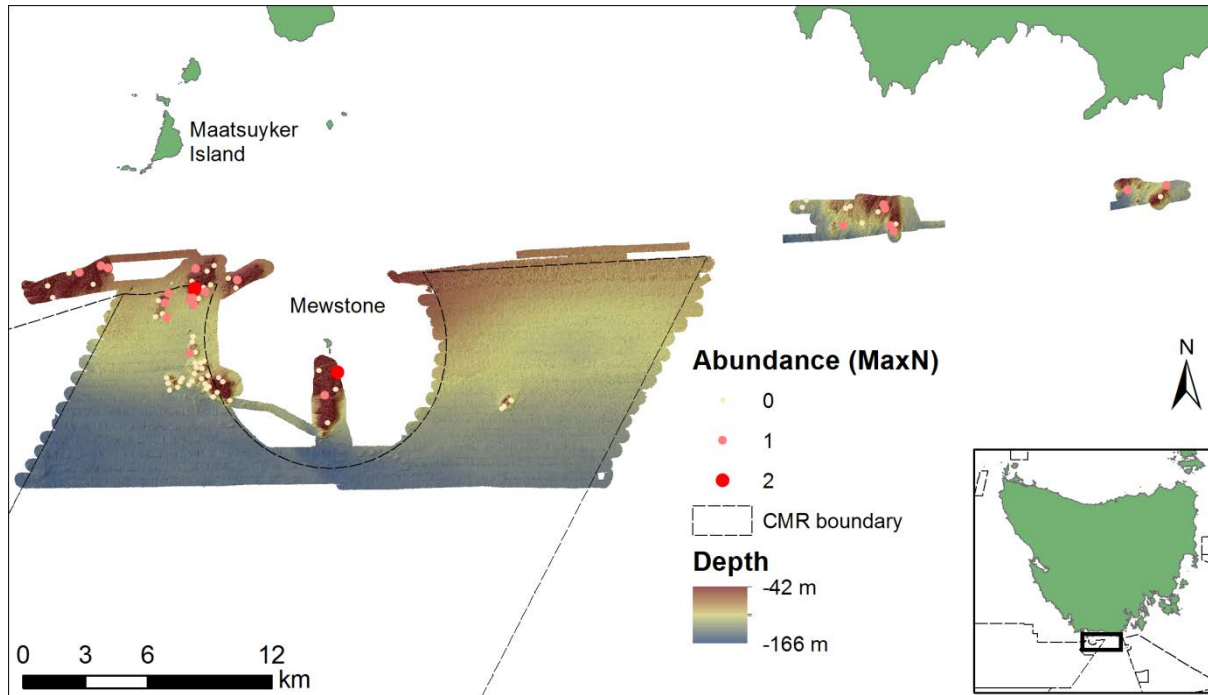


Figure 56. Relative abundance of draughtboard shark (*Cephaloscyllium laticeps*) as measured using BRUVS.

### 2.4.3 Detailed modelling of demersal fish data

Similar to the lobster data, additional model-based analyses were undertaken to further contrast the patterns in fish abundance and size between the CMR and adjacent fished reference reef areas across depth. The overall design of the sampling was based on this model-based analysis as it allows for sampling across a range of depths as well as protection (fished/unfished), including depths within the CMR not represented in the fished areas.

The same Bayesian model-based approach used as in the lobster analysis, and is detailed in Appendix 1. As with the above length-frequency analyses, detailed modelling was only undertaken on select fish species where sufficient data was available to generate meaningful models. These included: jackass morwong, ocean perch, morid cods, striped trumpeter and draughtboard shark.

Table 9 provides a summary of outputs from the model-based analyses on the effects of depth and protection on fish populations. It is important to note that most analyses results had non-statistically important probabilities, and would most probably be a non-significant effect in a traditional hypothesis testing framework with p-values. However, in a Bayesian framework, results greater than a posterior probability of 0.8 do indicate an increasing probability of a positive difference between CMR and fished populations.

Within this context, some interesting patterns in fish abundance, size and gender ratios were observed. These are presented in detail below.

Table 9. Summary of model outputs contrasting protection and depth effects on fishes in and around the Tasman Fracture CMR. Note probabilities are Bayesian probabilities (from 0 to 1) of each effect. Values >0.95 or <0.05 are considered statistically strong. Values >0.8 or <0.2 indicate increasing strength of the trend. For abundance the CMR effect is a multiplicative on a response scale. For average size the CMR effect is additive on a response scale. \* denotes statistically important result.

Species	Analysis	Probability	CMR effect	Depth effect
<i>Cephaloscyllium laticeps</i> (Draughtboard shark)	Abundance	0.73	2.33	General decrease with increasing depth
	Average size	0.48	-0.16	No clear effect
<i>Nemadactylus macropterus</i> (Jackass morwong)	Abundance	0.86	3.20	General increase with increasing depth
	Average size	0.46	-0.33	No clear effect
	Abundance of large sized fish	0.86	7.01	No clear effect
Moridae (Morid cods)	Abundance	0.94	2.05	Peak at c 60-80 m
	Average size	0.48	-0.19	No clear effect





<i>Helicolenus percoides</i> (Ocean perch)	Abundance	0.89	1.66	Two peaks in abundance, one at ~60 m and another at ~120 m
	Average size	0.48	-0.12	No clear effect
<i>Latris lineata</i> (Striped trumpeter)	Abundance	0.95 *	15.03	Peak at ~90 m
	Average size	0.48	-0.11	No clear effect
	Abundance of large sized fish	0.92	11.56	Peak at ~90 m

### *Effect of protection and depth on the abundance of key demersal fishes*

The subsequent figures (Figure 57-Figure 61) show the effects of depth and protection on fish abundance.

Depth had varying effects on the abundance of demersal fishes. For example, abundance of jackass morwong generally increased with increasing depth (Figure 57). By contrast, the abundance of morid cods, striped trumpeter and draughtboard sharks all appeared to be greatest in the shallow regions (c 60-80 m; Figure 59, Figure 60, Figure 61). The abundance of ocean perch showed a slightly different response to depth with two peaks in abundance, one at ~120 m and another at ~60 m (Figure 58).

Model-based analyses suggested that there was a positive effect of protection on the abundance of many of the demersal fish examined here. On a species by species basis, and accounting for depth related differences between sampling locations and treatments, jackass morwong was modelled to be 3.2 times more abundant within the CMR than the adjacent fished areas, ocean perch 1.7 times, Morid cods 2.1 times, striped trumpeter 15.0 times, and draughtboard sharks 2.33 times more abundant. With exception to overall abundance of striped trumpeter and Morid cods the probabilities associated with these estimates are not particularly strong, however, there is an indication that distinct patterns exist for jackass morwong and ocean perch, and that these patterns are also seen in the average size of jackass morwong and striped trumpeter. However, repeat surveys through time are required to validate the overall strength and temporal stability of these inferred patterns.



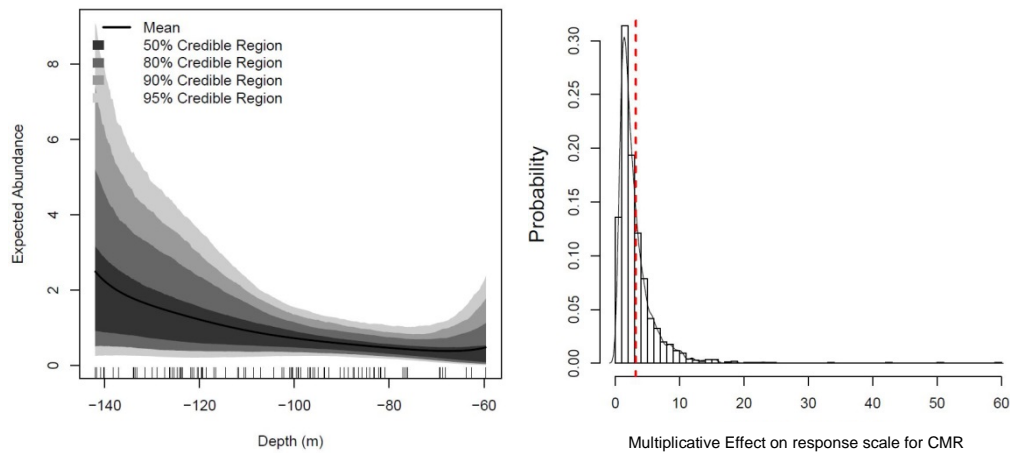


Figure 57. Depth (left) and protection (right) effects on abundance of jackass morwong (*Nemadactylus macropterus*). Solid line in left plot is the mean of the expected abundance and shading gives some point-wise credible intervals. Values greater than one in right plot imply greater abundance inside the CMR. Histogram and smoothed density are taken from the posterior samples. Dashed red vertical line is the mean estimate.

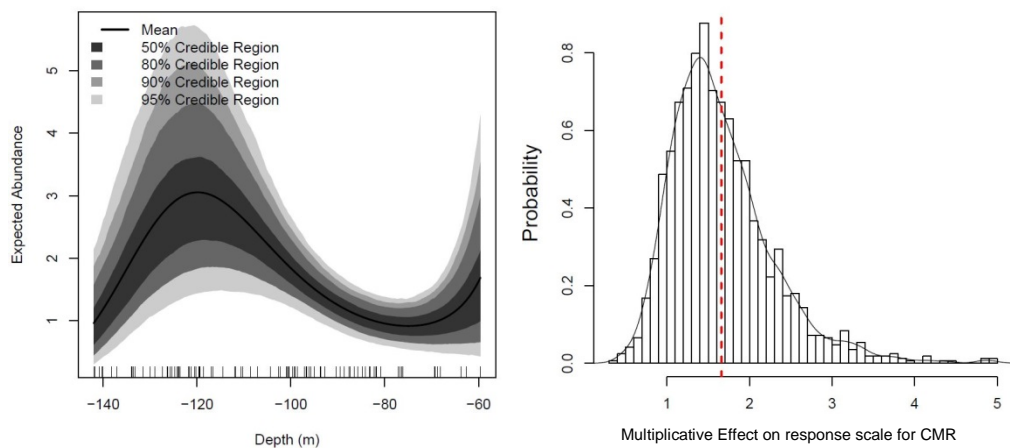


Figure 58. Depth (left) and protection (right) effects on abundance of ocean perch (*Helicolenus percoides*). Solid line in left plot is the mean of the expected abundance and shading gives some point-wise credible intervals. Values greater than one in right plot imply greater abundance inside the CMR. Histogram and smoothed density are taken from the posterior samples. Dashed red vertical line is the mean estimate.

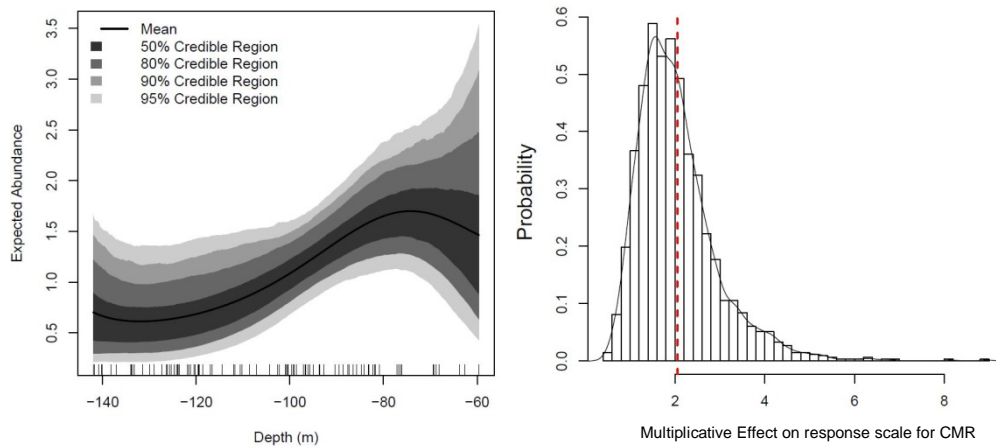


Figure 59. Depth (left) and protection (right) effects on abundance of morid cods. Solid line in left plot is the mean of the expected abundance and shading gives some point-wise credible intervals. Values greater than one in right plot imply greater abundance inside the CMR. Histogram and smoothed density are taken from the posterior samples. Dashed red vertical line is the mean estimate.

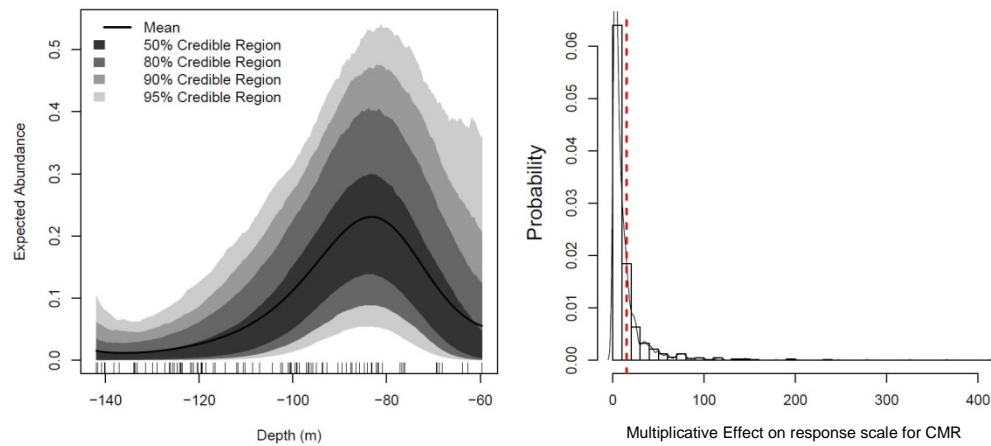


Figure 60. Depth (left) and protection (right) effects on abundance of striped trumpeter (*Latris lineata*). Solid line in left plot is the mean of the expected abundance and shading gives some point-wise credible intervals. Values greater than one in right plot imply greater abundance inside the CMR. Histogram and smoothed density are taken from the posterior samples. Dashed red vertical line is the mean estimate.

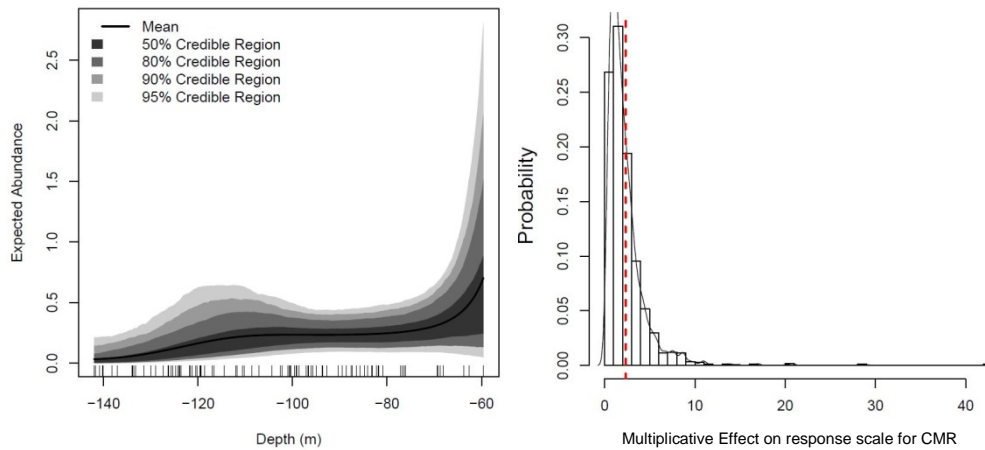


Figure 61. Depth (left) and protection (right) effects on abundance of draughtboard shark (*Cephaloscyllium laticeps*). Solid line in left plot is the mean of the expected abundance and shading gives some point-wise credible intervals. Values greater than one in right plot imply greater abundance inside the CMR. Histogram and smoothed density are taken from the posterior samples. Dashed red vertical line is the mean estimate.

### Effect of protection and depth on the mean size of key demersal fishes

The subsequent figures (Figure 62-Figure 66) show the effects of depth and protection on the mean size of the key fish species examined here.

The model-based analysis suggested that there was no strong variation in size with depth in any of the species examined (Figure 62-Figure 66). Similarly, only a very slight protection effect on mean fish size was evident (negative, close to zero), meaning that on average, fish were slightly smaller inside the CMR relative to adjacent fished areas.

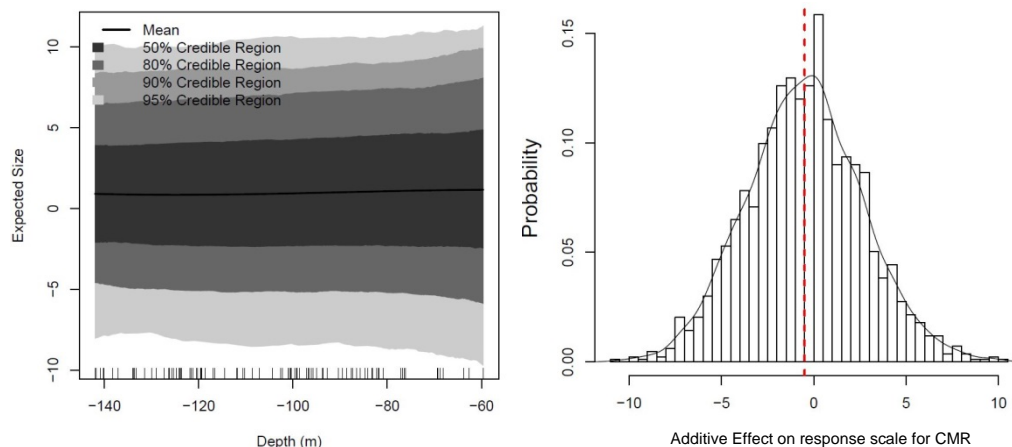


Figure 62. Depth (left) and protection (right) effects on mean size of jackass morwong (*Nemadactylus macropterus*). Solid line in left plot is the mean of the expected size and shading gives some point-wise credible intervals. Values less than zero in right plot imply smaller fish inside the CMR. Histogram and smoothed density are taken from the posterior samples. Dashed red vertical line is the mean estimate.

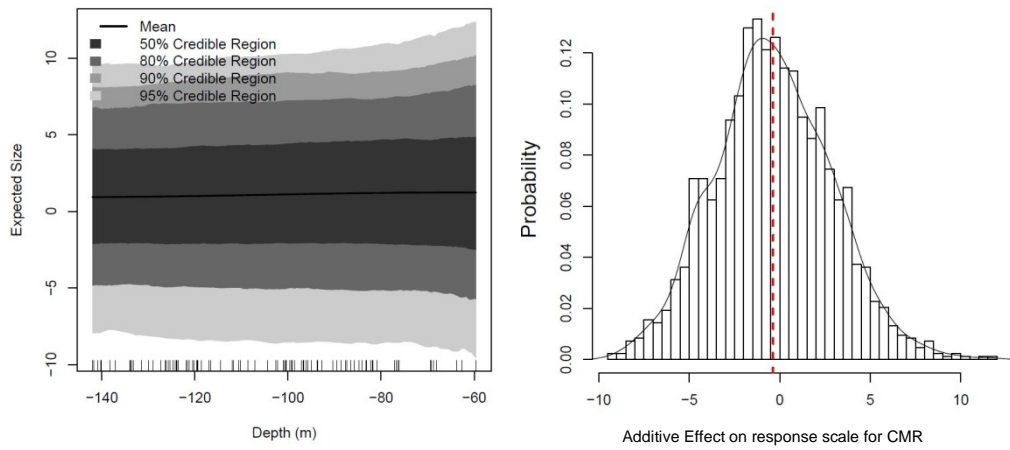


Figure 63. Depth (left) and protection (right) effects on mean size of ocean perch (*Helicolenus percooides*). Solid line in left plot is the mean of the expected size and shading gives some point-wise credible intervals. Values less than zero in right plot imply smaller fish inside the CMR. Histogram and smoothed density are taken from the posterior samples. Dashed red vertical line is the mean estimate.

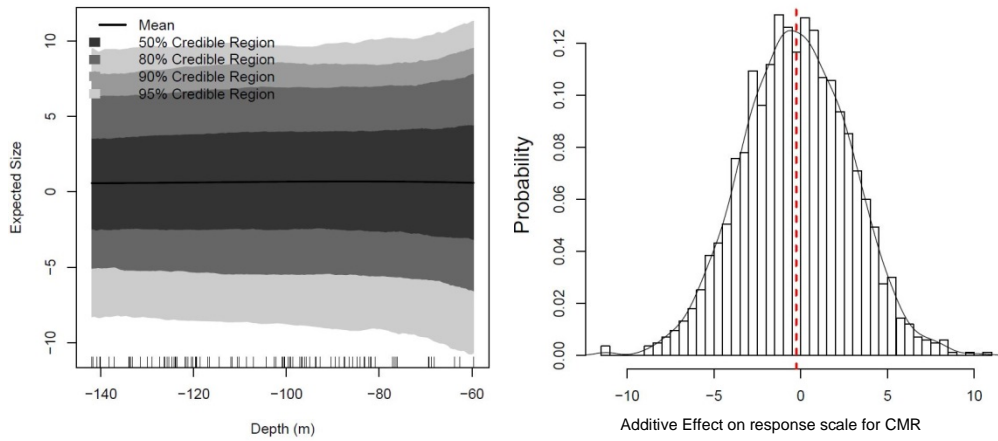


Figure 64. Depth (left) and protection (right) effects on mean size of morid cods. Solid line in left plot is the mean of the expected size and shading gives some point-wise credible intervals. Values less than zero in right plot imply smaller fish inside the CMR. Histogram and smoothed density are taken from the posterior samples. Dashed red vertical line is the mean estimate.

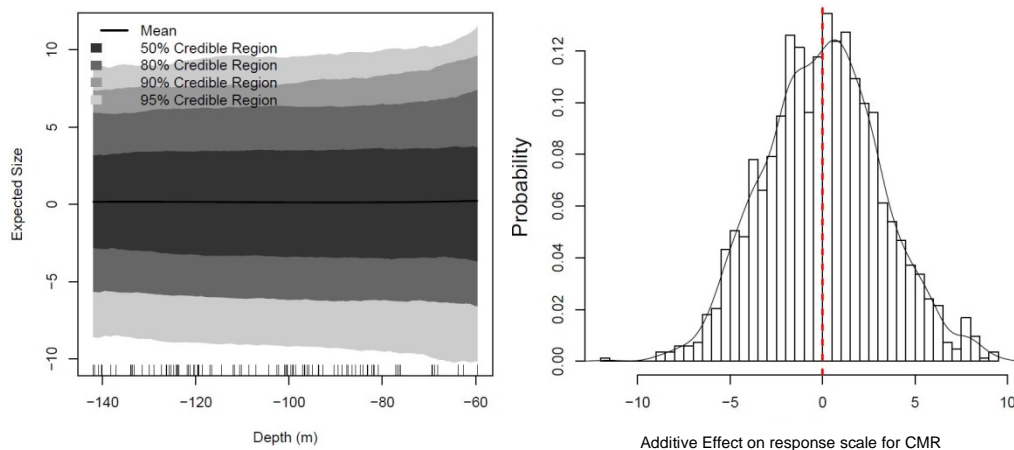


Figure 65. Depth (left) and protection (right) effects on mean size of striped trumpeter (*Latris lineata*). Solid line in left plot is the mean of the expected size and shading gives some point-wise credible intervals. Values greater than zero in right plot imply larger fish inside the CMR. Histogram and smoothed density are taken from the posterior samples. Dashed red vertical line is the mean estimate.

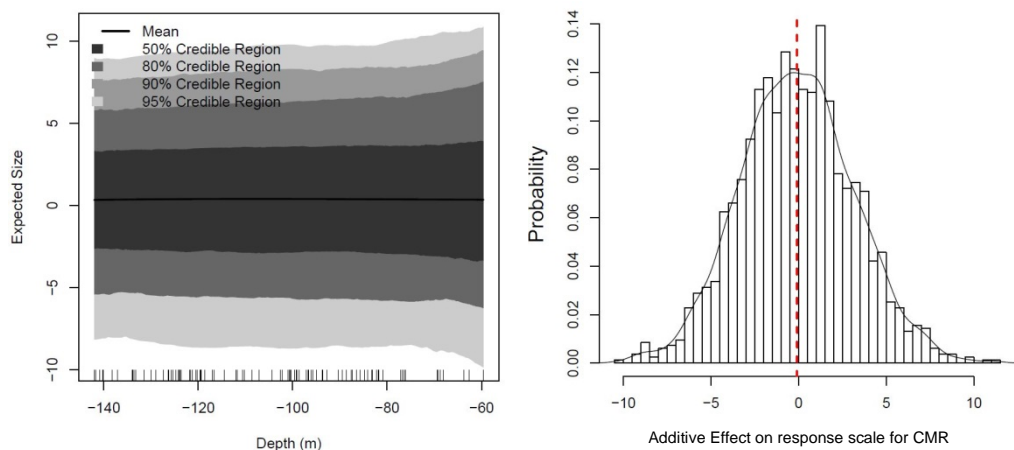


Figure 66. Depth (left) and protection (right) effects on mean size of draughtboard shark (*Cephaloscyllium laticeps*). Solid line in left plot is the mean of the expected size and shading gives some point-wise credible intervals. Values less than zero in right plot imply smaller fish inside the CMR. Histogram and smoothed density are taken from the posterior samples. Dashed red vertical line is the mean estimate.

### *Effect of protection and depth on the abundance of large-sized fish key demersal fishes*

Since fishing is generally size selective, and most abundance data is dominated by small juvenile fish that are not targeted by fishing gear, model-based analysis was also undertaken to determine if larger-sized fish differed across depth and with protection. For this analysis we only modelled two of the key fish species that are known to be directly targeted by fishing effort in the region and were of sufficient ranges of lengths. We applied a size threshold of 140 mm for jackass morwong as individuals below this size limit are most likely juveniles.

The second fish species, striped trumpeter, the size threshold of 550 mm was set as the size limit.

The model-based analysis on the abundance of large-sized jackass morwong suggested that there was a very small peak in abundance at 60 m (Figure 67). The model-based analysis also suggested that there was a positive protection effect (0.84) (Figure 67), with the 7 times more large sized jackass morwong (i.e. > 140 mm) inside the CMR.

The abundance of large-sized striped trumpeter showed similar variations with depth to that of the analysis based on overall abundance for this species, with a monotonic peak in abundance around 90 m (Figure 68). Protection had a moderately strong positive effect (0.92). The model indicated 11.6 times more large-sized striped trumpeter (i.e. >550 mm) inside the CMR compared to adjacent fished regions.

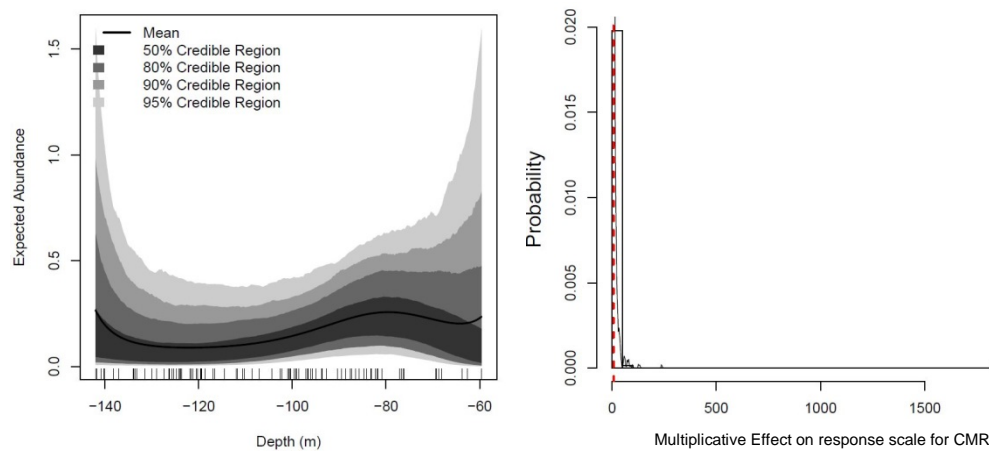


Figure 67. Depth (left) and protection (right) effects on the abundance of large-sized jackass morwong (*Nemadactylus macropterus*). Solid line in left plot is the mean of the expected abundance of large-sized fish and shading gives some point-wise credible intervals. Values greater than one in right plot imply greater abundance of large-sized fish inside the CMR. Histogram and smoothed density are taken from the posterior samples. Dashed red vertical line is the mean estimate.

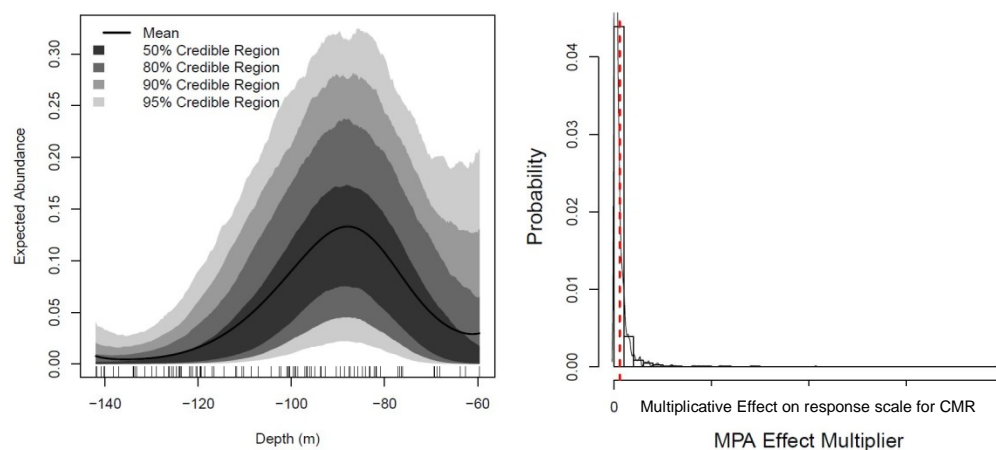


Figure 68. Depth (left) and protection (right) effects on the abundance of large-sized striped trumpeter (*Latris lineata*). Solid line in left plot is the mean of the expected abundance of large-sized fish and shading gives some point-wise credible intervals. Values greater than one in right plot imply greater abundance of large-sized fish

inside the CMR. Histogram and smoothed density are taken from the posterior samples. Dashed red vertical line is the mean estimate.





## 2.5 Discussion

Overall this study has contributed a considerable advance in our understanding of the seabed habitats and epibenthic species assemblages within the Tasman Fracture CMR and surrounding region, one that should be of value to both CMR and marine resource management.

### 2.5.1 Seabed mapping

The seabed mapping program using MBS provided a substantial improvement in our knowledge of the extent and distribution of reef and soft sediment systems within the region, including the offshore extent of coastal reef systems surrounding major regional feature such as South Cape, South East Cape, and offshore islands like The Mewstone. Of particular note were the observations that extensive reef systems extend off many of these features and provide significant habitat for many reef species, including the commercially targeted southern rock lobster. These systems, however, appear to generally be limited to 100 m maximum depth, potentially reflecting historical sea-levels and their influence on erosion of continental rock features, and deposition of sediment. The regional exception to this appears to be within the Tasman Fracture CMR, where a number of reef systems extent to depths of approximately 140 m. Overall though, such reef systems were a quite rare feature within the CMR and were restricted to the northern shelf region of the CMR, with the vast majority of the shelf region being composed of what appears to be soft sediments. Subsequent to the initial survey, a complimentary survey undertaken by CSIRO staff on the *R.V. Investigator* mapped the remaining habitat to the shelf-break, and found that it was composed entirely of soft sediments. While the area of continuous reef within the CMR was quite restricted, a broad region in the NE sector appeared to be strongly influenced by transported and mobile sediment/gravel/cobble at depths less than approximately 140 m. Presumably this is a depth zone subject to strong influence of swell action and currents, factors that at times, are able to actively transport the seabed material to form extensive dune systems and expose isolated patches of bedrock.

The biological sampling was based around a comparison of benthic biology within the CMR with that found in adjacent fished habitat of similar nature. However, this was somewhat limited from the outset due to the reef within the CMR being dominated by reef from 100 -140 m depth, whereas reef mapped outside the CMR was essentially restricted to 100 m depth due to an absence of reef at comparable depths to the CMR being found within the region. While such reef may be present in isolated outcrops, its presence wasn't indicated by previous mapping in the region, and there was insufficient time available to search for this during the study. This limitation will be discussed further later, however, finding and mapping suitable control reef systems of equivalent depth to the CMR reef systems is a high priority to underpin further monitoring programs.



## 2.5.2 Rock lobster

The lobster potting program was particularly effective in demonstrating the efficiency of a targeted sampling program to estimate abundances (catch) and size distributions of a known top predator and a key ecological species. Robust data was generated by the study, and provided new quantitative knowledge of the distribution of lobsters across the shelf and with depth in this region. It clearly demonstrated that lobster abundances drop off markedly below 100 m depth, and as the majority of reef within the CMR was deeper than 100 m, it predominantly represented sub-optimal habitat for this species. From the raw data overall abundances were found to be substantially higher in the fished reef systems as a result of this strong imbalance in sampling between shallower (50 - 100 m) depth reefs within fished areas, and the deeper (to 140 m) depth reefs within the CMR. When this depth imbalance was taken into account in the model-based analysis, a strong CMR effect was observed with the CMR predicted to support 3.68 times more lobster than adjacent fished areas. There was also a marked shift towards larger lobsters within the reserve relative to overall numbers in males, suggesting a slight effect of protection. Of note, was a similar trend for females, that despite females rarely being removed by the fishery (due to insufficient growth to reach legal size), the females were proportionally larger within the CMR and more abundant. This may be the result of a number of factors, including capture related mortality of sub-legal lobsters repeatedly caught and discarded in the fishery, or depth related gradients in density and food availability, and this pattern warrants further investigation from a fishery management perspective. The current dataset provides a robust baseline from which to document further protection-related trends through time, and a range of insights into lobster population demographics within this region to underpin further research. On the shallower reefs, it also indicates that lobsters are an abundant predator in this system (with in excess of 50 individuals per pot on some lifts) and are likely to play a major role in the functioning of benthic ecosystems in this region. However, as lobster abundance was significantly influenced by depth, future studies in this region will need to focus on identifying and sampling matching areas of deep reef within fished habitats to contrast better with the CMR, and/or focus on the current reef systems where depths are similar.

## 2.5.3 Benthic invertebrate assemblages

With 149 morphospecies identified from 261 of the AUV derived images (based on 25 random points per image), the Tasman Fracture CMR deep reef assemblage was quite diverse, but many of these morphospecies were relatively rare, with nearly 50 % only encountered once or twice across all images. This pattern of local rarity is increasingly being seen as typical of diverse deep reef systems as more regions around Australia are examined via image-based sampling. Interestingly, very few morphospecies had more than 1 % cover, suggesting that from an indicator perspective, detection of change in any particular species through time would need to focus either on large sample sizes of random imagery scored at the biodiversity level, or alternatively have sampling focussed on scoring only indicator species within image subsets. Key indicator species for this area would potentially be soft corals and other coral forms, as the Tasman Fracture CMR had a substantially greater coral cover than seen in other deep cross-shelf reef systems examined within SE Australia, where sponge cover typically dominates below algal depths. The comparison of the Tasman



Fracture CMR benthic invertebrate assemblage with those from comparable depths within the Huon, Freycinet and Flinders CMRs indicated that each represented a distinctly different assemblage, with each reserve contribution to the overall representation of biodiversity within the region. As discussed above, the predominance of soft corals differentiated the Tasman Fracture CMR assemblage, as did the high abundance of brittle stars; a feature rarely seen elsewhere in AUV-based surveys on shelf reef systems in Australia. Presumably these features relate to the unique ecosystem function and trophic pathways of this region, with these relationships now able to be modelled from our quantitative abundance data and tested through future experimental approaches. However, it should also be noted that based on the BRUV deployments the dominance of the brittle stars appeared to be mostly constrained to the reefs surveyed by the AUV located directly to the west of the Mewstone. Although seen on other BRUV deployments, the question remains to how widely distributed the brittle stars are throughout the Tasman Fracture CMR.

Overall, while the AUV component of this study was less successful than planned, the knowledge gained from the reef systems that were able to be sampled was invaluable in gaining an initial insight into the deep reef assemblages found within this region, and providing a first understanding of how these assemblages are structured. Despite the difficulty of operating in such difficult environments, further AUV surveys over the originally proposed extent of coverage remain a high priority for future research, to both ensure the patterns seen here are generalizable over the remaining CMR reef systems, and to provide a comparison with adjacent fished reference reef systems to understand the extent that such patterns are regionally representative and may be influenced by system-wide effects of fishing. While the latter effects are not expected to be seen at this early stage of protection, an early baseline is essential in the longer term for differentiating such effects from natural spatial variation due to local habitat effects.

#### 2.5.4 Fish assemblages

This study provided the first quantitative description of the demersal fish assemblages of the Tasman Fracture CMR and surrounding shelf reef systems, as well as an indication of the range of pelagic fish species that are associated with the region and found in CMR waters. The overall collection of species seen ranged from small handfish to large tuna. However, from the perspective of inventory of potentially resident species, and those most likely to derive benefit from the no-take zone of the CMR, it is the demersal species that make up the most likely indicator species for change through time. Not surprisingly, the schooling planktivorous species such as splendid and butterfly perch dominated these, indicating, as seen elsewhere on deep reefs surveyed in the SE region, that plankton provides a significant component of the pelagic to benthic coupling on these deep reef systems. The remaining demersal assemblage was fairly mixed, with no particular species dominating.

While the commercially targeted species, striped trumpeter, were anticipated to be moderately abundant on these deep reef systems based on patterns seen at similar depths within the Flinders CMR, they were relatively rare within this region, with only 32 encountered from the 92 BRUV deployments. Despite the low capture rate, the model-based analysis suggested this species was likely to be more abundant within the CMR at comparable depths, and with a greater abundance of large individuals. It must be stressed that a



considerably larger sample size is needed to improve confidence in this result if this species is to be used as a reliable indicator of the effects of protection. Another commercially targeted species (by trawl) the jackass morwong, was encountered in larger numbers (316) and on most BRUV deployments, and had a similar pattern to the trumpeter, being both more abundant within the CMR and having a greater proportion of larger individuals there. Due to the larger sample size, the results from the morwong are likely to be more robust than the trumpeter. However, in both cases additional replication would enhance the confidence in these trends.

As for the lobster results, the overall interpretation would be significantly enhanced if sampling was able to be evenly distributed across matching depth categories within both the CMR and reference locations, hence finding and mapping suitable reference reef system in depths from 100 to 140 m within this region is a priority action for implementation of longer term monitoring programs. Likewise, building confidence that the patterns observed relate to protection effects requires both a time series of observations to document protection-related trends, and ideally, additional replication to improve confidence in the trends seen. Ideally, these repeated observations would initially be at biologically meaningful periods (approximately 5 years), with additional replication requirements based on power analysis of the baseline data obtained here.

### 2.5.5 Conclusion

In summary, this study has been highly successful in providing a first baseline understanding of the types of habitats that characterise the Tasman Fracture CMR sanctuary zone on the shelf, and the species associated with rocky reef systems within the CMR and surrounding fished region. By utilising a range of quantitative sampling techniques, coupled with a strong model-based design, we have been able to provide robust estimates on the abundance (catch) and distribution of southern rock lobsters, reef-associated fish assemblages and benthic invertebrate cover of the reef systems. These provide considerable insights into the ecosystem functioning of these deep reef systems, where the abundance of lobsters suggest they play a significant role in structuring such systems, and the abundance of brittle stars and soft corals provide hints of the trophic pathways within these systems. The model-based analysis suggested there were protection-related patterns in the abundance of lobsters, including large male lobsters, as well as the overall abundance and proportion of large-sized individuals within several targeted fish species. Such changes are not unexpected given the CMR sanctuary zone has been protected from fishing for over seven years in an area subject to significant fishing pressure for lobsters in particular. However, as this was a “snapshot” study, these results need confirming through a time-series to fully differentiate protection related differences from those relating to spatial differences. Likewise, due to overall differences in the depths able to be sampled between the CMR and reference areas (relating to a lack of mapped reef below 120 m outside the CMR), this study required model-based designs to allow us to both derive a spatially-balanced survey of the CMR reef systems, as well as contrast changes with adjacent fished areas. We recommend that a similar study be undertaken at a biologically meaningful interval (approximately 5 years), and that in the intervening period, suitable reference reefs at depths of between 100-140 m be identified and mapped as a priority to allow depth stratified sampling to be undertaken in the future to more robustly differentiate depth related and protection related effects.



## 2.6 Summary of key findings

### 1. Seafloor mapping:

- The collection of fine-scale MBS has enabled the identification of reefs within the CMR. These reefs are generally sparse relative to soft-sediment habitats within the CMR, and are generally deeper than typical reef systems within this region. Of note, was the identification of what appears (based on the backscatter and limited exploration BRUV deployments over the region) to be a large expanse of mixed sediments (including cobble, large and small sand ripples) and low-profile reefs on the NE region of the CMR that is a complex habitat feature not previously seen during MBS mapping of Australia's continental shelf waters.
- The fine-resolution of the MBS thus provides us with a detailed inventory of seafloor features which were subsequently used to prioritize the sampling designs for lobster, benthic biota and fish surveys.

### 2. Lobster:

- Overall abundances (catch) per pot-lift were generally markedly lower within the CMR relative to the fished reference locations, driven by strong depth related declines in lobster abundance, and deeper reef within the CMR relative to nearby fished habitats. However, when corrected for by model-based analysis, the abundance of lobsters was actually found to be markedly higher in the CMR (see model summary below).
- Based on the descriptive statistics, the large, legal sized male lobsters provided a much larger proportion of the overall population in the CMR compared to the adjacent fished reference region (45% vs 18%).
- Of note is that very few legal sized females were caught, either in or out of the CMR. This is due to the biology of this species in this region, where female growth is particularly low following maturity. Although these females are not directly removed by the fishery, this does not mean that they are not exposed to other capture associated mortality (e.g. increased predation from octopus targeting lobsters caught in pots, predation from seals and seabird upon return to water by fishing vessel), and the descriptive results suggest they experience less incidental mortality within the CMR.
- The raw data was modelled (based on the initial statistical design) to account for the combined variations in depth, day of pot set and the influence of protection. The model results suggested that there was a strong positive effect of the CMR on total catch per pot, weaker yet positive average male lobster size, average legal-sized male abundance, proportion of females caught, and the proportion of legal males caught. Conversely, there was a weak negative effect of the CMR on average female lobster size (presumably because of greater survival of sub-legal sized females within the CMR). With the exception of the model based on lobster abundance per pot-lift (where a peak in catch around -80 m water depth was detected), depth appeared have little effect on the models. With exception to

overall abundance which yielded a strong signal, the remaining five models exhibited a weak to very weak signal and results should be interpreted with this in mind.

- Future lobster studies in this region/CMR need to better balance the range of depths sampled in the CMR with those sampled within the fishery. This will require discovery and mapping of additional deep reef (100 to 140 m) in the vicinity of the CMR, via targeted surveys or opportunities arising from transit voyages of *RV Investigator*.

### 3. Benthic biota:

- As a result of adverse weather and technical issues associated with AUV only two of the 21 proposed AUV missions were successfully completed. Despite this setback, the two successful transects yielded 18,420 images of seafloor benthos providing a significant advance in our knowledge of the benthic biota and habitats of this region and CMR
- The seafloor benthos appears to support a particularly high abundance of brittle stars which are clearly visible on the reef habitats. The brittle star communities have previously been observed on AUV imagery around the east-coast of Tasmania, but only on the interface between reef-sediment. To see such high abundances of these brittle stars on the reef proper is a noteworthy finding as these may have an important role in the ecosystem function of these deep reef systems.
- Likewise, the reef habitats appear to support a much greater proportion of soft corals than has previously been noted in description of cross-shelf communities in temperate Australia where sponge morphotypes normally dominate the benthic cover.
- Comparison of morphospecies assemblages recorded using the AUV from Tasman Fracture, Huon, Freycinet and Flinders CMRs revealed that each CMR contained a significantly different assemblage. Additionally, there appears to be a distinct division between the Tasman Fracture and Huon CMRs and the Freycinet and Flinders CMRs.
- The morphospecies assemblage and abundance was more variable in the Tasman Fracture and Huon CMRs compared to the Freycinet and Flinders CMRs.
- It appears that variations in the abundance of Bryozoa/Cnidaria/Hyrdoid matrix, the increased presence of *Capnella*-like soft corals and greater abundance brittle stars were the major morphospecies responsible for structuring biological differences between the southern and northern CMRs. It should be noted that the BRUV deployments indicate that the dominance of the brittle stars appear may be constrained to the reefs surveyed by the AUV located directly to the west of the Mewstone. However, additional AUV missions are required to quantitatively determine how widely distributed this brittle stars are throughout the CMR as they



were observed on other BRUV deployments but not in the same high abundances.

- A detailed analysis contrasting the effects of the CMR and depth was not possible from the Tasman Fracture dataset as only two missions were completed.
- It remains a priority to return to the region to collect additional AUV transects (as per initial sampling design) if, and when, additional funds become available.

#### 4. Demersal fishes

- A total of 92 deployments were achieved from the initially planned 100 deployments over four days.
- A total of 20929 individual fishes were recorded represented by 47 species from 33 families. There were slightly less species of fish recorded in the CMR (34 species) compared to the adjacent fished reference regions (39 species).
- Fish prevalence and abundance was generally low for the targeted fishes (especially striped trumpeter and jackass morwong). There does, however, appear to be a high prevalence of non-targeted species, including; butterfly perch, ocean reef perch, red cod, grubfish, lobster and even the occasional cephalopod in the CMR and adjacent fished reference regions.
- The observation of large schools of juvenile jackass morwong were unique (*c* 100-150 mm length) as juveniles of this species are usually associated with estuaries and other shallow-water coastal regions.
- Model-based analyses suggested a number of target or bycatch species were more abundant within the CMR, including striped trumpeter, jackass morwong, Morid cods and ocean perch. This increase in abundance also applied to large (legal sized) size class for striped trumpeter and jackass morwong. The overall abundance and the abundance of large-sized fish varied over depth, with depths *c* 60 – 90 m and >120 m being important. Interestingly, the analysis of overall mean fish size indicated that fish were generally smaller inside the CMR. It should be noted that due to low sample sizes of targeted fish species, these detailed model-based analyses need to be interpreted with caution as effect sizes were quite small.
- In contrast to previous BRUV surveys in other Tasmanian CMRs (e.g. Flinders CMR) where sufficient species abundances were recorded, the low abundances and prevalence's of targeted fish species in the Tasman Fracture region makes selecting suitable single-species biological indicators difficult. As with the lobster data, it remains a priority to undertake further work to refine survey effort and location (in regards to depth) to ensure adequate data is collected that would further refine the selection of suitable indicators.



### 3. APPENDIX 1: BAYESIAN MODEL PARAMETERS

The model resembles a regression-type model, where the outcome (e.g. abundance, length, proportion legal) were related to depth, pull date, and CMR effect. The model can be interpreted almost like any other regression model: the estimated parameters give a representation of the relationships in the data. We allow for non-linearity in the relationship between abundance and depth by including depth as a regression spline in the model. All models were geostatistical, in that they explicitly allowed for spatial dependence between pots. This was achieved using pot location as covariates, a spatial random effect, in the model. This allows for the fact that sites close together are more likely to have similar population characteristics (e.g. abundances). For the interpretation of the model however, this extra effect can largely be ignored.

Since the model is Bayesian we need to specify the priors used. They are: proper but vague priors for parameters for depth, pull date and CMR effect (normal with zero mean and variance 10). The random spatial field is assumed to have an exponential covariance function. The prior for the spatial dependence was uniform on the interval (0.04, 23) and was chosen so that the effective range could be very small and span the range of the data.

A total of 5 Markov Chain Monte Carlo chains were used for estimating the posterior for each of the parameters, with initialisation starting from a naive non-spatial generalised linear model. Each chain was one million iterations long and dependence on starting values was decreased by discarding the first 3000 samples (a burn in). Due to the strong autocorrelation in the chains for catch, all chains were thinned by taking every 3000<sup>th</sup> sample. Running multiple chains allowed the diagnostics to be run on chain convergence, in particular the Rubin-Gelman diagnostics. All chains appeared to pass this diagnostic, and so the samples from each of the chains were combined.

All models were fitted using the spBayes package (<https://cran.r-project.org/web/packages/spBayes/spBayes.pdf>) for R.









National Environmental  
Research Program

# MARINE BIODIVERSITY *hub*



THE UNIVERSITY OF  
WESTERN AUSTRALIA  
*Achieving International Excellence*



[www.nerpmarine.edu.au](http://www.nerpmarine.edu.au)

**Contact:**  
Neville Barrett

Institute for Marine and Antarctic  
Studies,  
University of Tasmania  
Private Bag 49, Hobart,  
Tasmania, 7001.

[neville.barrett@utas.edu.au](mailto:neville.barrett@utas.edu.au)